



DIPARTIMENTO SCIENZE DELLA VITA

**DOTTORATO DI RICERCA IN SCIENZE DELLA VITA
LIFE SCIENCES**

CICLO XXXVI

COORDINATRICE Prof. ssa Simona Maccherini

Water stress as a resource for the production of nutraceuticals with strong antioxidant
and wound healing properties

SETTORE SCIENTIFICO-DISCIPLINARE: CHIM/09

TUTOR: Prof. ssa Ylenia Zambito

DOTTORANDO: Dr. Luca Cerri

A.A. 2022-2023

INDEX

1. Abstract	1
2. Introduction	5
2.1. Cardiovascular diseases	5
2.2. Wound healing	5
2.2.1. Skin	6
2.2.2. Cornea	7
2.3. Respiratory system diseases	8
2.4 Polyphenols: classification and bioavailability	8
2.5. Products with nutraceutical value	9
2.6. Tomato	10
2.6.1. Tomato characterization	10
2.6.2. Beneficial effects	10
2.7. Olive	11
2.7.1. Olive characterization	11
2.7.2. Beneficial effects	11
2.8. Water stress and rescue of by-product	12
2.9. Micro and Nanotechnology and its application in nutraceutical	12
2.9.1. Polymeric material	13
2.9.3. Cyclodextrin	13
2.9.4. Cyclodextrin derivates	14
2.9.5. Hyaluronic acid	14
2.9.6. Chitosan	15
2.9.7. Chitosan derivates	16
3. Impact of Peels Extracts from an Italian Ancient Tomato Variety Grown under Drought Stress Conditions on Vascular Related Dysfunction	18
3.1. Introduction	18
3.2. Material and method	19
3.2.1. Material	19
3.2.2. Sample preparation	19
3.2.3. Tomato peel extract preparation	19
3.2.4. HPLC characterization	20
3.2.5. Antioxidant molecules	20
3.2.6. Lycopene detection	20

3.2.7. Ascorbic acid detection	21
3.2.8. FRAP assay	21
3.2.9. Total polyphenols content.....	21
3.2.10. Huvec isolation and culture	21
3.2.11. Cell treatment.....	21
3.2.12. Cell viability assay	22
3.2.13. ROS production.....	22
3.2.14. SOD, CAT and GPx activities	22
3.2.15. RED stability studies	22
3.2.16. Study of permeation of antioxidant molecules contained in RED across excised rat intestine.....	22
3.2.17. Statistical analysis	23
3.3. Results.....	23
3.3.1. Characterization of bioactive compounds	23
3.3.2. Dose and time dependent response of cell viability.....	24
3.3.3. Protective effect against oxidative stress	24
3.3.4. Reactive oxygen species production	25
3.3.5. Antioxidant enzymes activity.....	26
3.3.6. Studies on permeation of polyphenols contained in RED across excised rat intestine	26
3.4. Discussion	27
4. Olive leaf extracts from three Italian olive cultivars exposed to drought stress differentially protect cells against oxidative stress	29
4.1. Introduction	29
4.2. Materials and method.....	30
4.2.1. Materials.....	30
4.2.2. Leaves Sampling and Stress Condition	30
4.2.3. Determination of the Antioxidant Capacity and Polyphenols Content	30
4.2.4. Ferric Ion Reducing Antioxidant Power (FRAP)	31
4.2.5. Folin-Ciocalteu Method.....	31
4.2.6. Leaf Metabolite Extraction and Ultra-High-Performance Liquid Chromatography-Mass Spectrometry.....	31
4.2.7. Cell Viability Test by WST-1 Assay	32
4.2.8. ROS production.....	32
4.2.9. Permeation of antioxidants contained in OLE across excised rat intestine.....	32
4.2.10. Statistical analysis	32
4.3. Results.....	33

4.3.1. Antioxidant Capacity and Polyphenols Content.....	33
4.3.2. UHPLC phenolic characterisation.....	34
4.3.3. Cell Viability Test	36
4.3.4. OLEs protective effect from oxidative stress	37
4.3.5. OLE antioxidant activity as assessed by ROS production.....	39
4.3.6. Permeation of antioxidants contained in OLE across excised rat intestine.....	40
4.4. Discussion	41
5. Combination of Two Kinds of Medicated Microparticles Based on Hyaluronic Acid or Chitosan for a wound Healing Spray Patch.....	43
5.1 Introduction.....	43
5.2. Materials and method.....	44
5.2.1. Materials.....	44
5.2.2. Total Polyphenol Content (TPC) Determination in Olive Leaves Water Extract (OLE)	44
5.2.3. Bactericidal Assays	44
5.2.4. Preparation of Microparticles (MP) Using the Spray-Drying Technique.....	45
5.2.5. Determination of the OLE Content in Medicated MP	45
5.2.6. Dimensional and Morphological Analysis: Scanning Electron Microscopy (SEM) .	45
5.2.7. Thermogravimetric Analysis (TGA)	45
5.2.8. Determination of OLE Stability in MP.....	45
5.2.9. Determination of the MP Swelling Degree.....	46
5.2.10. Study of the Release Profiles from Medicated MP	46
5.2.11. Cell Culture Techniques	46
5.2.12. Cell Viability and Proliferation Test by WST-1 Assay	46
5.2.13. In Vitro Scratch Wound Healing Assay.....	46
5.3. Results.....	47
5.3.1. TPC Determination in OLE.....	47
5.3.2. OLE Antibacterial Activity	47
5.3.3. MP Characterization	48
5.3.4. TGA Analysis	49
5.3.5. Determination of OLE Stability in MP.....	49
5.3.6. Determination the MP Swelling Degree.....	50
5.3.7. Study of Release Profile from Medicated MP	51
5.3.8. Cell viability and proliferation test by WST-1 assay	52
5.3.9. <i>In vitro</i> scratch wound healing assay.....	54
5.4. Discussion	55

6. Olive Leaf Extract For Corneal Wound Healing	57
6.1. Introduction.....	57
6.2. Materials and method.....	58
6.2.1. Materials.....	58
6.2.2. Synthesis of Quaternarized Chitosan QA-Ch.....	58
6.2.3. Synthesis of QA-Ch-Metil- β -Cyclodextrin conjugate (QA-Ch-MCD).....	59
6.2.4. Lyophilization.....	59
6.2.5. Characterization of the QA-Ch-MCD conjugate.....	59
6.2.6. Cell Culture Techniques.....	59
6.2.7. Cell Viability assay.....	59
6.2.8. Preparation of polymeric complexes.....	60
6.2.9. OLE-GS stability study in simulated tear fluid (STF).....	60
6.2.10. Total polyphenols content (TPC).....	60
6.2.11. Differential Scanning Calorimetry (DSC).....	60
6.2.12. <i>In vitro</i> Scratch Test Wound healing assay.....	60
6.2.13. Antioxidant activity assay.....	61
6.2.14. <i>In Vivo</i> study.....	61
6.2.15. Statistics analysis.....	61
6.3. Results.....	61
6.3.1. Synthesis and characterization of QA-Ch and QA-Ch-MCD.....	61
6.3.2. OLE-GS stability study in STF.....	63
6.3.3. DSC.....	63
6.3.4. Biological investigation: Cell viability assay ad in vitro scratch test.....	64
6.3.5. Antioxidant activity assay.....	68
6.3.6. <i>In Vivo</i> study: Draize test.....	68
6.4. Discussion.....	69
7. Stabilization of nano-aggregates based on thiolated hydroxypropyl-β-cyclodextrin for pulmonary delivery	72
7.1. Introduction.....	72
7.2. Materials and methods.....	73
7.2.1. Materials.....	73
7.2.3. Synthesis and purification of thiolated hydroxypropyl- β -cyclodextrin (HP- β -CD-SH).....	73
7.2.4. Synthesis and purification of nanoparticles based on HP- β -CD-SH (HP- β -CD-SH-NP).....	74
7.2.10. Monolayer nebulization.....	75
7.3. Results.....	77

7.3.1. Synthesis and characterization of HP-β-CD-SH-NP	77
7.3.2. Determination of the association constant for cyclodextrins/DMS and cyclodextrins/OLE-GS	79
7.3.3. Study of DMS complexation with HP-β-CD-SH-NP	79
7.3.4. Cytotoxicity studies	80
7.3.5. Dimensional analysis and zeta potential of medicated formulations	81
7.3.7. Evaluation of the protective effect from oxidative stress of OLE-GS nebulized on the monolayer	83
7.4 Discussion	84
8. Conclusion	86
9. Acknowledgements	87
10. References	88

1. Abstract

The industrial processing of fruits and vegetables produce substantial quantities of by-products, such as peels and seeds, abundant in bioactive compounds. Repurposing and recycling these by-products not only contribute to waste reduction but also offer cost savings in waste treatment. These natural compounds find several applications in the food, pharmaceutical, and cosmetic industries. Notably, a wide range of waste products is generated during industrial processing, including peels, leaves, and seeds. Significant volumes of by-products are produced during the industrial processing of tomatoes and olives, particularly peels and leaves. Numerous studies underscore the potential health benefits associated with the consumption of these by-products. Moreover, water stress, defined as a lack water supply, can be used as a resource for nutraceutical production. This is particularly important in environments whit limited irrigation water accessibility and high water costs for agricultural practices.

Tomato by-products encompass a various range of biologically active substances and serve as a substantial source of natural antioxidant supplements for the human diet. The aim of the first study was to compare the antioxidant properties of a by-product from an ancient Tuscan tomato variety, Rosso di Pitigliano (RED), obtained through normal plant growth conditions (-Ctr) and conditions of drought stress (-Ds). The RED-Ds tomato peel extract exhibited a higher total polyphenol content than RED-Ctr. All tested extracts on HUVEC cells displayed no cytotoxic effects. A two-hour pretreatment with 5 μg GAE/mL (Gallic acid equivalent per mL) from either RED-Ctr or RED-Ds demonstrated protection against H_2O_2 -induced oxidative stress. Furthermore, it significantly reduced ROS production by elevating superoxide dismutase (SOD) and catalase (CAT) activity. The permeation of antioxidant molecules present in RED-Ctr or RED-Ds in excised rat intestine was consistently high, with no significant differences between the two RED types. In conclusion, the RED-Ds tomato peel extract emerges as a valuable source of bioactive molecules, exhibiting the capacity to safeguard HUVEC cells from oxidative stress induced by H_2O_2 more effectively than the related variety grown under normal conditions RED-Ctr.

The second work of this thesis was focused on the study olive leaves, an abundant by-product of olive oil production. The primary objective of the study was to assess the efficacy of olive leaf extracts from various varieties in addressing oxidative stress. Olive leaf extracts (OLE) are particularly rich in polyphenols, making them valuable for producing nutraceuticals with healthy properties. Polyphenols are the primary antioxidant molecules in plants and their content typically increases when plants undergo drought stress. This investigation focused on olive leaf extracts derived from three distinct Italian olive cultivars: Giarraffa, Leccino, and Maurino subjected to drought stress or grown under normal conditions. The evaluation encompassed antioxidant properties, phenolic profile, intestinal permeation, and protective effects against oxidative stress in a cell model based on human umbilical vein endothelial cells (HUVEC). OLEs from stressed Maurino and Giarraffa plants exhibited the most significant enhancement in antioxidant capacity compared to their respective controls. Maurino's phenolic profile showing a notable increase in compounds such as oleuropein and luteolin-7-O-rutinoside. All tested extracts subjected to water stress effectively protected HUVEC cells from oxidative stress by reducing reactive oxygen species (ROS) production. The protective effect was more pronounced in Giarraffa and Maurino OLEs exposed to drought stress compared to other extracts. The stressed Giarraffa olive leaf extract (OLE-GS) demonstrated a higher apparent permeability of antioxidant molecules compared to stressed Maurino olive leaf extract (OLE-MS). In conclusion, OLE-GS and OLE-MS show important antioxidant properties demonstrating their ability to protect HUVEC cells against oxidative stress. From this work, it was possible to observe that the OLEs obtained from plants cultivated under water stress conditions show a higher content of antioxidant molecules compared to extracts obtained from plants grown under normal conditions. Furthermore, these extracts exhibit a pronounced antioxidant action in containing

the production of ROS and reducing cell mortality compared to control OLEs following oxidative damage induced by H₂O₂, as highlighted in the HUVEC cell-based model proposed in the study. In particular, OLE-GS has proven to be the most effective in containing oxidative damage and, for this reason, it was the subject of further studies proposed in subsequent works.

OLE was deeply studied for its antioxidant and antibiotic properties, rendering it a valid resource for wound care applications. The third study aimed to incorporate OLE into microparticles (MPs) made of hyaluronic acid (MPHA-OLE) or chitosan (MPCs-OLE) to develop a spray patch for treating wounds in challenging anatomical areas. The produced MPs underwent characterization for particle size, OLE protection against degradation, absorption of wound exudate and also the ability to regulate OLE release. Both medicated and unmedicated MPHA and MPCs, as well as various mixture in different weight ratios, were subjected to in vitro testing using a mouse fibroblast cell line (BALB/3T3 clone A31) through the scratch wound healing assay. The size of the MPs consistently remained below 5 µm, making them suitable for the intended application. MPCs-OLE demonstrated a capability to slow down OLE release, with approximately 60% of the polyphenols released after 4 hours. Notably, both MPHA and MPCs exhibited the potential to expedite wound healing. A 50% MPHA-OLE and 50% MPCs-OLE mixture emerged as the most effective in accelerating the wound healing process. The combinations of MPHA-OLE and MPCs-OLE explored in this study exhibited characteristics well-suited for formulating a spray patch, presenting a beneficial way to repurpose waste products from olive growers. In conclusion, it has been demonstrated that OLE, thanks to its high content of antioxidant molecules, can be used for the development of a pharmaceutical form for skin wound repair. The encapsulation ensures a controlled release of OLE from MPCs and MPHA. All these mechanisms contribute to accelerating the wound healing process in the proposed cellular model. Based on these considerations, it has been considered using an OLE with pronounced antioxidant activities, such as OLE-GS, for the creation of an eye drop formulation for repairing corneal wounds.

After studying the potential use of Olive Leaf Extract (OLE) for the skin wound repair, it was decided to incorporate it into a formulation of eye drops designed to act as a healer for corneal wounds. In this regard, olive leaf extracts from the Giarrappa variety, obtained from trees subjected to water stress (OLE-GS), were chosen for the subsequent study. The focus of the fourth study was to develop medicated eye drop formulations containing OLE-GS for the purpose of corneal wound healing. The study was conducted starting from native chitosan (Ch), and then it was based on quaternary ammonium chitosan (QA-Ch 50-190 kDa) conjugated with methyl-β-CD (MCD), encoded as QA-Ch-MCD. The efficacy of ophthalmic drops, based on different prepared polymers either medicated or not with OLE-GS, in accelerating the healing of corneal wounds was assessed using a model of corneal cell monolayers of the HCE-T cell line, following the assay proposed in the preceding work. A cell viability assay conducted on the HCE-T cell line determined that a concentration of 10 µg/ml of QA-Ch-MCD was suitable for producing the polymer complexes. The mixture between QA-Ch and MCD (QA-Ch/OLE-GS) and Ch and MCD (Ch/MCD) was also prepared based on the weight ratio of MCD to QA-Ch-MCD. A scratch test was performed to select the concentration of OLE-GS to be used for the development of the polymeric complexes. The concentration of 100 µg/ml of OLE-GS was chosen. The samples tested for the wound healing assay included OLE-GS, QA-Ch-MCD, QA-Ch-MCD/OLE-GS, QA-Ch/MCD, QA-Ch/MCD/OLE-GS, Ch/MCD, Ch/MCD/OLE-GS, Ch, Ch/OLE-GS, MCD, and MCD/OLE-GS. None of the polymer solutions alone significantly reduced scratching compared to the control. All the polymer complexes demonstrated a notable improvement, with all formulations (except Ch/OLE-GS) significantly enhancing scratch closure compared to the control. Moreover, QA-Ch-MCD/OLE-GS exhibited superior efficacy in accelerating scratch closure compared to all other formulations tested and OLE-GS alone. The ability of the tested samples to protect against H₂O₂-induced oxidative damage was also evaluated on the HCE-T cell line. All formulations containing OLE-GS, as well as OLE-GS alone, increased cell viability following H₂O₂-induced oxidative

damage. Vehicles alone were also effective in protecting against oxidative damage, with the exception of MCD. A Draize test, utilizing male New Zealand albino rabbits, revealed that OLE-GS and QA-Ch-MCD/OLE-GS showed no signs of irritation, swelling, or redness after 24 hours. In conclusion, OLE-GS at the tested concentration demonstrated an improvement in corneal wound healing in the model used. Furthermore, when complexed with QA-Ch-MCD, this effect was even more pronounced. In conclusion, OLE-GS has demonstrated its ability to contribute to the healing of corneal wounds in the proposed cellular model. This effect is further amplified when OLE-GS is complexed with QA-Ch-MCD, which has proven to be the most effective in protecting the antioxidant molecules contained in it from degradation, thanks to the strong interaction between them. Pre-treatment of HCE-T with QA-Ch-MCD/OLE-GS has shown the ability to contain oxidative damage induced by H₂O₂. Furthermore, the QA-Ch-MCD/OLE-GS formulation did not show signs of irritation in the proposed in vivo model, suggesting its safety for use.

The interaction between the pulmonary and cardiovascular systems is gaining heightened attention. Patients with respiratory disorders such as chronic obstructive bronchoalveolar disease, idiopathic pulmonary fibrosis, and conditions affecting ventilatory control (such as sleep apnea syndromes, obesity, and hypoventilation) frequently exhibit vascular anomalies. In the context of the fifth study in this thesis, Olive Leaf Extract obtained from Giarraffa trees subjected to water stress (OLE-GS) was employed to formulate an inhalation product. Existing literature extensively documents the potential of polyphenols, with their robust antioxidant activity, for treating certain lung diseases. This study was focused on the development of formulations based cyclodextrins as solubility enhancers and mucoadhesive polymers able to interact with the mucous layer, enhancing drug bioavailability and local retention. Specifically, thiolated cyclodextrins, recognized for their robust mucoadhesive properties, were employed. The thiol groups of thiolated cyclodextrins form disulfide bridges with cysteine residues of mucins. Cross-linked thiolated cyclodextrins were used to enhance the pharmacological properties of corticosteroids such as dexamethasone (DMS) and deliver natural products based on polyphenols, such as OLE-GS, for treating pulmonary inflammation. The synthesis of thiolated hydroxypropyl beta cyclodextrin (HP-β-CD-SH) was performed from native hydroxypropyl beta cyclodextrin (HP-β-CD). The followed by cross-linked reaction was performed through the use of 1,11-bismaleimido-triethyleneglycol cross-linker (BM(PEG)3) in order to obtain HP-β-CD-SH-NP. Nanoaggregates of HP-β-CD-SH at a non-toxic concentration of 10 mg/ml with a low polydispersity index were formed. Then they were stabilized due to the cross-linking reaction with BM(PEG)3. Permeation studies, conducted using an in vitro Air-Liquid Interface (ALI) model consisting of NCI-H441 cells, revealed an increased drug concentration in the permeate when DMS was complexed with HP-β-CD-SH and HP-β-CD-SH-NP compared to native HP-β-CD. No significant differences were observed in the amount of DMS permeated between HP-β-CD-SH and HP-β-CD-SH-NP. In the context of ROS production and protection from oxidative damage, cyclodextrins were complexed with OLE-GS. Pretreatment with OLE-GS effectively reduced ROS production and enhanced cell viability compared to cells subjected to oxidative damage without pretreatment. While all formulations exhibited increased cell viability compared to OLE-GS alone, no significant differences were observed between the formulations. In particular, the complexation of OLE-GS with HP-β-CD-SH-NP led to a significant reduction in ROS production compared to any other sample tested. In conclusion, OLE-GS has proven to be effective in containing damages caused by oxidative stress in the proposed cellular model, and this effect is even more pronounced when it is complexed with the cyclodextrins used in this study. Crosslinking does not provide an advantage in DMS permeation, as demonstrated by the monolayer cell experiment. In particular, the crosslinking reaction with BM(PEG)3 of HP-β-CD-SH offers the advantage of creating stabilized nanoaggregates. These, by complexing OLE-GS, manage to enhance its antioxidant action compared to all other tested samples. Crosslinking represents a valuable resource, especially for carrying out localized actions, such as in the case

of pulmonary administration, making the antioxidant action of OLE-GS localized. This result aligns perfectly with the objectives set for the development of the formulation.

From the obtained results, it can be asserted that water stress represents a significant resource for the production of nutraceuticals with pronounced antioxidant power. This is because it can increase the production of antioxidant molecules in the extracts, making their activity even more pronounced. Moreover, encapsulating these extracts enhances their activity and prevents degradation, making them more active, stable, and useful for the treatment and prevention of diseases. In conclusion, cultivating native plants from the Mediterranean region through water stress, defined as a lack of water supply, is an important resource for the production of nutraceuticals with high antioxidant power. Developing these through the use of innovative pharmaceutical forms further enhances their potential utilization.

2. Introduction

2.1. Cardiovascular diseases

Cardiovascular diseases (CVDs) encompass a large spectrum of disorders affecting the heart and blood vessels, including conditions like coronary heart disease, cerebrovascular disease, and peripheral vessel disease. As demonstrated by a claim published from the World Health Organization (www.who.int, s.d.) CVDs as the leading causes of mortality worldwide. In the same year, the Tuscany Region reported a significant 39.9% of individuals succumbing to CVDs, as documented by the Tuscany Regional Health Agency (ARS Toscana) at ars.toscana.it (ars.toscana.it, s.d.). CVDs are preventable through the adoption of population-wide strategies addressing behavioral risk factors. These factors include tobacco use, unhealthy dietary habits, obesity, physical inactivity, and the harmful consumption of alcohol. Therefore, is possible to reduce the incidence of CVDs in proactive prevention. Early detection and the administration of appropriate medications, are essential for individuals with CVDs or those at high cardiovascular risk. With preventive measures and specific interventions, we can reduce the impact of CVDs on global health. A widely used cellular model for studying the effects of cardiovascular diseases is represented by HUVECs. HUVEC (Human Umbilical Vein Endothelial Cells) represents a main model for investigating a large range of diseases, encompassing cardiovascular and metabolic conditions (Figure 1). Numerous studies have shown the impact of antioxidant molecules obtained from natural products on HUVEC through in vitro experiments focusing on vascular dysfunction (Cao et al., 2017).

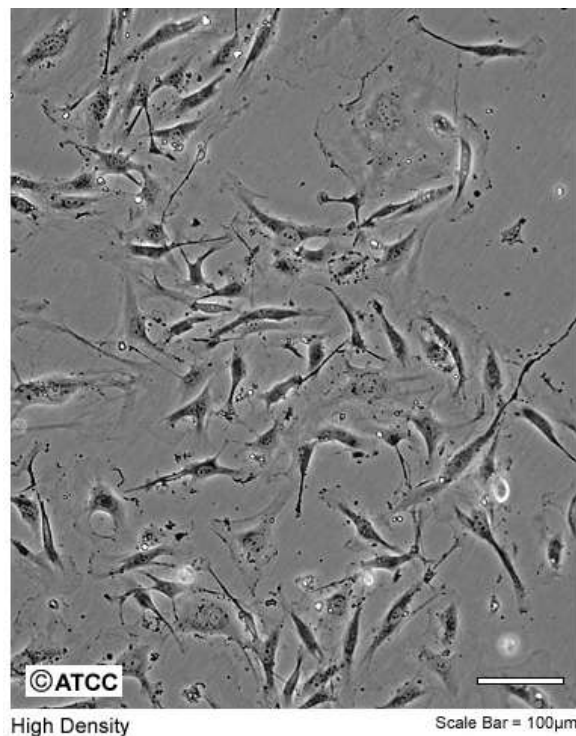


Figure 1. HUVEC Cells, scale bar 100 μm . (<https://www.atcc.org/products/crl-1730#detailed-product-images>, s.d.)

2.2. Wound healing

A wound represents a pathological condition that involves the rupture of the normal microstructure and function of the anatomical tissue. It can occur following chemical, thermal or physical injuries. Following the penetration of foreign bodies and organisms into the damaged tissue, the inflammatory response occurs. A wound can be classified as acute or chronic based on the duration of wound closure. Acute wounds include burns, traumatic injuries and wounds

non-infected surgically created. The healing process for acute wounds takes 8-12 weeks while for chronic wounds it takes more than 12 weeks. Wound area reduction is a dynamic biological process, caused by tissue rupture. Its healing involves numerous elements, such as platelets, leukocytes, monocytes, neutrophils, macrophages, fibroblasts, keratinocytes and endothelial and transient myofibroblasts, to maintain tissue integrity (Utami et al., 2020). The wound healing process is divided into four sequential phases which are (P.-H. Wang et al., 2018):

- Hemostasis: The initial phase of hemostasis involves the activation of platelets and of neutrophils at the wound site to remove bacteria to provide a suitable environment for wound healing. Subsequently, macrophages facilitate phagocytosis of the bacteria.
- Inflammatory phase and proliferative phase: require approximately 72 hours; in particular the proliferative phase is characterized by an accumulation of fibroblasts, keratinocytes and endothelial cells.
- Remodeling phase: represents the last phase of wound healing process. This phase is characterized by a balance between the apoptosis of existing cells and the production of new cells.

Historically, traditional medicinal plants have found an huge application in the wounds treatment. Several plant extracts were studied for their wound healing properties through both *in vitro* and *in vivo* studies. The presence of phytochemical components in these extracts contributes significantly to their therapeutic properties in wound repair. It is possible to state that nutraceutical products exhibit biological activities that play a crucial role in enhancing wound healing process (Polera et al., 2019).

2.2.1. Skin

The skin is the largest organ of the human organism and represents approximately 16% of total body weight. The skin mainly has the function of forming a barrier between the inside of the body and the external environment, in order to isolate and protect the organism from possible injuries and external pathogens. Starting from the most superficial portion and proceeding inwards, the skin is composed of the epidermis, dermis and hypodermis (Fore, 2006).

- Epidermis: serves as a barrier, preventing the penetration of water, foreign substances and microorganisms from the outside. The epidermis does not have vessels and consequently the nutrients reach it from the capillaries of the dermis. In this layer the most present cells are keratinocytes. These cells are able to synthesize keratin to protect the underlying tissues from heat, pathogenic microorganisms and chemicals.
- Dermis: it is formed by thick connective tissue, rich in blood vessels and nerve endings. The most present cells are fibroblasts whose purpose concerns the synthesis of the constituent elements of the extracellular matrix.
- Hypodermis: It is made by connective tissue and represents a storage site for fats.

A highly accredited *in vitro* model for the study of the skin is represented by the BALB/3T3 murine embryonic fibroblast cell line clone A31 (Figure 2) (Fabiano et al., 2021).

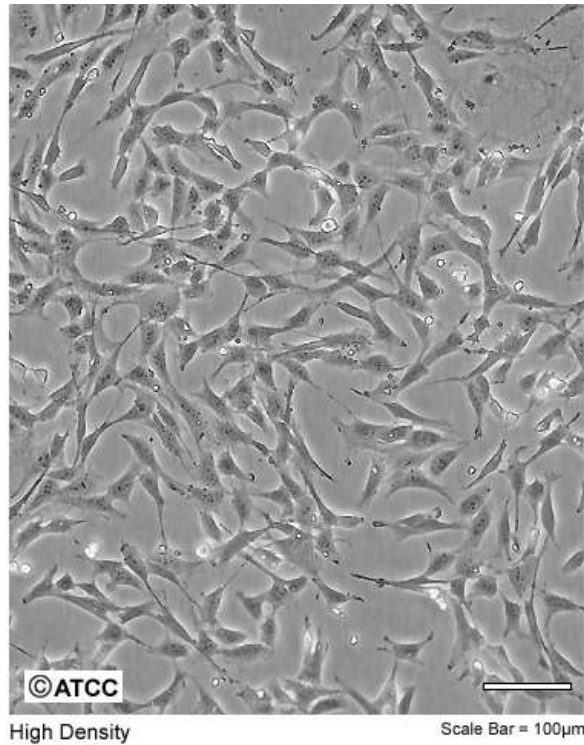


Figure 2. BALB/3T3 clone A31 a cell line. (<https://www.atcc.org/products/ccl-163#detailed-product-images>, s.d.)

2.2.2. Cornea

The cornea is a vital transparent tissue. It performs crucial functions, its primary role being a protective barrier. The epithelium, crucial to this protective function, acts a defense against pathogens. Tight junctions are fundamental for this barrier activity. Basement membrane and Bowman's layer provide to support cornea posteriorly. The stroma, represent the majority of the corneal volume. It offers structural support, clarity and contributes to ocular immunity. The posterior cornea, composed of Descemet's membrane and endothelium, is essential for stromal dehydration (Eghrari et al., 2015). The cornea, like the skin, can suffer a large number of injuries which can be chemical and mechanical. The *in vitro* model represented by the human corneal epithelial cell line (HCE-T) (Figure 3) is one of the main accredited methods for the studies of some ocular pathology as dry eye disease and in particular for the study of the cornea wound healing process.

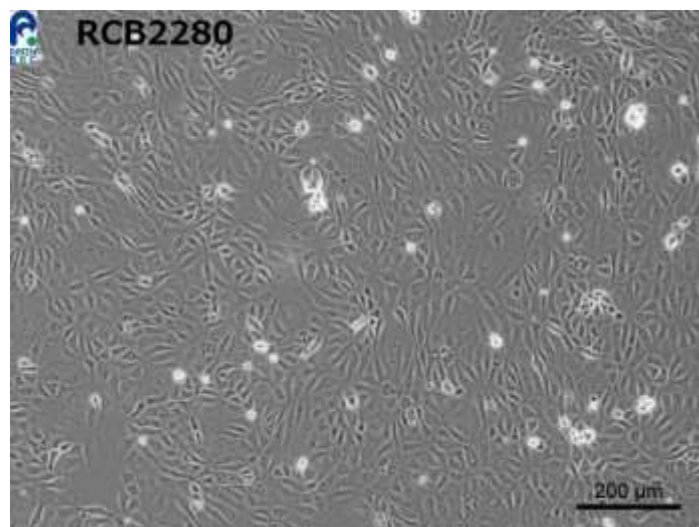


Figure 3. HCE-T cells. (https://cellbank.brc.riken.jp/cell_bank/CellInfo/?cellNo=RCB2280, s.d.)

2.3. Respiratory system diseases

The relationship between the pulmonary and cardiovascular systems is gaining heightened recognition, in fact patients with respiratory disorders, such as chronic obstructive bronchoalveolar disease, idiopathic pulmonary fibrosis and disorders affecting ventilatory control (as sleep apnea syndromes and obesity hypoventilation syndrome), often exhibit vascular abnormalities. Pulmonary hypertension can lead to severe ventricular dysfunction in the context of lung disease (Han et al., 2007). In chronic obstructive pulmonary disease (COPD), exacerbations are events marked by a negative impact on disease progression, comorbidities and mortality. However, also the non-respiratory diseases (such as heart failure and thromboembolism), may also have an important impact on disease progression (MacLeod et al., 2021). Furthermore, the administration of nutraceuticals can be used in the context of both preventing and for the treating of COPD. Scientific evidence suggests that some foods and nutrients, in particular nutraceuticals shown antioxidant and anti-inflammatory properties able to enhance pulmonary function, reduce lung function decline, and decrease the risk of COPD. It is well reported as several type of nutraceutical may have a beneficial impact on COPD. This consent to health professionals to suggest to patients a correct lifestyle able improved pulmonary health (Scoditti et al., 2019). A highly accredited *in vitro* model for carrying out *in vitro* biological evaluations for respiratory system pathologies is represented by the immortalized human lung adenocarcinoma cell line NCI-H441 (ATCC HTB-174), type II alveolar cells, capable of forming a polarized differentiated monolayer (Figure 4) (Vizzoni et al., 2023).

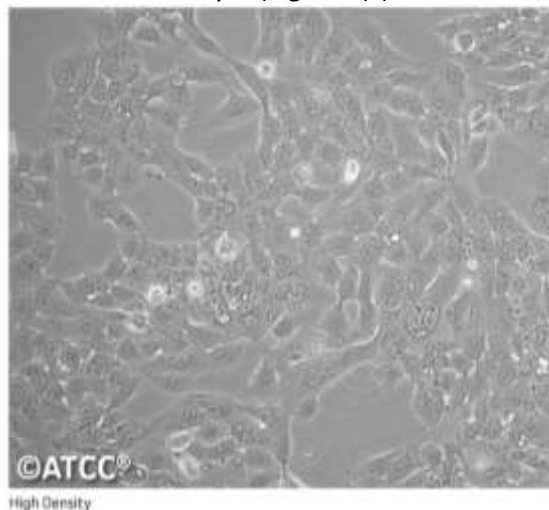


Figure 4. NCI-H441 cells. (<https://www.atcc.org/products/htb-174>, s.d.)

2.4 Polyphenols: classification and bioavailability

Polyphenols constitute biologically active compounds found in plant derivatives or produced as secondary metabolites, categorized into three primary classes based on their chemical structure: phenolic acids, flavonoids, and non-flavonoids (including stilbenes like resveratrol and lignans) (Figure 5). These compounds are present in fruits, vegetables, nuts, and their derivatives, showcasing significant antioxidant and anti-inflammatory properties. The majority of polyphenols are flavonoids, encompassing anthocyanins (such as cyanidin) and anthoxanthins (including flavonols as quercetin and flavanols as catechin), which contribute both antioxidant and anti-inflammatory attributes (H. Wang et al., 1999). It is possible found flavonoids in chocolate, tea and wine that are particularly rich in proanthocyanidins, quercetin, and epicatechin. Flavonoids share a diphenylpropane chemical structure, comprising two benzene rings and one pyranic ring, with -OH and -O-R groups typically at positions 7 and 4', respectively. Other substituents (R groups) vary for each type of flavonoid. Coumaric and ferulic acid, cyanidin, catechin, and quercetin stand out as major polyphenols in this context. Oxidative stress plays an important role in numerous chronic and degenerative pathologies, including atherosclerosis.

Several studies were aimed towards identifying antioxidant compounds capable of preventing the progression of such diseases. Many polyphenols exhibit radical-scavenging and antioxidant activities, particularly evident in cell-free systems and *in vitro* cellular studies (Mitjans et al., 2011). Numerous studies described the anti-inflammatory properties of polyphenols, demonstrating their ability to impede tumor development, modulate the immune system, enhance capillary resistance by acting on blood vessel constituents, and safeguard the cardiovascular system. Consequently, numerous plant extracts rich in these phenolic molecules are used as supplements or integrated in pharmaceutical formulations (Munin & Edwards-Lévy, 2011).

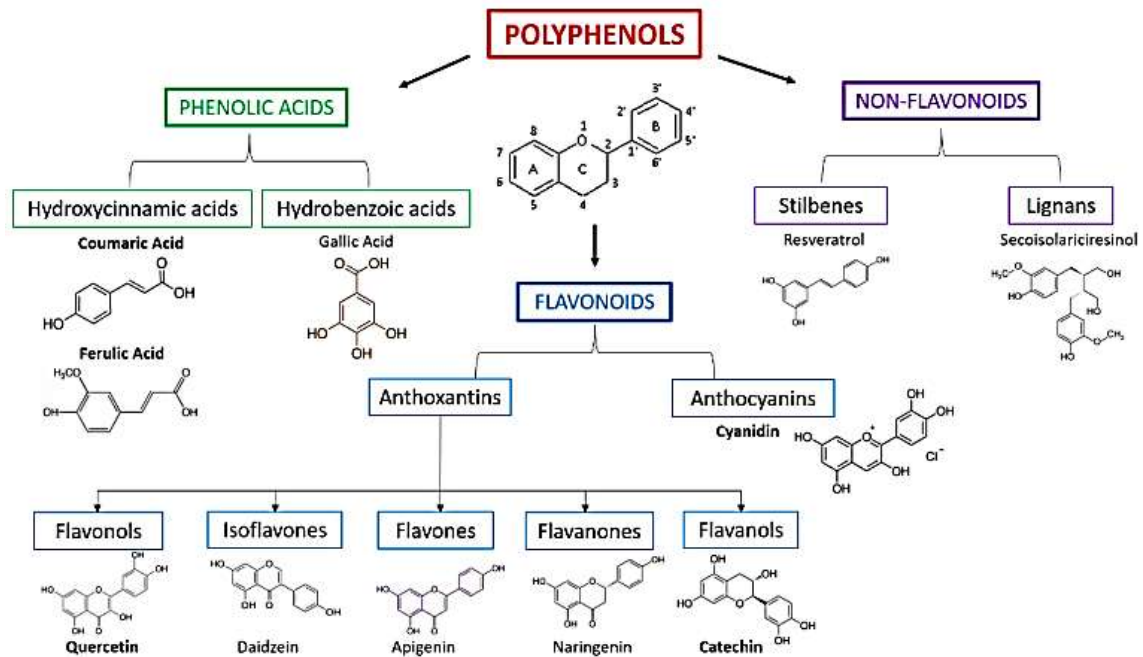


Figure 5. Schematic classification of polyphenols and some examples.

2.5. Products with nutraceutical value

The term "nutraceutical" was coined in 1989 by Stephan DeFelice by combining "nutrition" and "pharmaceutical." DeFelice's definition of nutraceutical is: "a food (or a part of food) that provides medical or health benefits, including the prevention and/or treatment of diseases (Kalra, 2003). In particular, nutraceuticals have shown benefits in terms of providing physiological advantages and protection against chronic inflammatory disorders, such as cardiovascular diseases (CVDs). (Kuppusamy et al., 2014). It is well demonstrated the importance of administration of nutraceutical products as a strategy to prevent inflammation and atherosclerosis (ATS) and its complications, such as cardiovascular diseases (CVD). It is mentioned that many *in vitro* studies have demonstrated the beneficial effects of natural products and their derivatives in protecting human endothelial cells from aging and oxidative stress (Felice et al., 2019). Moreover, it is reported that polyphenols contained in nutraceuticals can be used for the treatment of inflammatory pulmonary diseases due to potent anti-oxidant and anti-inflammatory activity (Trotta & Scalia, 2017). Furthermore it is reported that the active molecules contained in nutraceuticals can find application in the wound healing process (Fabiano et al., 2021).

2.6. Tomato

The tomato (*Solanum lycopersicum* L.) (Figure 6) is an edible Mediterranean plant well known for its beneficial properties (Kavitha et al., 2014). Consumed fresh or processed, tomatoes are one of the most consumed vegetables in the world. It was stated during the 13th World Processing Tomato Congress, in June 2018, that since 1994 the production and processing of tomatoes has grown globally by 59%. As reported by Ismea in 2017 held in Rome, California, Italy and China are the largest tomato producers in the world. Other producing countries include Spain, Turkey and Portugal (Van Eck et al., 2006) (*Ismea, 2017. Report - I numeri della filiera del pomodoro da industria. Roma, June 2017, s.d.*).



Figure 6. Tomato rosso di Pitigliano

2.6.1. Tomato characterization

Due to their substantial consumption, tomatoes and tomato-based products play a vital role in our dietary intake (Padalino et al., 2017). Tomatoes are rich in various beneficial compounds, including carotenoids like lycopene, ascorbic acid (vitamin C), vitamin E, and a range of phenolic compounds, notably flavonoids and hydroxycinnamic acids (García-Valverde et al., 2013). Lycopene is the primary antioxidant present in fresh tomatoes and processed tomato products. Due to its long-chain conjugated double bonds, lycopene possesses superior antioxidative properties compared to compounds such as luteolin or β -carotene. Moreover, the lycopene content contributes to the characteristic red coloration of tomatoes (Kalióra et al., 2006). Furthermore, phenolic compounds are the main contributors of the antioxidant capacity of tomato fruits among the various antioxidant compounds they contain. In addition to phenols, increased consumption of flavonoids, vitamin C, and carotenoids further augments the antioxidant potential of fruits and vegetables. Tomatoes are particularly rich in lycopene and β -carotene (Hernández et al., 2007).

2.6.2. Beneficial effects

Numerous studies have provided important evidence suggesting that bioactive compounds found in foods, particularly tomato products, may offer significant advantages in the prevention of cardiovascular disease (Cámara et al., 2022). These potential benefits have been attributed, in part, to the elevated levels of lycopene present in tomatoes. Epidemiological investigations have consistently demonstrated an important connection between tomato administration and a reduced risk of chronic degenerative diseases, in particular cardiovascular diseases, cancer and neurodegenerative diseases (Steven et al., 2019).

2.7. Olive

The olive trees have a well know nutritional and medicinal value in particular due to its oil obtained from the fruits and the for the leaves (Figure 7). The olive occupies a principal role in the Mediterranean area. The country of this area are responsible of 98% of the global production (approximately 11 million tons). This prominence extends far beyond its economic impact, as it plays a vital role in the dietary habits and tradition in country where it is cultivated. The olive has an important role across European Mediterranean islands and nations, including Spain, Italy, France, Greece, Israel, Morocco, Tunisia, and Turkey due to its the application in traditional remedies. Recently, olive byproducts derived from olive tree cultivation, such as the olive leaves, attract a growing interest by their nutraceutical value (El & Karakaya, 2009).



Figure 7. Olive leaf

2.7.1. Olive characterization

Olea europaea L. garners attention in research, due to for its significance in the culinary realm. Its fruits and oil are used as fundamental components of the daily diet for a substantial portion of the global population. However, the leaves of the olive tree have a particular importance, owing to their secondary metabolites, exemplified by compounds like oleuropein. These compounds have crucial roles as key constituents with beneficial effects on metabolism when employed as traditional herbal remedies. These advantageous properties can be attributed to the phenolic compounds found within olive leaves (J. A. Pereira et al., 2006). It is possible to divide the phenolic compounds principally present in olive leaves in five groups: oleuropeosides (oleuropein and verbascoside); flavones (luteolin-7-glucoside, apigenin-7-glucoside, diosmetin-7-glucoside, luteolin, and diosmetin); flavonols (rutin); flavan-3-ols (catechin), and substituted phenols (tyrosol, hydroxytyrosol, vanillin, vanillic acid, and caffeic acid). Oleuropein is the principal compound present in olive leaves, followed by hydroxytyrosol, the flavone-7-glucosides of luteolin and apigenin, and verbascoside. In particular hydroxytyrosol is a precursor of oleuropein. Verbascoside is a conjugated glucoside of hydroxytyrosol and caffeic acid (Benavente-García et al., 2000).

2.7.2. Beneficial effects

The beneficial effects of virgin olive oil are mainly due to the presence of polyphenols. These compounds have been widely studied in recent years. In particular oleuropein, the most present polyphenol in olive leaves. It is able to prevents the heart disease's by protecting membrane from lipid oxidation. Furthermore, has an antiarrhythmic action, improve lipid metabolism, and prevent hypertensive. Hydroxytyrosol is an oleuropein derivative. It is able to prevent heart disease's and tumoral diseases with similar effects of oleuropein (Somova et al., 2003) (A. P. Pereira et al., 2007). Moreover, hydroxytyrosol play an important role against atherosclerosis and

in the prevention diabetic neuropathy (Sato et al., 2007). Oleocanthal is a molecule naturally present in olive oil with a well know anti-inflammatory activity. Moreover, is well know that oleuropein possesses remarkable antioxidant properties. These properties enable it to mitigate tissue damage and promote more efficient wound healing processes (Alquraishi et al., 2023).

2.8. Water stress and rescue of by-product

Beyond the bioactive constituents with the potential for creating health-focused products, there's a compelling opportunity to reuse substances from agricultural by-products. The industrial processing of vegetables and fruits produce huge quantities of by-products, such as peels and seeds, which are abundant in bioactive compounds. The reuse and the recycling of these by-products can lead to save money waste treatment. These naturally compounds have versatile applications in the food, pharmaceuticals, and cosmetics areas. Additionally, what stands out is the significant variety of beneficial waste products generated, including peels (constituting approximately 60%) and seeds (making up around 40%). In the course of industrial tomato processing, substantial quantities of by-products, notably peels with high nutritional value (Szabo et al., 2018), are produced. Several studies have explored the potential health benefits of these by-products (Felice et al., 2020). Moreover, Olive leaf extract (OLE), derived from biowaste, is widely utilized as a food supplement and an over-the-counter drug due to its positive effects. Recent research has shown that OLE is a valid resource in relation to its impact on oxidative stress in the development of vascular disease. These particular benefits in use of OLE are due to the presence of phenolic compounds, as oleuropein, that are well known for their health effects (De la Ossa et al., 2019). Moreover, as reported from Barbagallo et al. (Barbagallo et al., 2013) water stress, in the sense of lack of water supply, can represent a solution for the production of nutraceuticals. Water stress can be effectively used through the implementation of water-saving irrigation strategies, aiming to enhance the quality and nutritional attributes of vegetables and fruits while concurrently fostering water conservation. This becomes particularly crucial in the cultivation of processing tomatoes in semi-arid environments, where the challenges of the cost and accessibility of irrigation water are significant issues for agricultural practices.

2.9. Micro and Nanotechnology and its application in nutraceutical

To contrast the low oral bioavailability of polyphenols, nanotechnology has been exploited in the field of nutraceuticals. This application of nanotechnologies in the medicine is known as nanomedicine. Nanomedicine, with a primary focus on innovative drug delivery systems, offers advantage in enhancing the delivery of nutraceuticals. The delivery of nutraceuticals through nanosystems aims to achieve two protective mechanisms (Fang & Bhandari, 2010):

- maintaining the active molecular form and protect the active from degradation until consumption
- delivering this form to the physiological target in the organism

Several types of nanosystems are under investigation for the delivery of polyphenols. Nanoparticles (NPs), due to their subcellular size, are able to improve the bioavailability of nutraceutical compounds. Specifically, they prolong the residence time of polyphenols in the gastrointestinal (GI) tract, reduce intestinal clearance mechanisms and increasing the available surface in ordre to facilitate the interaction with the biological target. Moreover, NPs can cross tissues through fine capillaries and are efficiently taken up by cells. This mechanism facilitates the delivery of nutraceutical to target sites in the body (Kawashima, 2001). The main advantages in the use of nanomedicine are: the increase in bioavailability, specific targeting and controlled release. Furthermore, it is possible to state that nanoencapsulation improves bioavailability and increases solubility of poor soluble drugs. All this manages to increase the bioactivity of various nutraceutical compounds (S. Wang et al., 2014). As well as NPs, microparticles (MPs) have gained prominence as widely utilized carriers to enhance the bioavailability and biodistribution of both lipophilic and hydrophilic drugs. Thanks to this feature, it is possible to design and manufacture

MPs with programmable and time-controlled drug release (Lagreca et al., 2020). Furthermore, it is widely reported in the literature that the formation of polymeric complexes can enhance the bioavailability and absorption of drugs. In fact, poorly soluble drugs can be brought into solution, and labile active principles can be protected from oxidation through interaction with complexing polymer agents (J. Chen et al., 2014; Kurkov & Loftsson, 2013).

2.9.1. Polymeric material

Nanosystems are characterized as solid colloidal particles with a diameter between 1 and 1000 nm. They can be classified into nanospheres and nanocapsules. In particular, the nanospheres contain the drug dispersed in the polymeric matrix or adsorbed on their surface. The polymer matrix can be natural or synthetic. The choice of polymer is often oriented towards natural polymers due to their biocompatibility, biodegradability and low toxicity. The ability of polymeric nanoparticles to be internalized by cells and to facilitate the absorption of phenolic compounds is well known (Felice et al., 2012). Moreover, mucoadhesive nanoparticles demonstrate an augmented capacity to enhance the bioavailability of encapsulated drugs compared to the less mucoadhesive nanoparticles (Fabiano et al., 2018). In particular, among polymeric matrices, chitosan, hyaluronic acid and cyclodextrin are regarded as polymers of primary interest.

2.9.3. Cyclodextrin

Cyclodextrins (CDs) represent cyclic oligosaccharides composed of α -D glucopyranoside units, interconnected in a cyclic configuration through $\alpha(1-4)$ glucosidic bonds. This family of compounds encompasses three primary members: α -cyclodextrins, characterized by six glucosidic residues; β -cyclodextrins, composed of seven residues; and γ -cyclodextrins, featuring eight residues (Figure 8). The CDs manifest a structure as a truncated toroidal cone: the internal cavity exhibits hydrophobic properties, while the external surface is rendered hydrophilic by the presence of hydroxyl groups (Szejtli, 1998). Specifically, the secondary hydroxyl groups of glucopyranose (C2 and C3) are situated along the broadest section of the toroidal structure. In contrast, the primary hydroxyls (C6) are positioned around the lower edge, corresponding to the narrower region. The primary hydroxyls exhibit unrestricted rotational flexibility, resulting in a reduction in diameter at the lower periphery. The secondary hydroxyl groups lack this rotational freedom. The hydrophobic cavity of cyclodextrins is formed by CH groups and the hydrogen bonds formed between the H and O of glycoside groups. In particular, the hydroxyl group in position 2 of glucopyranose has the capacity to establish a hydrogen bond with the hydroxyl group in position 3 of the adjacent unit. This intermolecular hydrogen bonding forms the foundation of the inflexible structure observed in cyclodextrins and explain the limited solubility of β -cyclodextrins in water. In the case of α -cyclodextrins, the glucopyranose unit assumes a distorted position, allowing only the formation of four hydrogen bonds. On the other hands, γ -cyclodextrins due to their pliable non-planar structure, are the most water-soluble among cyclodextrins (Loftsson & Brewster, 1996).

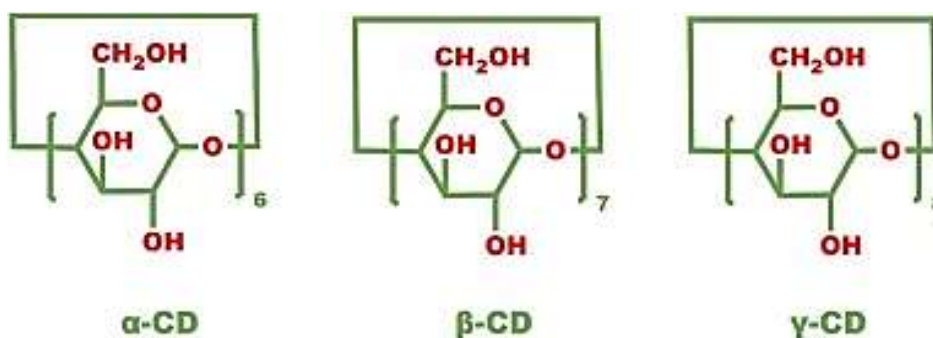


Figure 8. structure of α , β , and γ cyclodextrin (He et al., 2024)

The interaction between cyclodextrins and poorly soluble molecules in aqueous solutions induces various chemical and physical transformations in the guest molecule. In aqueous environments, the hydrophobic cavity of cyclodextrins is initially occupied by water molecules. Due to the hydrophobic nature of the cavity, these water molecules can be readily displaced by other, less polar molecules, forming an inclusion complex. This complex is stabilized through a combination of Van der Waals forces, hydrogen bonds, and electrostatic interactions. The affinity a molecule for the cyclodextrin cavity is in dependence of its own size and the size of the cyclodextrin employed in the process (Kurkov & Loftsson, 2013).

2.9.4. Cyclodextrin derivatives

Natural cyclodextrins are obtained through the enzymatic hydrolysis of starch derived from rice, corn, and potatoes. The enzyme responsible of this reaction is the cyclodextrin glucanotransferases. This is sourced from plants or microorganisms. The β -cyclodextrin is the most widely utilized natural variant due to its well-suited cavity dimensions, able to host drugs with molecular weights falling between 200 and 800 g/mol (Lachowicz et al., 2020). Derived or semi-synthetic cyclodextrins have been crafted to enhance the physicochemical characteristics of their natural counterparts. This enhancement is achieved through the substitution of hydrogen atoms on the hydroxyl groups of each glucose unit. Among the various derived cyclodextrins are reported alkylated cyclodextrins, polymeric cyclodextrins and thiolated cyclodextrins. These modifications offer a strategy to optimizing the properties of cyclodextrins for specific applications (Kurkov & Loftsson, 2013). Thiolated cyclodextrins exhibit the ability to establish disulfide bonds with cysteine-rich subdomains present in mucus glycoproteins. This interaction imparts elevated mucoadhesive properties to thiolated cyclodextrins, underscoring their potential for enhanced adhesion to mucosal surfaces (Grassiri et al., 2022). Numerous studies affirm that β -cyclodextrins (β -CD) represent biocompatible macrocyclic options for formulating diverse composites with enhanced functionalities. The creation of stabilized structures is achievable through the reaction between a cross-linking agent and β -cyclodextrins. The carboxyl and hydroxyl groups present in the cross-linking agents function as "structural bridges," contributing to an augmented solubility of β -CD. This process leads to the development of cross-linked β -CD structures characterized by intricate architectures and targeted functionalities (He et al., 2024).

2.9.5. Hyaluronic acid

Hyaluronic acid (HA), a discovery credited to Karl Meyer and John Palmer in 1934, was initially isolated from the vitreous humor of a bovine eye. This glycosaminoglycan (GAG) is a polymer characterized by lengthy linear chains of disaccharide units alternating with aminosaccharide units (Figure 9). HA is present in various tissues, including joints, skin, the human umbilical cord, as well as connective, epithelial, and nervous tissues. It serves as a fundamental component of the extracellular matrix and is notably found in the bone marrow, articular cartilage, and synovial fluid (Gupta, 2019). HA is structured as a linear polymer with a high molecular weight. HA consists of repetitive disaccharide units of D-glucuronic acid and N-acetyl-D-glucosamine, interconnected by β -1,4 glycosidic bonds (Gupta et al., 2019). Under physiological conditions, the carboxyl groups of D-glucuronic acid become ionized, conferring upon the hyaluronic acid molecule the remarkable ability to coordinate water molecules, resulting in a heightened state of hydration (Harrer et al., 2021). Extensive research has been conducted over the years to explore the applications of HA in the development of pharmaceutical dosage forms, particularly in medicine and cosmetics. In the medical area, these forms have proven to be suitable in treating conditions such as osteoarthritis, an inflammatory condition characterized by progressive cartilaginous degeneration that intensifies with age (Gupta et al., 2019). Additionally, HA finds application in the medical treatment of skin lesions, where its use accelerates the healing process. Ophthalmic surgery benefits from HA in addressing dry eye syndrome and eyelid retraction (Zamani et al., 2008). In the cosmetic area, HA plays a crucial role in combatting age-

related imperfections (Andre, 2004). The introduction of these injections, known as Dermal Fillers, serves as a prominent alternative to cosmetic surgery. Among the diverse Dermal Fillers available, those based on HA are the most widely used. This preference is attributed to HA's excellent tolerability within the body, due to its biodegradability and biocompatibility (Safran et al., 2021).

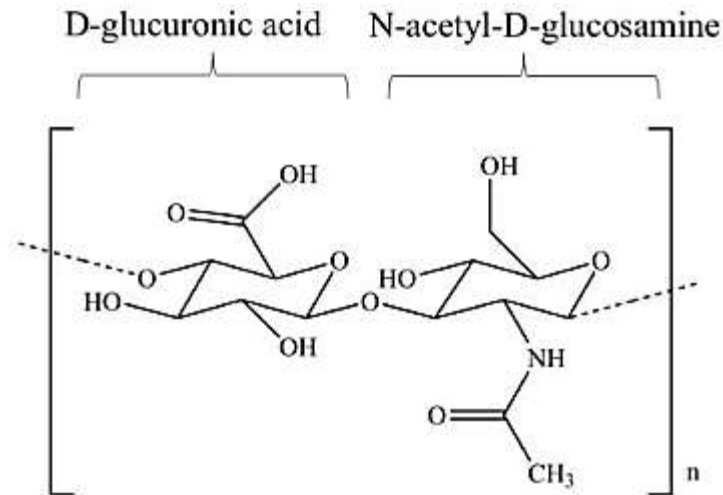


Figure 9. hyaluronic acid structure

2.9.6. Chitosan

Chitosan (Ch) is a cationic polysaccharide composed by D-glucosamine and N-acetyl-D-glucosamine units, intricately connected through β (1-4) glycosidic bonds. Chitosan is obtained from the incomplete deacetylation of chitin, a homopolymer consisting of β (1-4) linked N-acetyl-D-glucosamine (Figure 10). It is possible to collect chitin prevalent by the exoskeletons of crustaceans and mollusks, the cell walls of fungi, and the cuticles of insects. The biological properties of chitosan, including biocompatibility, biodegradability, mucoadhesivity, and non-toxicity, contribute to its versatility. Additionally, chitosan exhibits antimicrobial, antiviral, and immunoadjuvant activities. Chitosan initially exhibits insolubility in water. It is soluble under acidic conditions. Furthermore, the acetylation of extensively deacetylated chitin can yield soluble chitosan. Consequently, chitosan is commercially available in more forms distinguished by variations in molecular weight (MW) and deacetylation degree. Furthermore, the inherent -NH₂ and -OH groups on its repeating units allow for modifications, leading to various derivatives. Chitosan, with its notable capacity to enhance drug penetration across cellular monolayers has emerged as a valuable component in drug delivery systems. Chitosan is suitable in the development of novel therapeutic delivery systems, such as oral administration of nanoparticles, skin administration of microparticles, or for the production of eye drop formulation. Chitosan has an important role in nanomedicine, showing its potential to elevate the efficacy of nutraceuticals and drug delivery systems (Kerch, 2015).

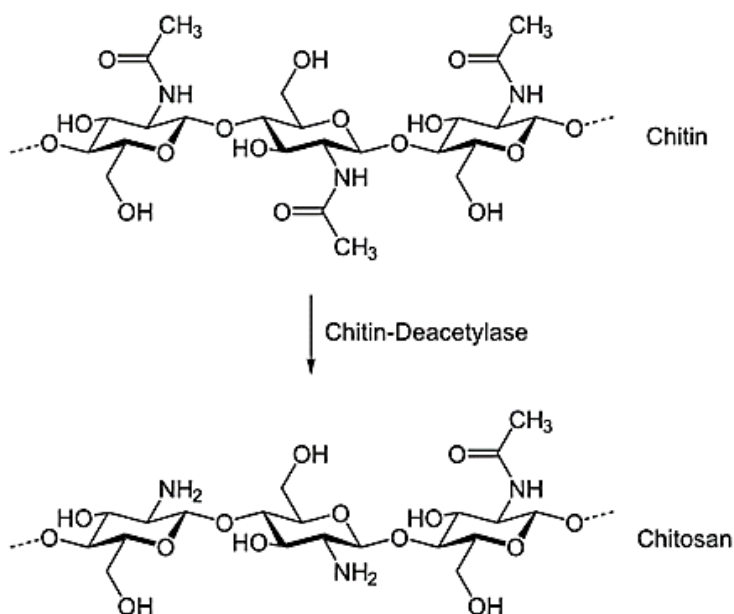


Figure 10. Chemical structures of chitin and chitosan.

2.9.7. Chitosan derivatives

The utilization of chitosan must overcome significant challenges due to its limited mucoadhesive strength and water solubility at neutral and basic pH levels. All these features suggest to explore chemical modifications in order to enhance its applications (M Ways et al., 2018). In its protonated form, chitosan facilitates the paracellular transport of hydrophilic drugs due to the combining bioadhesion and a transient widening of tight junctions in the membrane. The introduction of positive charges to the polymer chain has been studied in order to superate these challenges. N,O-[N,N-diethylaminomethyl(diethyl dimethylene ammonium)_n methyl] chitosan, or quaternary ammonium chitosan (QA-Ch) (Figure 11), is obtained by the reaction of chitosan with 2-diethylaminoethyl chloride (DEAE-Cl) under varied conditions. The resulting quaternary ammonium ions are able to permeabilize the epithelium and enhance polymer mucoadhesion, forming the foundation of the polymer's bioactivity. The augmented adhesive properties of QA-Ch not only extend the contact time with mucosal membranes but also prolong the residence time of vehiculated drugs or small molecules. This prolonged interaction enhances the concentration gradient at the absorption site. Meanwhile, QA-Ch facilitate drug transport, increasing bioavailability, and allowing for a reduction in dosage and administration frequency. In this context, QA-Ch represent as a promising category of mucoadhesive polymers. In particular QA-Ch is a source for the future development of effective and safe non-invasive delivery systems, for example for the delivery of polyphenols. The antioxidant, anti-inflammatory, antidiabetic, and anticancer properties of chitosan and its derivatives, as previously reported (Kerch, 2015) encourage their utilization in the prevention, delay, mitigation, and treatment of various diseases, especially when combined with natural antioxidant molecules.

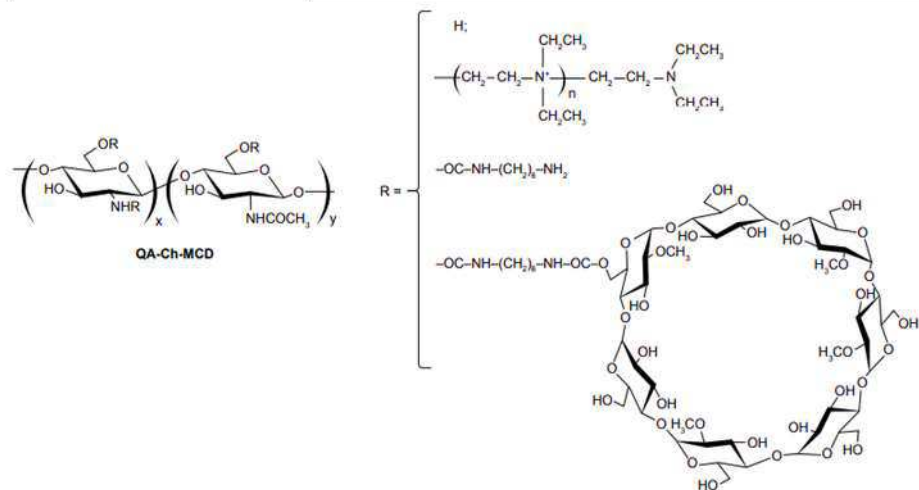


Figure 11. chemical structure of quaternarized chitosan functionalized with methyl- β -cyclodextrin (Zambito et al., 2022).

3. Impact of Peels Extracts from an Italian Ancient Tomato Variety Grown under Drought Stress Conditions on Vascular Related Dysfunction

The tomato (*Solanum lycopersicum* L.) is an edible Mediterranean plant known for its beneficial properties. Epidemiological studies suggest a strong association between tomato consumption and decreased risk of chronic degenerative diseases. Tomatoes are known for their content in carotenoids, lycopene, ascorbic acid, vitamin E and phenol compounds, in particular, flavonoids and hydroxycinnamic acids (Frusciante et al., 2007). Under stressful conditions, an increase in enzymatic or non-enzymatic antioxidant compounds in nature may occur. Water stress can affect fruit diameter and composition, lycopene and total soluble sugar content (Klunklin & Savage, 2017). The aim of the work was to compare the antioxidant properties of a by-product from an ancient Tuscan tomato variety, Rosso di Pitigliano (RED), obtained by growing plants in normal conditions (-Ctr) or in drought stress conditions (-Ds) for their beneficial effects on vascular related dysfunction. RED-Ds tomato peel extract possessed higher total polyphenols content compared to RED-Ctr (361.32 ± 7.204 mg vs. 152.46 ± 1.568 mg GAE/100 g fresh weight (gallic acid equivalent per 100 g fresh weight product)). All extracts were non-cytotoxic. Two hours pre-treatment with the equivalent gallic acid concentration of $5 \mu\text{g/mL}$ from RED-Ctr or RED-Ds showed protection from H_2O_2 -induced oxidative stress and drastically reduced reactive oxygen species (ROS) production raising superoxide dismutase (SOD) and catalase (CAT) activity. The permeation of antioxidant molecules contained in RED-Ctr or RED-Ds across excised rat intestine was high with non-significant difference between the two RED types ($41.9 \pm 9.6\%$ vs. $26.6 \pm 7.8\%$). RED-Ds tomato peel extract represents a good source of bioactive molecules, which protects HUVECs from oxidative stress at low concentration.

3.1. Introduction

The tomato (*Solanum lycopersicum* L.) is an edible Mediterranean plant already known for its beneficial properties. Whether it is fresh or processed, it is one of the most consumed vegetables worldwide (Kavitha et al., 2014) and a key component of the daily meals in many countries. Epidemiological studies have revealed a strong association between tomato consumption and decreased risk of chronic degenerative diseases such as cancer, cardiovascular and neurodegenerative pathologies (Perveen et al., 2015). In virtue of their high consumption, tomatoes and tomato products represent an important source of natural antioxidants, including carotenoids and phenolic compounds that are contained in the human diet (Friedman, 2013). Tomatoes are well known for their content in carotenoids such as lycopene as well as ascorbic acid, vitamin E and phenol compounds, in particular, flavonoids and hydroxycinnamic acids (García-Valverde et al., 2013). Lycopene and β -carotene are the main C40 carotenoids found in tomatoes [13], whilst the chemical class of polyphenols is represented by rutin (quercetin3-O-rutinoside), quercetin, naringenin and chalconaringenin, which are just a few of the various flavonoids found in this fruit, together with organic acids such as benzoic, protocatechuic and cinnamic (Slimestad & Verheul, 2009). Many articles have reported the presence of flavonoids and hydroxycinnamic acids in tomatoes (Jesús Periago et al., 2009). This group of polyphenols includes a variety of chemical structures that act on antioxidant enzymes such as superoxide dismutase (SOD), catalase (CAT) and glutathione peroxidase (GPx), resulting in very efficient peroxy radicals scavenger activity (Pietta, 2000). The above are three key enzymes in the first line defense. They are very fast in neutralizing any potentially oxidative molecules in the cells (Ighodaro & Akinloye, 2018). Tomato plants adapt to different climatic conditions and to abiotic stress, such as the shortage of water which is one of the most serious problems concerning crops (Morales et al., 2015). Unfortunately, tomato plants are highly sensitive to drought stress. The lack or shortage of water is the most common environmental factor that influences plant growth and productivity/yield (Joshi et al., 2016). In the future, water will become a strategic resource and, therefore, industrial and agricultural processes requiring low water consumption must be

developed. Plants have adopted various strategies to cope with water deficiency, including changes in growth and development (Osakabe et al., 2014). In normal conditions, antioxidant defense systems are in a dynamic balance in plant cells, whereas stress conditions may result in an increase in antioxidant compounds that are either enzymatic or non-enzymatic in nature (W.-B. Wang et al., 2009). Water shortage stress can affect the yield of tomato crops, the volume, diameter and composition of the fruits, e.g., lycopene and total soluble sugars content (Sivakumar & Srividhya, 2016). Moreover, what is remarkable is the amount of various kinds of useful waste products, such as peels (about 60%) and seeds (around 40%). During the industrial processing of tomatoes, large quantities of by-products are generated, such as peels, which have high nutritional value (Szabo et al., 2018). Many studies have tested their potential beneficial effects on health (Felice et al., 2020) and optimized the extraction process of carotenoids from tomato skins (Pellicanò et al., 2020). Moreover, it is important to recycle industrial tomato processing waste to reduce the environmental impact of agro-industrial transformation processes. Hydroxycinnamic acids, such as chlorogenic, caffeic, ferulic and p-coumaric, contribute to the antioxidant ability of tomatoes and their derivatives. HUVEC is an excellent model to study a broad array of diseases, including cardiovascular and metabolic diseases (Cao et al., 2017). So several studies have tested antioxidant molecules derived from natural products on HUVEC by *in vitro* experiments related to vascular dysfunction (Felice et al., 2020). The aim of the present study was to compare the antioxidant properties of a by-product from an ancient Tuscan tomato variety, Rosso di Pitigliano, which is obtained by growing plants in normal conditions or in drought stress conditions. To this purpose an *in vitro* model of human endothelial vascular cells, the HUVEC, was used. The Rosso di Pitigliano variety was chosen from nine local Tuscan varieties in virtue of its highest concentration of antioxidants. Furthermore, the extracts were evaluated both *in vitro* and *ex vivo* in order to compare their beneficial effects on vascular related dysfunction following oral intake.

3.2. Material and method

3.2.1. Material

Hexane, acetone, and Folin-Ciocalteu reagent were procured from Sigma-Aldrich (Milan, Italy). H₂O₂ was obtained from Farmac-Zabban S.p.a. (Calderara di Reno, BO, Italy), and gelatin was sourced from Sigma-Aldrich (Milan, Italy). Medium 199 (M199), fetal bovine serum (FBS), penicillin-streptomycin solution, l-glutamine, and HEPES buffer were provided by Hospira S.r.l. (Naples, Italy). The WST-1 assay reagent (4-[3-(4-iodophenyl)-2-(4-nitrophenyl)-2H-5-tetrazolium]-1,3-benzenedisulfonate) was purchased from Roche Applied Science (Mannheim, Germany), while the CM-H2DCFDA reagent (5-(and-6)-chloromethyl-2',7'-dichloro-di-hydro-fluorescein diacetate, acetyl ester) was supplied by Invitrogen (Thermo Fisher Scientific).

3.2.2. Sample preparation

The selected tomato variety, Rosso di Pitigliano (RED), was cultivated by growing plants under both normal and drought stress conditions. For each condition, four plants were utilized, all cultivated in a greenhouse at the Botanical Garden, University of Siena, Italy. First to start the water stress treatment, all plants were adequately irrigated. The start of drought stress commenced when the first fruits began to develop. At the initial point, the plants stood at approximately 120 cm in height. The water stress condition persisted for a duration of 20 days (Landi et al., 2016). Ripe tomatoes (*Solanum lycopersicum* L.) were harvested between August 1 and August 31, 2019, and the fruits were refrigerated at -80 °C in order to arrest their natural biological processes.

3.2.3. Tomato peel extract preparation

The lyophilized tomato peel sample was prepared following the method proposed by Beconcini et al. (Beconcini et al., 2018), with some modifications. Initially, frozen tomatoes were manually

peeled. Then, 2 g of tomato peel was accurately weighed. Subsequently, 6 mL of water was added to the peeled tomatoes. The resulting mixture underwent homogenization (Ultra-Turrax® T25 based IKA, Saint Louis, MS, USA) for approximately 3 minutes, followed by sonication (Elma Transsonic T 460/H, Wetzikon, Switzerland) for 20 minutes to ensure thorough cellular decomposition. After an additional minute of homogenization, the mixture underwent centrifugation for 5 minutes at 13,000 rpm (Eppendorf® 5415D centrifuge, Hamburg, Germany) in order to separate biomolecules from the pellet. The supernatant obtained was then filtered through a 0.45 µm cellulose acetate membrane filter (Sartorius, Göttingen, Germany). The resulting tomato peel extracts were subsequently freeze-dried for 48 hours using a freeze dryer (LIO 5P, Spascal, Italy). The freeze-dried tomato peel extracts were transferred to airtight containers and stored at -20 °C. For subsequent analyses, the freeze-dried tomato peel extracts were appropriately diluted in water.

3.2.4. HPLC characterization

Identification by HPLC methodology was performed to determine antioxidant molecules, lycopene and ascorbic acid as described below.

3.2.5. Antioxidant molecules

Rutin, quercetin, naringenin, and caffeic acid were quantified using High-Performance Liquid Chromatography (HPLC) with a Perkin Elmer Nelson 3200 Series instrument equipped with an RP-C18 column (SUPELCO Kromasil 100A-5u-C18, 4.6 mm × 250 mm). The extraction process followed the methodology proposed by Berni et al. (Berni et al., 2018) One gram of each fruit peel was combined with 1 mL of 70% acetone containing 1% (v/v) HCl and 0.02 mg/mL of TBHQ (tert-Butylhydroquinone). The mixture underwent homogenization using an Ultra-Turrax (IKA®), and 0.2 mL of HCl (1.2 M) was subsequently added. The resulting blend was incubated at 90 °C with continuous stirring for 2 hours. After cooling to room temperature and sonication for 3 minutes, the extract was centrifuged for 5 minutes at 3000 × g and filtered through a 0.45 µm membrane filter. HPLC measurements were conducted following the approach proposed by Kumar et al. (Kumar et al., 2008) with minor adjustments. The mobile phase consisted of two solvents: water (A) and acetonitrile with 0.02% trifluoroacetic acid (TFA) (B). A linear gradient elution was employed: 80% A and 20% B (0–5 min), 60% A and 40% B (5–8 min), 50% A and 50% B (8–12 min), 60% A and 40% B (12–17 min), and 80% A and 20% B (17–21 min). The flow rate was maintained at 1 mL/min, and absorbance readings were set at 365 nm for rutin and quercetin, 325 nm for caffeic acid, and 280 nm for naringenin for 21-minute runtime. For the quantification of rutin, quercetin, naringenin, and caffeic acid were used calibration curves made with standards with a range of concentration between 5 and 80 µg/mL (Sigma Chemical, St. Louis, MI, USA).

3.2.6. Lycopene detection

The extraction of lycopene was performed as reported (Barba et al., 2006). In this method, 0.3 g of tomato peel was combined with 10 mL of hexane/acetone/ethanol (50:25:25 v/v/v) and homogenized using an Ultra-Turrax (IKA®). Subsequently, 1.5 mL of distilled water was added, followed by vortexing. Later, 1 mL of the upper layer was then subjected to vacuum drying, and the resulting dry extract was resuspended in 0.4 mL of a tetrahydrofuran (THF)/acetonitrile (ACN)/methanol (15:30:55 v/v/v) solution. For High-Performance Liquid Chromatography (HPLC) analysis, the mobile phase consisted of methanol/ACN (90:10 v/v) with triethanolamine (TEA) at 9 mM, flowing at a rate of 0.9 mL/min through an RP-C18 column (SUPELCO Kromasil 100A-5u-C18, 4.6 mm × 250 mm). Detection occurred at an absorbance of 475 nm, with a total run time of 20 minutes. Quantification was achieved through a standard calibration curve, with a range of concentrations between 6.25 and 100 µg/mL of lycopene standard (Sigma Chemical, St. Louis, MI, USA).

3.2.7. Ascorbic acid detection

Ascorbic acid extraction was performed as following described. First, 1 g of tomato peel was solved in 2 mL of distilled water, followed by homogenization using an Ultra-Turrax (IKA®) and subsequent filtration through a 0.45 µm membrane filter (Scherer et al., 2012). For High-Performance Liquid Chromatography (HPLC), an RP-C18 column (SUPELCO Kromasil 100A-5u-C18, 4.6 mm × 250 mm) was used. The mobile phase consisted of a 0.01 mol/L KH₂PO₄ buffer solution adjusted to pH 2.6 with o-phosphoric acid, flowing at a rate of 0.5 mL/min, and detection absorbance set at 250 nm. Quantification was achieved through a standard calibration curve with a range of concentration between 6.25 and 100 µg/mL, using an ascorbic acid standard (Sigma Chemical, St. Louis, MI, USA).

3.2.8. FRAP assay

The total antioxidant potential of tomato peel extracts was assessed utilizing the Ferric Reducing antioxidant Power (FRAP) (Benzie & Strain, 1996). This method is based on the reduction of Fe³⁺-2,4,6-Tri(2-pyridyl)-s-triazine (TPTZ) to a blue-colored Fe²⁺-TPTZ complex. The FRAP reagent was freshly prepared and the solution was incubated at 37 °C for one hour. Subsequently, the absorbance was measured at 593 nm using a UV-Vis spectrophotometer (Perkin Elmer, Lambda 25 spectrophotometer, Waltham, MA, USA). FRAP values for the samples, expressed as µmol of Fe²⁺ per g of fresh weight (FW). For this issue a standard curve was developed constructed with ferrous sulfate as the standard.

3.2.9. Total polyphenols content

The Total Phenolic Content (TPC) in tomato peel extracts from fresh fruit was quantified using the Folin-Ciocalteu spectrophotometric method (Singleton et al., 1999). The absorbance was measured at 765 nm. The results were derived from a standard curve constructed with gallic acid (GA) (Sigma-Aldrich) and were reported as milligrams of gallic acid equivalent (GAE) per 100 grams of fresh weight (FW).

3.2.10. Huvec isolation and culture

Human Umbilical Vein Endothelial Cells (HUVEC) were harvested and isolated through enzymatic digestion following the method proposed by Jaffe et al. (Jaffe et al., 1973) The isolated cells were centrifuged, and the resulting cell pellet was plated on gelatin-precoated flasks. After incubating for 24 hours at 37°C, 5% CO₂, in Medium 199 (Life Sciences Grand Island, NY, USA) supplemented with 10% fetal bovine serum (FBS), antibiotics (penicillin-streptomycin), growth factors (heparin, 50 U/mL, and endothelial cell growth factor, 10 mg/mL) (all from Sigma-Aldrich, St. Louis, MO, USA), L-glutamine, and HEPES buffer, the growth medium was replaced to eliminate excess red blood cells.

3.2.11. Cell treatment

The Human Umbilical Vein Endothelial Cells (HUVEC) between passages P2-P4 were subjected to the following protocol (Felice et al., 2020). In brief, the cells were treated for 2 hours and 24 hours with varying concentrations of Total Phenolic Content (TPC) (5, 20, 50, or 100 µg GAE/mL) derived from tomato peel extracts of the RED variety. These extracts were obtained from plants cultivated under normal or drought stress conditions, and the treatments were administered in growth medium containing 5% FBS. Untreated cells served as a positive control. Subsequently, the cells were rinsed with PBS and exposed to 100 µM H₂O₂ for 1 hour to induce oxidative stress, with the concentration and duration chosen according to established guidelines (De la Ossa et al., 2019). Following each treatment, the cells were assessed for viability and reactive oxygen species (ROS) production.

3.2.12. Cell viability assay

Cell viability was evaluated using the WST-1 colorimetric assay following the treatment of HUVEC with either the test samples or H₂O₂ (100 μM). At the conclusion of the treatment period, the cells were incubated with tetrazolium salt (10 μL/well) for 3 hours at 37°C in 5% CO₂. Formazan formation was quantified by measuring absorbance at 450 nm using a multiplatform reader (Thermo Scientific Multiskan FC photometer for microplates, Thermo Fisher Scientific Oy, Vantaa, Finland). Absorbance directly correlated with the number of metabolically active cells, and viability was expressed as a percentage of viable cells (Cesare et al., 2021).

3.2.13. ROS production

The intracellular production of reactive oxygen species (ROS) was evaluated using the fluorescent probe CM-H₂DCFDA, a cell-permeable indicator for these compounds. In accordance with previous protocols (Felice et al., 2020), during the final 15 minutes of treatment with RED-Ctr, RED-Ds, or H₂O₂, Human Umbilical Vein Endothelial Cells (HUVEC) were co-incubated with CM-H₂DCFDA (10 μM/well) dissolved in PBS in the dark at room temperature. The microplate reader (Fluorometer Thermo Scientific Fluoroskan Ascent Microplate) was employed to measure the increase in fluorescence over time, with excitation at 488 nm and emission at 510 nm capturing ROS production.

3.2.14. SOD, CAT and GPx activities

Following pre-treatment with 5 μg GAE/mL of RED-Ctr and RED-Ds for 2 hours or 24 hours with H₂O₂ (100 μM), the cells were detached and later they were lysated. The resulting supernatant was collected, and the enzymatic activities of Catalase (CAT), Superoxide Dismutase (SOD), and Glutathione Peroxidase (GPx) were determined using commercially available kits, provide from Cayman (Cayman Chemical Company, Ann Arbor, Michigan, MI, USA). The measured values were expressed in U/mL for SOD activity and nmol/min/mL for CAT and GPx activity (Cesare et al., 2021).

3.2.15. RED stability studies

RED-Ctr and RED-Ds stability at pH 1.2 was evaluated (Beconcini et al., 2018). A solution of RED-Ctr or RED-Ds was added to simulated gastric fluid pH 1.2 (SGF) warmed at 37 °C in a water bath with continuous stirring. At 30 minutes intervals for a total of 240 minutes, 50 μL samples were withdrawn and subjected to analysis for antioxidant molecule content using the Folin-Ciocalteu method (Singleton et al., 1999).

3.2.16. Study of permeation of antioxidant molecules contained in RED across excised rat intestine

These experiments were conducted following established procedures in previous works (Zambito & Colo, 2010). In summary, the intestinal mucosa was excised from non-fasted male Witstar rats weighing between 250–300 g. All procedures were conducted under veterinary supervision, and the protocols received approval from the scientific-ethical committee of the Italian University and Ministry of University and Research. The intestine was longitudinally cut into strips, cleansed of luminal content, and affixed in Ussing type cells (0.78 cm² exposed surface) without removing the underlying muscle layer. After a 20 minutes equilibration period at 37 °C, RED-Ctr or RED-Ds, at a concentration equivalent to 110 μg GAE/mL in phosphate buffer pH 7.4 (0.13 M), was introduced into the apical chamber. Three milliliters of fresh phosphate buffer pH 7.4 (0.13 M) were placed in the acceptor compartment. Cloxicarb (95% O₂ plus 5% CO₂ mix) was bubbled in both compartments to ensure tissue oxygenation and stirring. The study focused on the apical to basolateral transport of tomato extracts. At 30 minutes intervals, for a total of 150 minutes, 100 μL samples were withdrawn from the acceptor and refilled with fresh pre-thermostated medium. The analysis of antioxidant molecules permeated was conducted by the Folin-Ciocalteu method, as previously described (Felice et al., 2012). The mean cumulative

percentage permeated within a given time frame was calculated to construct each permeation profile.

3.2.17. Statistical analysis

Results are expressed as means \pm standard deviation (SD) derived from a minimum of three independent experiments. The distribution of data was assessed using the one-sample Kolmogorov–Smirnov test, confirming a normal distribution. Group differences were analyzed using one-way ANOVA, followed by post hoc tests such as Turkey’s or Bonferroni’s multiple comparison test. In *ex vivo* experiments, the significance of differences between two values was determined by Student’s t-test. Statistical significance was considered at p-values below 0.05, leading to the rejection of the null hypothesis. The statistical analysis of the data was conducted using GraphPad Prism Software v. 7.0 (GraphPad Software Inc., San Diego, CA, USA).

3.3. Results

3.3.1. Characterization of bioactive compounds

Table 1 displays the antioxidant activity evaluated through the ferric-reducing antioxidant power (FRAP) assay and the total phenolic content (TPC) determined by the Folin-Ciocalteu assay. It is important to note that although the term TPC is used, the Folin-Ciocalteu reagent may react not only with phenolic compounds but also with other extract components possessing reducing characteristics. By the results is possible to note that plants subjected to drought stress conditions exhibited higher TPC compared to those grown in normal conditions. However, no significant difference in antioxidant activity determined by the FRAP assay was observed between the two extracts.

Plant Grow Condition	Antioxidant Activity ($\mu\text{mol Fe}^{2+}/\text{g}$ Fresh Weight) \pm SD	Total Polyphenols Content (mg GAE/100 g Fresh Weight) \pm SD
Ctr	23.885 \pm 0.375	152.46 \pm 1.568
Ds	26.052 \pm 0.556	361.32 \pm 7.204*

Table 1: Rosso di Pitigliano (RED) tomato peel extract characterization. Plants were obtained under normal growth (Ctr) or under drought stress (Ds) conditions. * Significantly different from each other ($p < 0.05$).

Based on the results obtained for the identification of bioactive compounds in tomato peel performed by high-performance liquid chromatography (HPLC) reported in table 2 is possible to state that there is an absence of significant differences between the peel extracts of Rosso di Pitigliano (RED) grown in normal conditions (-Ctr) and those subjected to drought stress (-Ds), except for lycopene. In RED-Ds peel extracts, moderate increases were observed in rutin, caffeic acid, and naringenin compared to RED-Ctr. Quercetin and chlorogenic acid were undetectable. Vitamin C was in the same amount in both extracts

Plant Grow Condition	Lycopene	Vitamin C	Rutin	Caffeic acid	Naringenin	Quercetin
Ctr	171.0 ± 1.4*	30.5 ± 8.81	11.60 ± 0.33	0.83 ± 0.08	1.13 ± 0.08	/
Ds	95.48 ± 6.39	39.6 ± 0	12.59 ± 0.14	1.19 ± 0.08	1.32 ± 0.03	/

Table 2: Bioactive compounds profile of the tomato peel of RED varieties grown in different conditions. Data are expressed in mg/100 g of fresh fruit (FW) ± SD. *Significantly different from each other ($p < 0.05$). Ctr: normal plant growth conditions; Ds: drought stress condition.

3.3.2. Dose and time dependent response of cell viability

Cell viability was assessed using the WST-1 colorimetric assay. HUVECs were treated for 2 hours and 24 hours with varying concentrations of TPC from RED tomato peel extracts (5-20-50-100 µg GAE/ml), obtained from plants grown under normal (Ctr) or drought stress (Ds) conditions. The treatment durations was according established protocols (Felice et al., 2020). The results obtained after 2 hours or 24 hours of treatment (Figure 1a, 1b) indicate the absence of toxicity at all tested concentrations. An enhancement in cell viability was observed after 24 hours of treatment with 5 µg GAE/mL of RED-Ds extracts compared to the control ($p < 0.0001$). This data suggests the protective effect of the extracts, preventing the decrease in cell viability usually observed after 24 hours of culture.

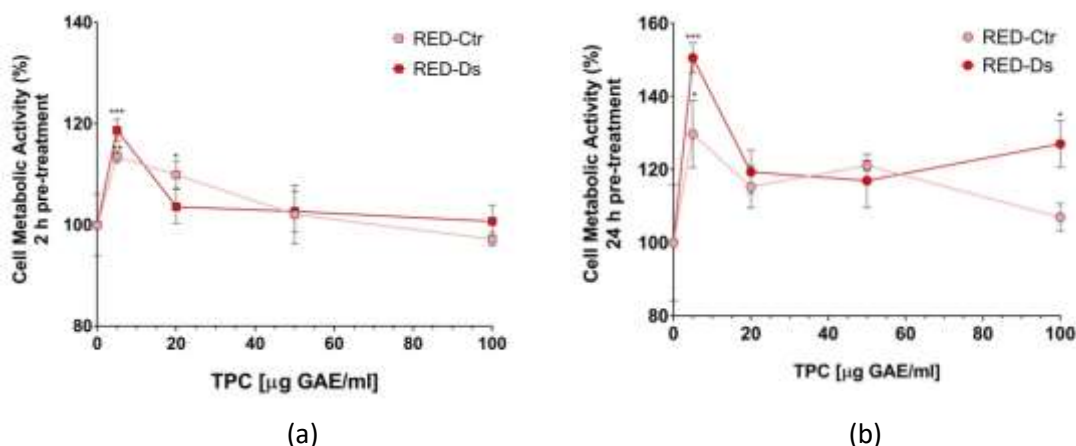


Figure 1. Dose- and time-dependence of cell metabolic activity. HUVECs were cultured 2 h (a) or 24 h (b) with different concentrations of total polyphenols contained (TPC) in Rosso di Pitigliano (RED) tomato peel extracts (5-20-50-100 µg GAE/ml), obtained under normal plant growing conditions (Ctr) or in dehydration conditions (Ds). Data are expressed as % of metabolically active cells on an untreated cell basis (control). Graphical data are represented as mean ± SD of three separate experiments run in triplicate. * $p < 0.05$, ** $p < 0.005$, *** $p < 0.0001$ vs Control (untreated cells).

3.3.3. Protective effect against oxidative stress

The protective impact of tomato peel extracts against oxidative stress was evaluated using an active antioxidant concentration of 5 µg/mL GAE (figure 2a, 2b). Gallic acid (GA) was used as standard at the same concentration served as a positive control. The data revealed that HUVECs treatment with H_2O_2 significantly decreased viable cell numbers, expressed as a percentage of metabolic cell activity relative to untreated cells. No protective effect was observed after 24 hours of pre-treatment, while a protective effect following 2 hours pre-treatment with both RED-Ctr and RED-Ds tomato peel extracts ($p < 0.0005$ and $p < 0.05$ vs. H_2O_2 treated cells, respectively) was observed (Figure). The same concentrations of standard GA exhibited cell protection after 2 hours ($p < 0.005$ vs. H_2O_2) but not after 24 hours of pre-treatment.

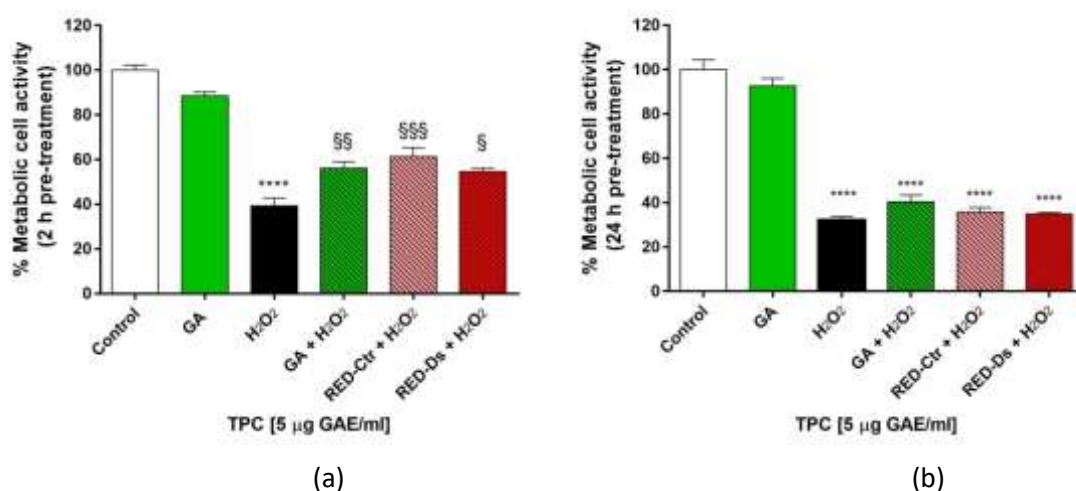


Figure 2. Cell viability after (a) 2 h or (b) 24 h pre-treatment with 5 µg GAE/ml TPC from Rosso di Pitigliano peel extracts or with 5 µg/ml gallic acid (GA) as positive control, and subsequent 1 h treatment with H₂O₂ (100 µM). RED-Ctr: plants grown in normal condition; RED-Ds: plants grown in drought stress condition. **** p < 0.0001 vs Control (untreated cells); § p < 0.05, §§ p < 0.005 and §§§ p < 0.0005 vs H₂O₂.

3.3.4. Reactive oxygen species production

By measure of ROS production was evaluated the antioxidant potential of bioactive molecules in tomato peel, both in the presence and absence of H₂O₂-induced stress on HUVEC (figure 3a, 3b). After a 2 hours or 24 hours of pre-treatment with 5 µg GAE/mL of tomato peel extracts the ROS production in HUVEC was examined. GA was used as standard, serving as a positive control at the same concentration. Treatment of HUVEC with H₂O₂ significantly elevated intracellular ROS production compared to untreated cells (p < 0.0001). As is possible to note in Figure 3a, after 2 hours of pre-incubation, RED-Ds significantly reduced ROS production compared to H₂O₂ treatment alone (p < 0.005). However, the 24-hour pre-treatment with either RED-Ctr or RED-Ds did not prevent the increase in ROS production induced by H₂O₂ (Figure 3b). In particular, 5 µg/mL GA exhibited a protective effect only after 2 hours of pre-treatment.

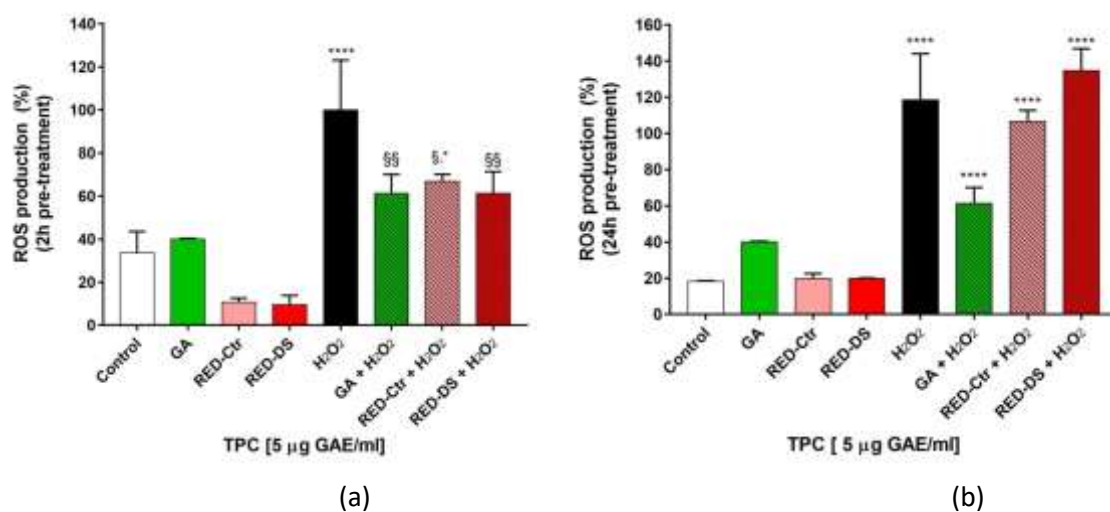


Figure 3: Reactive Oxygen Species (ROS) production in HUVEC pre-treated with 5 µg GAE/mL of total polyphenol content (TPC) of Rosso di Pitigliano peel extracts or with 5 µg/mL gallic acid (GA) as positive control for 2 h (a) and 24 h (b) and with H₂O₂ (100 µM) for 1 h. RED-Ctr: plants

grown in normal condition; RED-Ds: plants grown in drought stress condition. Data are expressed as % ROS production and are representative of three separate experiments run in triplicate. * $p < 0.05$ and **** $p < 0.0001$ vs. Control (untreated cells); § $p < 0.05$, §§ $p < 0.005$ vs. H_2O_2

3.3.5. Antioxidant enzymes activity

The activity of SOD, CAT, and GPx enzymes in HUVEC was assessed in order to evaluate the antioxidant activity by measuring pre-treated for 2 hours (figure 4a) or 24 hours (figure 4b) with $5 \mu\text{g}$ GAE/ml of tomato peel extracts, $5 \mu\text{g}/\text{mL}$ GA as a positive control, and H_2O_2 ($100 \mu\text{M}$) for 1 hour. In Figure 4a and 4b is possible to note that the treatment of HUVEC with H_2O_2 significantly reduced the activity of antioxidant enzymes compared to untreated cells ($p < 0.005$). However, the 2-hour pre-treatment of cells with RED-Ds prevented the negative effect of H_2O_2 by influencing SOD and CAT enzymes. Figure 4b shows no effect of RED-Ds on CAT and GPx activity after 24-hour pre-treatment, while RED-Ctr was observed to affect SOD activity. The GA positive control exhibited a protective effect after either 2 hours or 24 hours of pre-treatment by influencing CAT, SOD, and GPx after 2 hours and SOD after 24 hours of pre-treatment.

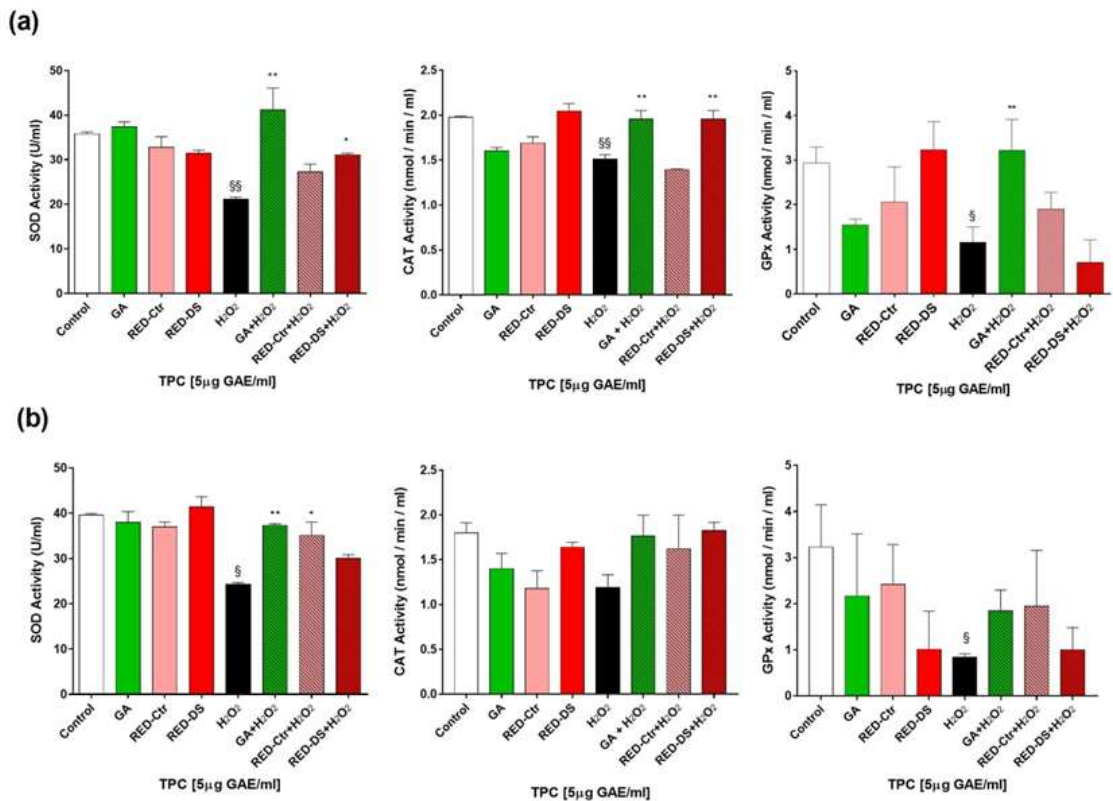


Figure 4. Activity of SOD, CAT and GPx enzymes in HUVEC pre-treated for 2 h (a) and 24 h (b) with $5 \mu\text{g}$ GAE/ml of tomato peel extracts, or with $5 \mu\text{g}/\text{ml}$ gallic acid (GA) as positive control, and with H_2O_2 ($100 \mu\text{M}$) for 1 h. RED-Ctr: plants grown in normal condition; RED-Ds: plants grown in drought stress condition. * $p < 0.05$, ** $p < 0.005$ vs H_2O_2 ; § $p < 0.05$, §§ $p < 0.005$ vs Control.

3.3.6. Studies on permeation of polyphenols contained in RED across excised rat intestine

The excised jejunal rat epithelium was selected as one of the *ex vivo* intestinal models for studying the permeability of antioxidant molecules (Legen et al., 2005). The data of the permeation of antioxidant molecules of both RED-Ctr and RED-Ds across the excised jejunal rat epithelium indicate a non-significant difference in the permeated fraction of antioxidant

molecules between the two extracts under comparison. The mean cumulative permeated fractions are $41.9 \pm 9.6\%$ for RED-Ctr and $26.6 \pm 7.8\%$ for RED-Ds, suggesting that antioxidants from RED-Ctr exhibit greater permeability. Figure 5 illustrates that, over time, the fraction of antioxidant molecules permeated gradually increases up to 150 minutes with RED-Ctr, while RED-Ds reaches a maximum permeation at 120 minutes. These behaviours may be attributed to the variations in the composition of the extracts. It is important to note that the introduction of Clioixcarb into the ussing chambers during the permeation experiment created a strongly oxidizing environment. This condition could potentially lead to the degradation of antioxidant molecules, as previously observed with grape seed extracts (Felice et al., 2012). Notably, a more pronounced oxidation of antioxidants in RED-Ds compared to those in RED-Ctr was observed, indicating a higher antioxidant potential in the RED-Ds extract.

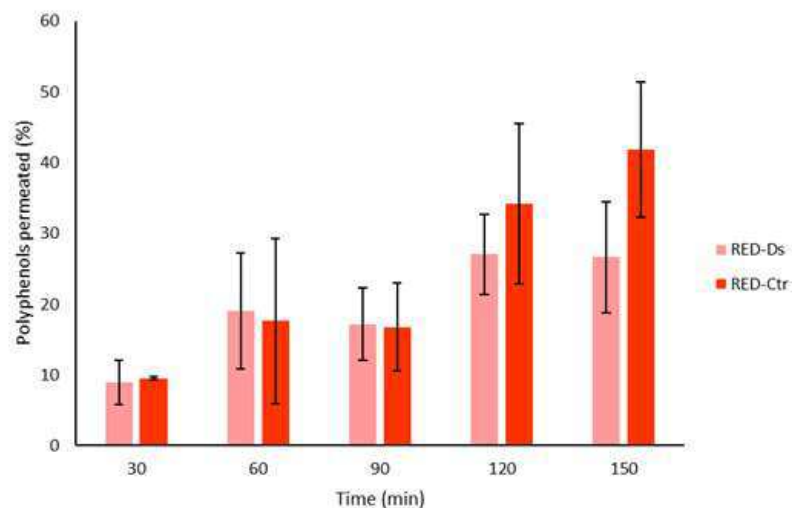


Figure 5. Data on permeation of polyphenols contained in RED-Ctr or RED-Ds in phosphate buffer, pH 7.4 0.13 M, at the equivalent gallic acid concentration (GAE) of $110 \mu\text{g/mL}$ across the excised jejunal rat epithelium (n=4).

3.4. Discussion

The tomato plays a pivotal role in the Mediterranean diet, particularly in semi-arid regions where its cultivation often relies on irrigation to combat drought events linked to climate change (Ighodaro & Akinloye, 2018). An important issue of environmental sustainability is addressing the management of by-products generated during tomato processing. In order to minimize waste and cut down on disposal costs it is possible to reuse these by-products. These by-products contain a diverse of biologically active substances. Through both in vitro and in vivo studies, these substances have exhibited antioxidant, lipid-lowering, and anticarcinogenic properties (Morales et al., 2015). Many of these bioactive compounds are products of secondary plant metabolism, synthesized in response to biotic stresses and normal physiological processes. Drought stress, a significant factor altering plant physiology, triggers the strengthening of the plant's antioxidant defenses (Cao et al., 2017). Important increases in biomolecules, antioxidant activity, and total polyphenols have been consistently observed in studies involving tomato plants subjected to water stress (Beconcini et al., 2018). This study was aimed to compare the antioxidant effects of molecules found in the peels of a variety of Tuscan tomatoes grown under normal conditions with those grown under drought stress conditions. In line with other works (Cao et al., 2017), our results reveal a significantly higher content of phenolic compounds in peel extracts from plants exposed to water stress ($361.32 \text{ mg GAE/100 g FW}$) compared to those grown under normal conditions ($152.46 \text{ mg GAE/100 g FW}$). Additionally, a subtle increase in vitamin C, rutin, caffeic acid, and naringenin was noted in stressed plants. These results indicate that water stress may influence the total polyphenol content of tomato peels, where lycopene

constitutes the primary compound in RED tomatoes' skin. Lycopene, constituting over 80% of the total carotenoid content in fully ripe tomatoes, is the most present antioxidant in tomatoes, and it is responsible for its red color (Huang & Zhu, 2016). Our data indicate a decrease in lycopene levels in plants subjected to drought stress, aligning with other studies (Anderson et al., 2017). The irrigation process appears to significantly impact lycopene biosynthesis (Fрати et al., 2014), with variations may be due to the genotype responsiveness to diverse water conditions. The literature extensively highlights the use of foods and dietary supplements to contrast a large spectrum of health diseases, including cardiovascular diseases (CVD), disorders associated with oxidative stress, allergies, cancer, diabetes, immune system complications, inflammatory obesity, and diabetes, as documented in Parkinson's work (Yoon, 2017). In our investigation, we evaluate the protective impact of Tuscan tomato peel extracts on endothelial cells. Our data indicate that lower concentrations of RED exhibit a significant capacity to decrease the cell viability after 24 hours of treatment when compared to untreated cells. The induction of oxidative stress leads to cell apoptosis, particularly when endogenous antioxidant factors are diminished (Laplante & Sabatini, 2012). Vascular oxidative stress is implicated in the mechanisms underlying vascular dysfunction and plays a pivotal role in various cardiovascular pathologies. Our study reveals that a low concentration of total polyphenols (TPC) and a brief treatment duration with RED-Ds are able to reduce hydrogen peroxide-induced oxidative stress. This results in cytoprotective effects on human umbilical vein endothelial cells (HUVECs), accompanied by a significant reduction in reactive oxygen species (ROS) production compared to untreated cells. The direct antioxidant potential of RED-Ds peel extract aligning with the reported activity of carotenoids against hydrogen peroxide (Mirzoev et al., 2016). Furthermore, our data reveals that RED-Ds antioxidant properties are connected with its influence on the activity of superoxide dismutase (SOD) and catalase (CAT) enzymes. This study demonstrates that the extract derived from plants grown under conditions of water stress, RED-Ds, exhibits antioxidant activity on HUVECs. It is possible to state that RED-Ds could contribute to the prevention of cardiovascular diseases (CVD). The presence of bioactive compounds in Tuscan tomato peel extracts, including carotenoids, vitamins, and polyphenols, can be attributed to their protective effects, which likely interact synergistically (Bell et al., 2016). Numerous studies have demonstrated that the combinations of antioxidants can impact synergistic antioxidant capacity. For instance, the biological activity of lycopene may be augmented in the presence of other active antioxidant compounds such as vitamin C, β -carotene, or vitamin E (Klein, 2015). However, it's important to note that specific concentrations and combinations of antioxidants can also exert antagonistic effects (Bodine et al., 2001). The cellular protective effect observed in tomato peel extracts may be attributed to the optimal concentrations and combinations of antioxidants present in RED-Ds peels. Moreover, by the permeation data of polyphenols in the permeation experiments, it can be possible to affirm that these bioactive molecules reach the target site in sufficient concentrations to execute their protective actions on endothelial cells. In the *in vitro* model, in the cases of RED-Ctr and RED-Ds, it is possible to note a permeation of total polyphenols equivalent to approximately 30% of the applied dose (110 μg GAE/ml) is observed. Experiments on human umbilical vein endothelial cells (HUVEC) have indicated their activity at a concentration as low as 5 μg GAE/ml. Natural extracts have exhibited efficacy against chronic diseases, including cardiovascular diseases (CVD). With the integration of nutraceuticals in the diet is possible to contrast the development of CVD and also serve as defense mechanism against oxidative stress. As observed during the coronavirus (COVID-19) pandemic, a correct diet rich in functional compounds can improve the immune system's capability to prevent and control pathogenic viral infections (Lecker et al., 2004).

4. Olive leaf extracts from three Italian olive cultivars exposed to drought stress differentially protect cells against oxidative stress

Olive leaves are an abundant by-product of olive oil production. Olive leaf extracts (OLEs) are rich in polyphenols, which can be used for health benefits. As polyphenols are the major antioxidant molecules in plants, plants typically increase their polyphenol content when exposed to drought stress. However, the phenolic profile of OLE can vary depending on the origin and variety of the plant material. In this work, olive leaf extracts from three different Italian olive cultivars ('Giarraffa', 'Leccino' and 'Maurino'), exposed or not to drought stress, were studied in terms of antioxidant properties and profile, intestinal permeation, and protection against oxidative stress of HUVECs cells, since HUVECs are considered as a model to study a wide range of diseases. OLE from stressed Maurino and Giarraffa plants showed the highest increase in antioxidant capacity compared to controls. The phenolic profile of 'Maurino' was mainly increased by water deficit, with a large increase in the compounds oleuropein and luteolin-7-O-rutinoside. All tested extracts exposed to water stress protected HUVECs against oxidative stress by reducing ROS production, and this effect was more pronounced in OLE from 'Giarraffa' and 'Maurino' exposed to drought stress compared to all other extracts. Finally, OLE from the stressed group of 'Giarraffa' showed a higher apparent permeability of antioxidant molecules than that of 'Maurino'.

4.1. Introduction

The olive tree (*Olea europaea* L.) is one of the most widespread plants with high nutraceutical properties, in fact more than 8 million hectares of olive trees are cultivated worldwide, 98% of which are in the Mediterranean area (Talhaoui et al., 2015). Every year, the economically and culturally rich production of olive oil generates a large amount of leaves and branches derived from pruning and harvesting. In particular, for every litre of olive oil produced, about 6 kg of leaves are discarded (Avraamides & Fatta, 2008) and, usually, burned or grinded and scattered on fields (Guinda et al., 2015). Numerous reports have described the importance of olive leaves by-products as a rich source of bioactive compounds (Selim et al., 2022). The antioxidant activity of olive leaves extracts (OLEs) is due to the presence of polyphenols (Tarchoune et al., 2019) that makes them an ideal candidate in medical, cosmetic, and pharmaceutical field (Erbay & Icier, 2010). For example, OLE's protective effects against oxidative stress were found in endothelial cells (De la Ossa et al., 2019), in renal cells exposed to cadmium (Ranieri et al., 2019) in bronchial epithelial cells affected by cystic fibrosis (Allegretta et al., 2023). Oleuropein is the most abundant compound in OLE (Ortega-García & Peragón, 2009) and is thought to be primarily responsible for its pharmacological effects. However, OLE contains a wide variety of flavonoids, which are the most abundant group of polyphenols in olive leaves. Therefore, the use of whole extracts may provide greater antioxidant capacity and health benefits than isolated compounds, thanks to the synergistic effects of all the polyphenols present (Borjan et al., 2020). In plants, polyphenols are involved in the tolerance to various abiotic stresses, such as extreme temperatures, drought, flood, light, salt, and heavy metals (Šamec et al., 2021). Thanks to its long term adaptation to the dry conditions of the Mediterranean, the olive tree is considered a woody plant model to study drought stress responses (Diaz-Espejo et al., 2018). Several studies report the accumulation of phenolic compounds in response to drought (cit.). The increase in the content of total polyphenols as a consequence of drought stress contributes to an increase in the antioxidant properties of the extracts (Cesare et al., 2021). However, the phenolic profile of OLE varies depending on the origin and the variety of the plant material (Irakli et al., 2018). The Italian National Register catalogues up to 700 olive cultivars (as defined in D.M. 7521 March 4, 2016). We have previously analysed three Italian olive cultivars under drought stress conditions, selected on the basis of their geographical origin (Parri et al., 2023). The cultivars 'Leccino' and 'Maurino' are thought to be derived from a local oleaster of central Italy (D'Agostino

et al., 2018). The former is cultivated worldwide thanks to its resistance to the bacterium *Xylella fastidiosa* (De Pascali et al., 2019); the latter is mainly distributed in central Italy. 'Giarraffa' is genetically distant from other Italian olive cultivars and was probably introduced from Spain and Morocco (D'Agostino et al., 2018). It is mainly cultivated in Sicily. The cultivars showed different physiological responses to drought. In this work, OLEs from 'Giarraffa', 'Leccino', and 'Maurino', exposed or not to drought stress, were studied in terms of antioxidant properties and profile, protection against oxidative stress of HUVECs cells and intestinal permeation. HUVECs are an excellent model to study a wide range of diseases, such as cardiovascular and metabolic diseases, therefore several studies have evaluated antioxidant molecules from natural products on HUVECs through in vitro experiments related to vascular dysfunction (Medina-Leyte et al., 2020). The aim of this work is to observe whether the phenolic profile induced by drought stress differs from that of controls and whether OLEs derived from cultivars with different drought response provide different ROS protection in human cells. The result could convert an agri-by-product into a high value nutraceutical compound.

4.2. Materials and method

4.2.1. Materials

Olive leaf extracts of the Giarraffa (OLE-G), Leccino (OLE-L) and Maurino (OLE-M) varieties and the extracts obtained from the same cultivars subjected to water stress (OLE-GS, OLE-LS, OLE-MS) were collected at Life Sciences Department of the University of Siena, Siena (SI), Italy. The Human umbilical vein endothelial cells (HUVEC) were purchased from Lonza (Basel, Switzerland). MCDB 131 Medium was purchased from Gibco-Thermo Fischer (Waltham, Massachusetts, USA). Fetal Bovine Serum (FBS), L- Glutamine and heparin sodium salt from porcine intestinal mucosa were purchased from Sigma-Aldrich (Darmstadt, Germany). Human FGF-basic and Human EGF (Animal Free) were purchased from Peprotech (Waltham, Massachusetts, USA). Cell proliferation reagent (WST-1) was provided by Roche diagnostic (Mannheim, Germany). The fluorescent probe 2,7-dichloro-di-hydro-fluorescein diacetate, acetyl ester (CM-H2DCFDA) was provided by Invitrogen (Carlsbad, CA, USA). Gallic acid (GA), ferrous chloride, and Folin-Ciocalteu reagent were purchased from Merck (Darmstadt, Germany).

4.2.2. Leaves Sampling and Stress Condition

Leaves were collected from certified 18-month-old olive trees (*Olea europaea* L., cultivars Leccino, Maurino and Giarraffa) provided by "Spoolivi" (Società Pesciatina di Orticoltura, Pescaia, PT, Italy). Growing conditions and drought treatments of the plants have already been described in detail by (Parri et al., 2023). Briefly, for each cultivar, 10 plants were completely water deprived for 4 weeks (OLE-GS, OLE-LS, OLE-MS for 'Giarraffa', 'Leccino', and 'Maurino' stress groups) and 10 plants were fully watered (OLE-G, OLE-L, OLE-M for 'Giarraffa', 'Leccino', and 'Maurino' control groups). For each experimental group, a pool of about 40 leaves was sampled at t0, t1, t2, t3 and t4, corresponding to the start of withholding irrigation and the first, second, third and fourth weeks of water deprivation, respectively. Leaves were collected, immediately frozen at -80°C, and used for the following analysis.

4.2.3. Determination of the Antioxidant Capacity and Polyphenols Content

The extracts were prepared following the procedure described by Fabiano et al. (Fabiano et al., 2021) slightly modified. In detail, frozen leaves (1 g) were ground in liquid nitrogen and the powder resuspended in 3 mL of 70% acetone. Samples were homogenised with Ultra-Turrax T-25 basic (IKA®-Werke GmbH & Co. KG, Staufen im Breisgau, Germany) for 3 min and sonicated with an ultrasonic bath (Transsonic T 460/H Elma, Singen, Germany) for 20 min. The homogenate was centrifuged at 4000 × g for 5 min at 4 °C. Part of the supernatants containing the antioxidant extracts were used for FRAP analysis and Folin-Ciocalteu method. Part of the supernatants was filtered through a 0.45 µm cellulose acetate membrane filter (Sartorius, Göttingen, Germany),

frozen, and freeze-dried 48 h (freeze dryer LIO 5P, Spascal, Italy). The lyophilized olive leaves were used for the Cell Viability Test by WST-1 Assay, ROS production analysis, and permeation of antioxidants contained in OLE across the excised rat intestine.

4.2.4. Ferric Ion Reducing Antioxidant Power (FRAP)

FRAP method was carried out to determine the antioxidant capacity (Benzie & Strain, 1996). For each reaction, 20 μL of extract was mixed with 2040 μL of 300 mM acetate buffer pH 3.6, 200 μL of 10 mM TPTZ (2,4,6-tripyridyl-s-triazine), and 200 μL of 20 mM FeCl_3 . After 1 h-incubation at 37°C, the absorbance of samples was measured using a UV-Vis spectrophotometer (wavelength set at 563 nm). The absorbance values were interpolated on a standard curve using known ferrous sulfate solutions. The antioxidant power of each group was expressed in mmol of ferrous chloride equivalent per 100 g of matter. For each time point, results are expressed as an average of six replicas \pm the standard deviation.

4.2.5. Folin-Ciocalteu Method

The total polyphenols content was determined by the Folin-Ciocalteu colorimetric assay (Singleton & Rossi, 1965). For each reaction, 500 μL of extract was mixed with 3950 μL of distilled water, 250 μL of Folin-Ciocalteu reagent, and 750 μL of a sodium carbonate saturated solution (Na_2CO_3) for each reaction. After a 30-minute incubation at 37 °C, the absorbance of each sample was measured at 795 nm using a UV-Vis spectrophotometer. The absorbance value was interpolated using a standard curve of a known gallic acid solution. Total phenolic content was measured in milligrams of gallic acid equivalents (GAE) per 100 g of matter. For each time point, results are expressed as an average of six replicas \pm the standard deviation.

4.2.6. Leaf Metabolite Extraction and Ultra-High-Performance Liquid Chromatography-Mass Spectrometry

Only the leaves sampled at t4 were used for this extraction. Approximately 4 g of frozen olive leaves were dried for 7 days at 40°C. The leaves were then grinded in a small mill and the powder used for metabolites extraction. Two extraction cycles were performed with methanol (1:10, w:v). The dry methanolic extract obtained was weighted, and 50 mg were collected and dissolved in 1 mL of methanol PA. Samples with a concentration of 10 mg/mL were filtered (0.2 mL nylon membrane from Whatman, Medstone, UK) and injected in the ultra-high performance liquid chromatography–mass spectrometry (UHPLC–MS) (Thermo Scientific Ultimate 3000RSLC Dionex, Waltham, MA, USA). The chromatography analysis was performed according to the described at Dias et al. (Dias et al., 2019). The UHPLC–MS was equipped with a Dionex UltiMate 3000 RS diode array detector with a mass spectrometer, and a Thermo Scientific Hypersil GOLD column (particle size of 1.9 μm and temperature of 30°C). The mobile phase contained a degassed and filtered acetonitrile and 0.1% formic acid (v/v) with a flow rate of 0.2 mL min⁻¹. In the first 14 min, the solvent gradient was 5% acetonitrile, followed by 40% formic acid (2 min), 100% formic acid (7 min), and 5% formic acid (the last 10 min). Four microL of the sample were injected into the UHPLC–MS equipment. The UV–vis spectral data were collected (250 and 500 nm) and the chromatograms recorded for 280 nm. The mass spectrometer (LTQ XL Linear Ion Trap 2D) contained an orthogonal electrospray ion source (ESI) and operated in negative-ion mode with an electrospray ionization source of 5.00 kV (ESI capillarity temperature of 275 C) covering a mass range of 50.00 - 2000.00 m/z. The collision-induced dissociation MS/MS and MSn experiments were acquired for precursor ions. The retention times, UV-vis spectra, and spectral data obtained were then compared with those of standard compounds to identify the phenolic compounds. A semi-quantitative analysis was done by peak integration through the standard external method, using the closest standard compound. The detection and quantification limits were performed through calibration curves performed with reference compounds (quercetin for flavonoids and oleuropein for secoiridoids). Calibration curves were obtained by injection of different concentrations of quercetin ($y = 4\text{E}+06x - 390882$ and $R^2 =$

0.99) and oleuropein ($y = 1E+06x - 6948$ and $R^2 = 0.98$) using the same conditions used for the sample analysis. The results are expressed in mg of the compound / g of leaf DW and presented as the mean \pm standard deviation of 3 independent analyses per sampling time and treatment.

4.2.7. Cell Viability Test by WST-1 Assay

The viability of HUVEC was assessed by the WST-1 assay. For this purpose, 2×10^4 cells per well were seeded in 96-well plates and placed in an incubator for 24h at 37 °C and 5% CO₂. Fifteen hours after seeding the cells were incubated for 4 hours with the OLEs at concentrations in the 1-50 $\mu\text{g}/\text{mL}$ range. The samples to be tested were dissolved in fresh medium and filtered through 0.45 μm cellulose acetate filter prior contact with the cells. Following the 4-hour treatment the cells were washed with fresh medium to completely remove any residual extract, then incubated at 37°C for 2h with WST-1 diluted 1:10. The amount of formazan produced was evaluated at 450 nm. After washing, some of the cells were subjected to oxidative stress by incubating them for 1 hour with 500 μM H₂O₂. In this case the WST-1 reagent was added after completely removing H₂O₂ from the wells through a suitable washing.

4.2.8. ROS production

ROS production was evaluated as previously described (Felice et al., 2020). HUVECs during the last 30 minutes of treatment with OLEs or H₂O₂ were incubated with the fluorescent probe 2,7-dichloro-di-hydro-fluorescein diacetate, acetyl ester (CM-H2DCFDA) dissolved in PBS at a concentration of 10 $\mu\text{M}/\text{well}$ in the dark at room temperature. At the end of the experiment, ROS production was detected measuring the increase in fluorescence at excitation of 488 nm and emission of 510 nm.

4.2.9. Permeation of antioxidants contained in OLE across excised rat intestine

A well-known procedure (Zambito & Colo, 2010) (Zambito et al., 2009) was carried out. Briefly, the intestinal mucosa was excised from non-fasted male Wistar rats weighing 250-300 g. All experiments were performed under veterinary supervision and the protocols were approved by the scientific-ethical committee of the Italian University and the Ministry of University and Research. The intestine was cut longitudinally into strips, rinsed free of luminal contents and mounted in Ussing type cells (0.78 cm² exposed surface) without removing the underlying muscle layer. After 20 minutes of equilibration at 37°C, OLE-G, OLE-GS, OLE-M, or OLE-MS dispersed in phosphate buffer pH 7.4 (0.13 M) was added to the apical chamber. The experiment was performed with OLEs at the same extract concentration of 3 mg/mL and the same GAE content of 0.16 mg/mL. Three mL of fresh phosphate buffer pH 7.4 (0.13 M) was added to the acceptor chamber. Clioxcarb (95% O₂ plus 5% CO₂ mix) was bubbled in both compartments to ensure oxygenation of tissue, and stirring. The apical to basolateral transport of OLEs was studied. At 30 min intervals of a total of 150 min, 1 mL sample was withdrawn from the acceptor and replaced with fresh pre-thermostated medium. The amount of antioxidant molecules permeated was determined by analysing the samples by the Folin-Ciocalteu method.

4.2.10. Statistical analysis

All data are expressed as mean \pm standard deviation (SD). Six independent replicates were performed for each experiment. Data were tested for normality of distribution using the Shapiro-Wilk test. Significant differences between the extracts analysed were determined by one-way ANOVA. When ANOVA showed $p \leq 0.05$, a post-hoc test (Bonferroni correction) was performed. $p \leq 0.05$ was considered to indicate a significant difference.

4.3. Results

4.3.1. Antioxidant Capacity and Polyphenols Content

Figure 1 shows the antioxidant capacity of leaves collected at different time points. After two weeks of stress, the first difference between OLE-G and OLE-GS appeared (Figure 1). However, as the drought stress progressed, the antioxidant capacity increased in all cultivars: OLE-GS, OLE-LS and OLE-MS were significantly different from their respective controls at t4. At this time point, OLE-GS and OLE-MS showed a higher antioxidant value (22.6 mmol Fe²⁺ 100 g⁻¹ and 21.3 mmol Fe²⁺ 100 g⁻¹, respectively) compared to OLE-LS (12.2 mmol Fe²⁺ 100 g⁻¹).

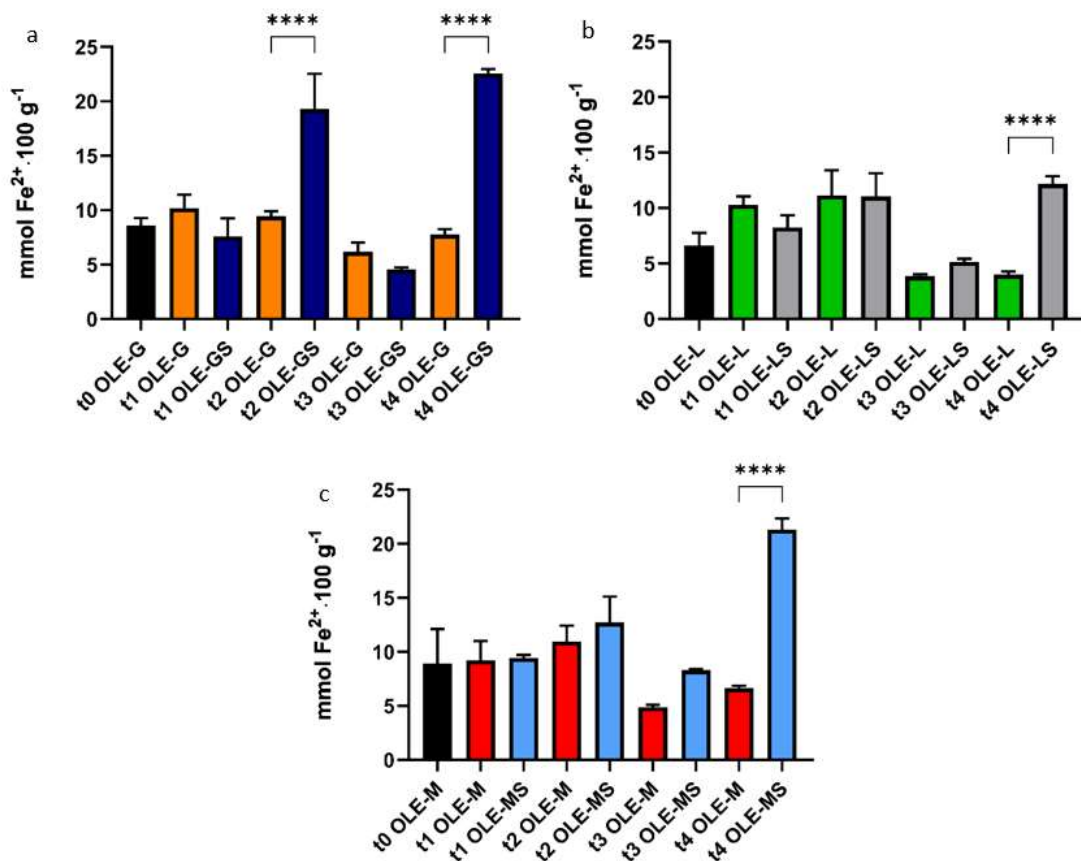


Figure 1. Antioxidant Capacity of (a) OLE-G and OLE-GS; (b) OLE-L and OLE-LS; (c) OLE-M and OLE-MS, from t0 to t4. Asterisks indicate a statistically significant difference (****: $p < 0.001$) between the stressed group and its respective control. In each panel, unstressed and stressed samples are indicated by different colours, regardless of the time of analysis.

The polyphenol content of each group during the experimental period is shown in Figure 2. The polyphenol content increased after four weeks of drought stress, when all the stressed groups differed significantly from their respective control. As shown in figure 2, the polyphenol content in OLE-GS already increased at t2 (39.4 mg GAE 100 g⁻¹), but the highest value was reached at t4 (52.2 mg GAE 100 g⁻¹). Despite the different antioxidant capacities, the polyphenol content in OLE-GS, OLE-LS, and OLE-MS were very similar at t4 (51.3, 49.9, 50.3 mg GAE 100 g⁻¹, respectively).

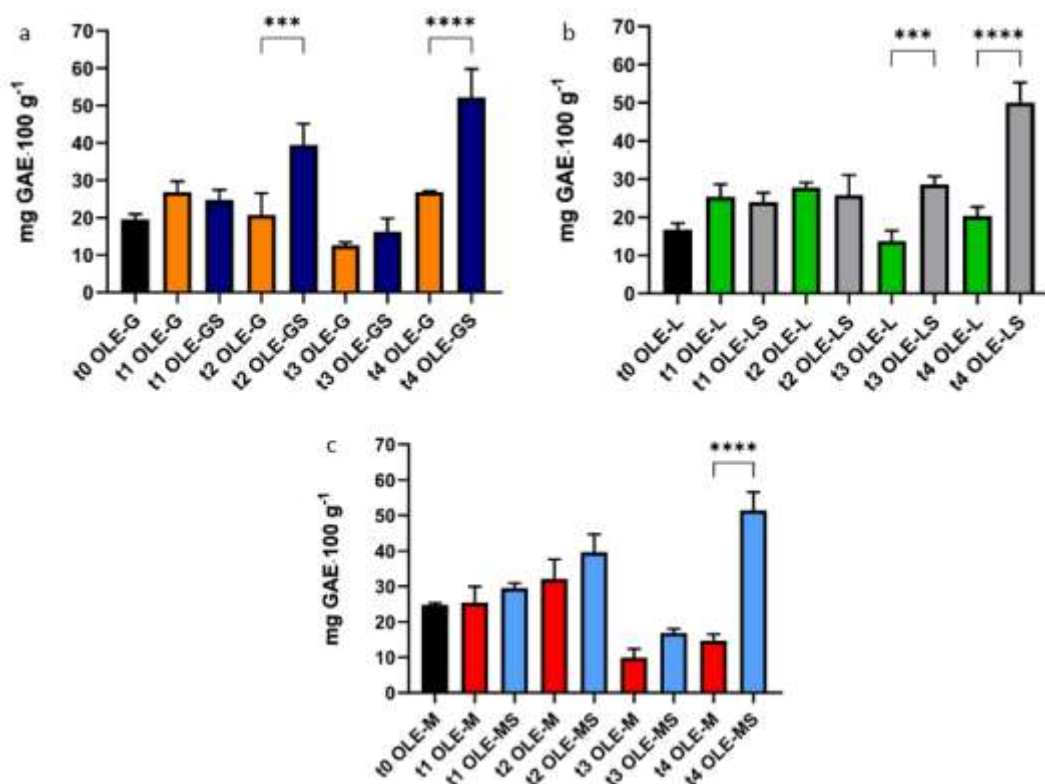


Figure 2. Polyphenols content of (a) OLE-G and OLE-GS; (b) OLE-L and OLE-LS; (c) OLE-M and OLE-MS, from t0 to t4. Asterisks indicate a statistically significant difference (****: $p < 0.001$; *** $p < 0.001$) between the stressed group and its respective control.

The strongest response, both in terms of antioxidant capacity and polyphenol content, was observed after four weeks of stress. Therefore, for all cultivars, leaves collected at t4 were selected for UHPLC characterization and analysis on human cells.

4.3.2. UHPLC phenolic characterisation

In total, sixteen compounds were quantified: three secoiridoids and thirteen flavonoids. There were some differences between the extracts. In OLE-L, only one secoiridoid (aldehyde form of decarboxyl elenolic acid) could be detected, whereas the flavonoids chrysoeriol-7-O-glucoside and luteolin-7-O-glucoside could not be detected in either OLE-L or OLE-LS. In the same retention time (12.1 min), the extracts from 'Giarrappa' contained luteolin-7 associated with rutinoside instead of glucoside, as occurred in the extracts from 'Leccino' and 'Maurino'. The total amount of phenolic compounds is higher in OLE-LS (46.1 mg/g DW) and OLE-MS (79.1 mg/g DW) compared to their respective controls (40.7 mg/g DW in OLE-L and 39.9 mg/g in OLE-M). In OLE-LS the increase is mostly due to the higher amount of detected secoiridoids (10.0 mg/g DW) compared to OLE-L (4.3 mg/g DW). OLE-MS showed a higher detected amount of both secoiridoids (27.7 mg/g DW) and flavonoids (51.4 mg/g DW) compared to OLE-M (3.2 mg/g DW and 36.7 mg/g DW, respectively). Conversely, OLE-GS showed a decrease in the total amount of phenolic compounds detected (29.4 mg/g DW) compared to OLE-G (33.2 mg/g DW) due to a lower amount of flavonoids detected (30.4 mg/g DW in OLE-G, 26.7 mg/g DW in OLE-GS). The extracts from OLE-MS presented the highest ($p < 0.05$) amounts of oleuropein and oleuropein aglicone, dihydroquercetin, luteolin-7-O-rutinoside and chrysoeriol-7-O-glucoside, and OLE-M the highest ($p < 0.05$) level of diosmetin (Table). In turn, OLE-L showed the highest ($p < 0.05$) content of aldehyde form of decarboxyl elenolic acid, and OLE-LS the highest ($p < 0.05$) levels of apigenin-O-dideoxyhexoside-hexoside, apigenin-7-O-rutinoside and luteolin-7-O-glucoside (Table 1).

Rt (min.)	Compound	[M-H] -(m/z)	MS ² (m/z) Fragments	OLE-G	OLE-GS	OLE-L	OLE-LS	OLE-M	OLE-MS
Secoiridoids									
10.3	Oleuropein aglicone	377	197/153	1.140 ± 0.109 ^b	0.596 ± 0.025 ^d	nd	1.244 ± 0.022 ^b	0.875 ± 0.024 ^c	1.797 ± 0.005 ^a
10.8	Aldehydic form of decarboxyl elenolic acid	215	197/153/ 171/ 185	0.475 ± 0.118 ^b	0.752 ± 0.076 ^b	4.314 ± 0.681 ^a	0.708 ± 0.033 ^b	0.653 ± 0.184 ^b	0.973 ± 0.014 ^b
14.4	Oleuropein Flavonoids	539	377/307/275	1.228 ± 0.276 ^c	1.377 ± 0.106 ^c	nd	8.095 ± 0.494 ^b	1.661 ± 0.845 ^c	24.897 ± 1.353 ^a
11.9	Dihydroquercetin	303	285/177/ 125	2.506 ± 0.145 ^c	2.722 ± 0.032 ^c	2.655 ± 0.014 ^c	2.391 ± 0.204 ^c	3.430 ± 0.048 ^b	5.279 ± 0.089 ^a
12.1	Luteolin-7- <i>O</i> -rutinoside	593	447/285	nd	nd	2.584 ± 0.015 ^d	4.261 ± 0.167 ^b	3.008 ± 0.046 ^c	10.366 ± 0.125 ^a
12.1	Luteolin-7- <i>O</i> -glucoside is.1	447	287/285	2.029 ± 0.070	2.305 ± 0.171	nd	nd	nd	nd
12.4	Apigenin - <i>O</i> - dideoxyhexoside-hexoxide	449	269	1.826 ± 0.023 ^d	1.726 ± 0.016 ^d	2.628 ± 0.015 ^b	2.992 ± 0.015 ^a	2.250 ± 0.025 ^c	2.479 ± 0.174 ^b
12.8	Apigenin-7- <i>O</i> -rutinoside is.1	577	269	3.471 ± 0.125 ^c	2.350 ± 0.050 ^e	4.797 ± 0.090 ^b	5.364 ± 0.071 ^a	2.688 ± 0.023 ^d	3.621 ± 0.047 ^c
13.0	Apigenin-7- <i>O</i> -rutinoside is.2	577	269	2.485 ± 0.102 ^c	2.099 ± 0.107 ^d	2.849 ± 0.036 ^b	3.296 ± 0.199 ^a	2.283 ± 0.041 ^c	2.979 ± 0.037 ^b
13.3	Luteolin-7- <i>O</i> -glucoside is.2	447	285	3.737 ± 0.163 ^{bc}	3.035 ± 0.462 ^{bc}	2.762 ± 0.233 ^c	6.135 ± 0.250 ^a	4.039 ± 0.139 ^b	7.161 ± 0.638 ^a
13.5	Chrysoeriol-7- <i>O</i> -glucoside	461	299/446	2.198 ± 0.099 ^c	1.669 ± 0.007 ^d	nd	nd	2.840 ± 0.112 ^b	4.111 ± 0.127 ^a
13.9	Luteolin-7- <i>O</i> -glucoside is.3	447	285	2.215 ± 0.145 ^b	1.741 ± 0.063 ^c	nd	nd	2.506 ± 0.173 ^{ab}	2.878 ± 0.187 ^a
15.7	Luteolin	285	285	2.668 ± 0.018 ^c	3.098 ± 0.290 ^c	7.160 ± 0.197 ^a	3.109 ± 0.014 ^c	4.905 ± 0.119 ^b	4.546 ± 0.200 ^b
16.7	Apigenin-7- <i>O</i> -rutinoside	577	269	2.000 ± 0.004 ^c	1.651 ± 0.078 ^d	2.086 ± 0.034 ^c	2.262 ± 0.019 ^b	2.339 ± 0.073 ^b	2.619 ± 0.046 ^a
17.4	Apigenin	269	269/225	2.612 ± 0.041 ^d	2.010 ± 0.077 ^e	5.982 ± 0.089 ^a	3.956 ± 0.042 ^b	2.884 ± 0.012 ^c	2.701 ± 0.010 ^d
17.8	Diosmetin	299	284	2.637 ± 0.028 ^c	2.283 ± 0.049 ^d	2.877 ± 0.020 ^b	2.277 ± 0.005 ^d	3.537 ± 0.047 ^a	2.674 ± 0.014 ^c

Table 1. Phenolic profile (mg/g DW) of OLE-G, OLE-GS, OLE-L, OLE-LS, OLE-M, and OLE-MS extracts. Values are mean ± standard deviation (n = 3–4). Rt—retention time; Nd—not detected; is. —isomer. For each compound, different letters denote significant difference (p < 0.05) between the values.

Figure 3 shows the heat map of the fold changes of the phenolic metabolites extracted from the three cultivars. In cultivar Giarraffa, drought stress caused, in general, a decrease of the phenolic content of OLE-GS/OLE-G, with the exception of the secoiridoids aldehyde form of decarboxyl elenolic acid and oleuropein and the flavonoids dihydroquercetin, luteolin-7-O-glucoside is.1 and luteolin, which slightly increased. In contrast, a more heterogeneous response profile was observed in OLE-LS/OLE-L, with a similar number of compounds increased and decreased by drought stress. The phenolic pool of 'Maurino' was mostly increased by water deficit, with a large increase of oleuropein and luteolin-7-O-rutinoside.

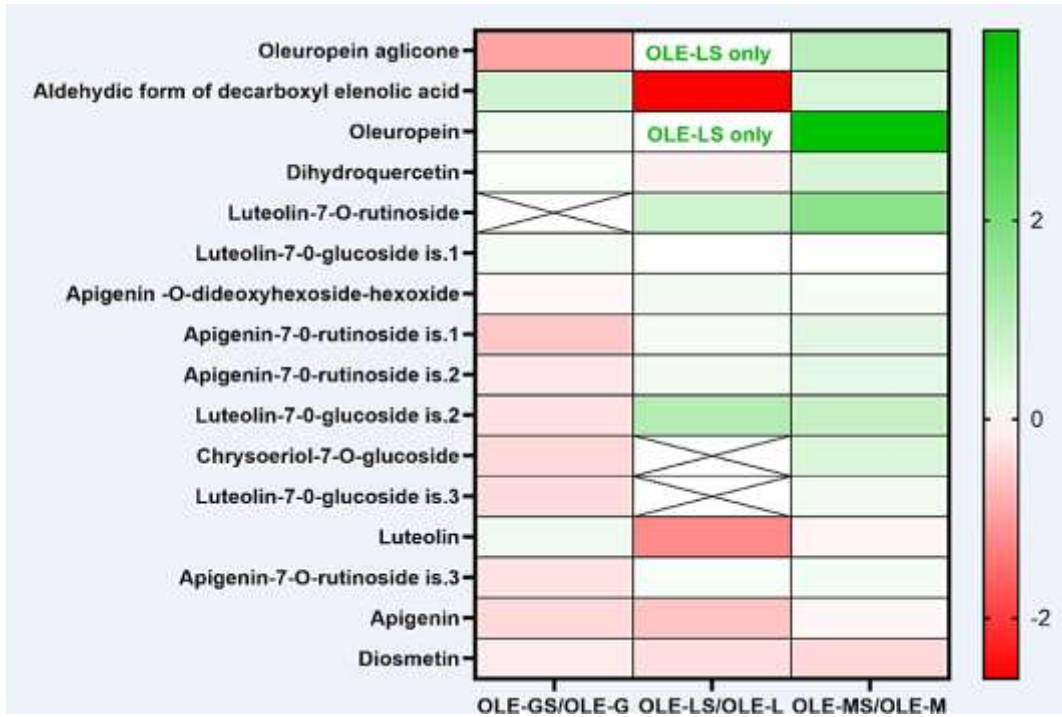


Figure 3. Heat map of the fold changes (\log_2 (stressed/control)) in phenolic metabolites of Giarraffa (OLE-GS/OLE-G), Leccino (OLE-LS/OLE-L), and Maurino (OLE-MS/OLE-M).

4.3.3. Cell Viability Test

Figure shows the viability of HUVEC treated with increasing concentrations of OLE-G and OLE-GS (Figure 4a), OLE-L and OLE-LS (Figure 4b) and OLE-M and OLE-MS (Figure 4c). The data appearing in Figure 4a show that OLE-G and OLE-GS are cytotoxic at concentrations above 10 $\mu\text{g}/\text{mL}$. Figures 4b and 4c show that the olive leaf extracts of the Leccino and Maurino varieties have a low cytotoxicity at any of the concentrations tested. Therefore, the concentration of 10 $\mu\text{g}/\text{mL}$ was chosen to carry out the subsequent experiments.

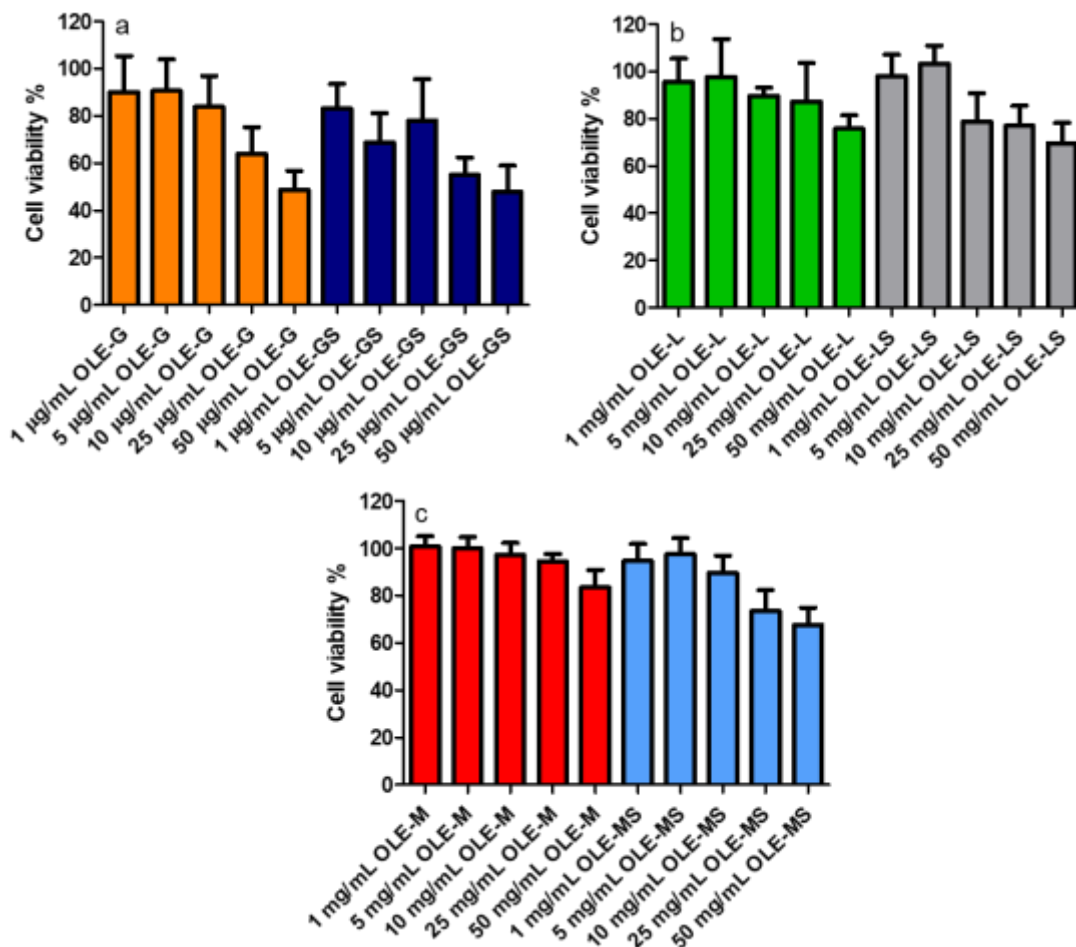


Figure 4. HUVEC viability after 4 h of incubation with: (a) OLE-G and OLE-GS; (b) OLE-L and OLE-LS; (c) OLE-M and OLE-MS in culture medium. Data are expressed as % viable cells referred to 100% control (untreated cells). Data are reported as mean \pm SD (n = 6).

4.3.4. OLEs protective effect from oxidative stress

With this test the influence of the treatment with OLEs on the viability of HUVECs after oxidative stress induced by H_2O_2 was evaluated. The OLEs were obtained from plants either subjected or not to water stress. Figure 5 shows data on the protection of HUVECs from oxidative damage after 2 hours of pretreatment with OLEs at a non-toxic concentration of 10 μ g/mL, and subsequent treatment with 500 μ M H_2O_2 for 1 hour. The data show that oxidative stress significantly reduced the number of viable cells compared to Control (cells with medium only). Pretreatment of HUVECs with all the extracts under study at a concentration of 10 μ g/mL reduced H_2O_2 cytotoxicity significantly. Apparently, the extracts from the Giarraffa and Maurino varieties subjected to water stress (OLE-GS and OLE-MS) are significantly more effective than the corresponding extracts from olive trees not subjected to water stress (OLE-G and OLE-M).

Figure 6 shows data on the protection of HUVECs from oxidative damage after 2 hours of pre-treatment with OLEs and gallic acid (GA) at the same polyphenol concentration of 0.5 μ g/mL, and subsequent treatment with 500 μ M of H_2O_2 for 1 hour. Also in this case, oxidative stress significantly reduced the number of viable cells compared to the control (cells with medium). HUVEC cells pre-treatment with all extracts at a concentration of 0.5 μ g/mL of GAE showed a significant protective activity against the H_2O_2 oxidative damage, compared to GA pre-treatment. However, there are no statistical differences between the various OLEs tested.

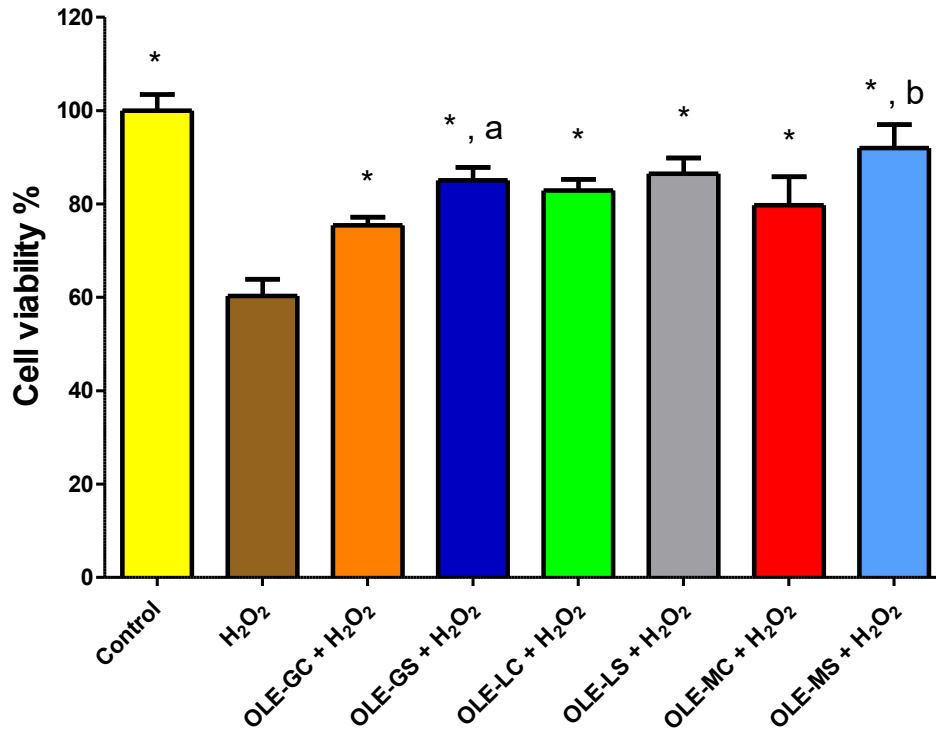


Figure 5. HUVEC viability after 2 h pre-treatment with OLE-G, OLE-GS, OLE-L, OLE-LS, OLE-M and OLE-MS (10 $\mu\text{g}/\text{mL}$) in culture medium, and subsequent 1 h treatment with 500 μM H₂O₂. Data are expressed as % viable cells compared to negative control (H₂O₂). *, significantly different from H₂O₂, $p < 0.05$; a, significantly different from OLE-G, $p < 0.05$; b, significantly different from OLE-M, $p < 0.05$.

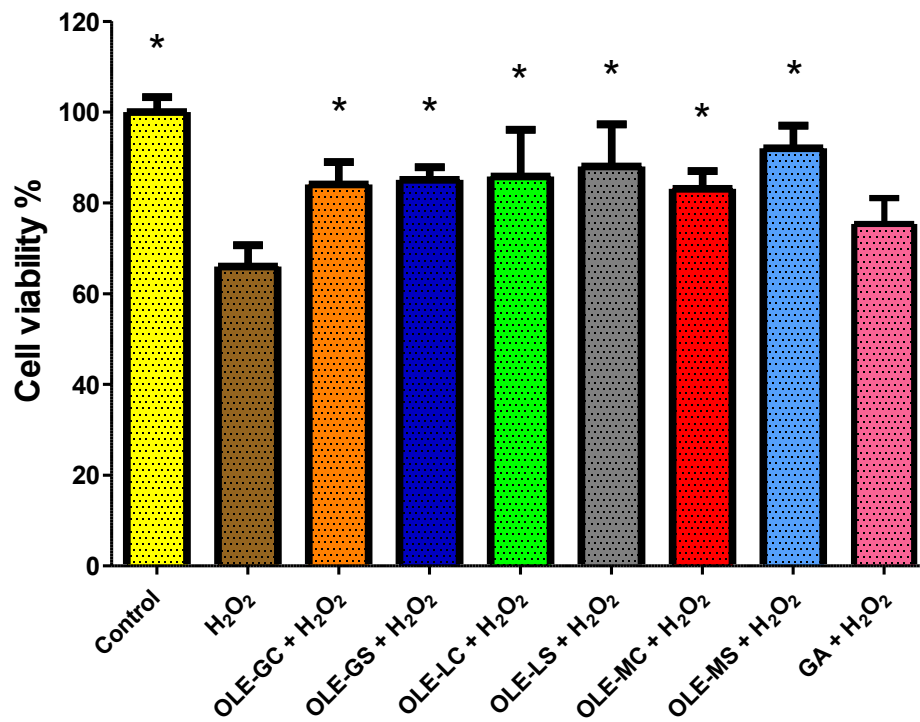


Figure 6. HUVEC viability after 2 h pre-treatment with OLE-G, OLE-GS, OLE-L, OLE-LS, OLE-M, OLE-MS and GA (0.5 $\mu\text{g}/\text{mL}$ GAE) in culture medium, and subsequent 1 h treatment with 500 μM H₂O₂. Data are expressed as % viable cells compared to negative control (H₂O₂). *, significantly different from H₂O₂, $p < 0.05$.

4.3.5. OLE antioxidant activity as assessed by ROS production

Figure 7 shows the data for ROS production in HUVECs pretreated or not with the OLEs of interest and then subjected to oxidative stress. As can be seen, ROS production after cell treatment with H₂O₂ is significantly higher than ROS production in cells incubated with control (plain medium). All extracts tested, except OLE-M, can significantly reduce ROS production compared to cells treated with H₂O₂. Apparently, OLE-GS and OLE-MS can significantly reduce ROS production, more effectively than OLE-G and OLE-M, respectively. On the other hand, no significant differences are observed between OLE-L and OLE-LS. The results obtained with this test are in perfect agreement with those reported in figure 5 and figure 6. These results can be attributed to the fact that OLE-GS and OLE-MS have a significantly higher content of polyphenols and antioxidants than all the other extracts and are not significantly different from each other.

ROS production was also evaluated in HUVECs with OLEs at the same GAE concentration (0.5 µg/mL GAE). GA was also tested as a positive control (Figure 8). All extracts tested significantly reduced ROS production compared to H₂O₂ treated cells. Surprisingly, ROS production in OLE-GS treated cells was significantly lower than that in OLE-G and GA treated cells. This result demonstrates that extracts from olive leaves subjected to water stress contain antioxidant molecules with greater reducing power than those extracted from non-stressed olive trees.

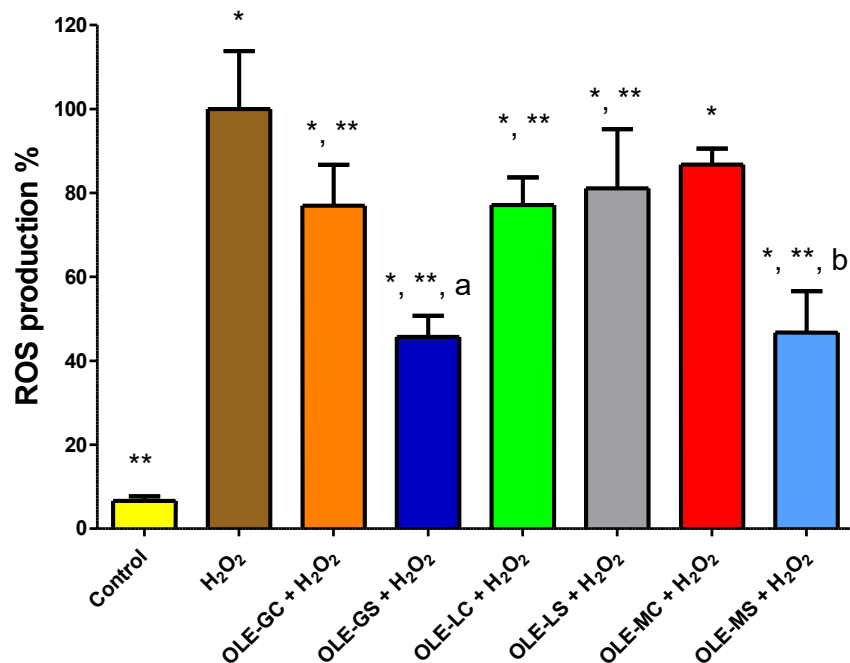


Figure 7. Reactive oxygen species (ROS) production in HUVECs treated with OLE-G, OLE-GS, OLE-L, OLE-LS, OLE-M, and OLE-MS (10 µg/mL) in culture medium, and subsequent treatment with 500 µM H₂O₂ for 1 h. Data are expressed as % ROS production on the basis of cells simply treated with H₂O₂. *, Significantly different from Control, p<0.05; **, Significantly different from H₂O₂, p<0.05; a, significantly different from OLE-G, p<0.05; b, significantly different from OLE-M, p<0.05

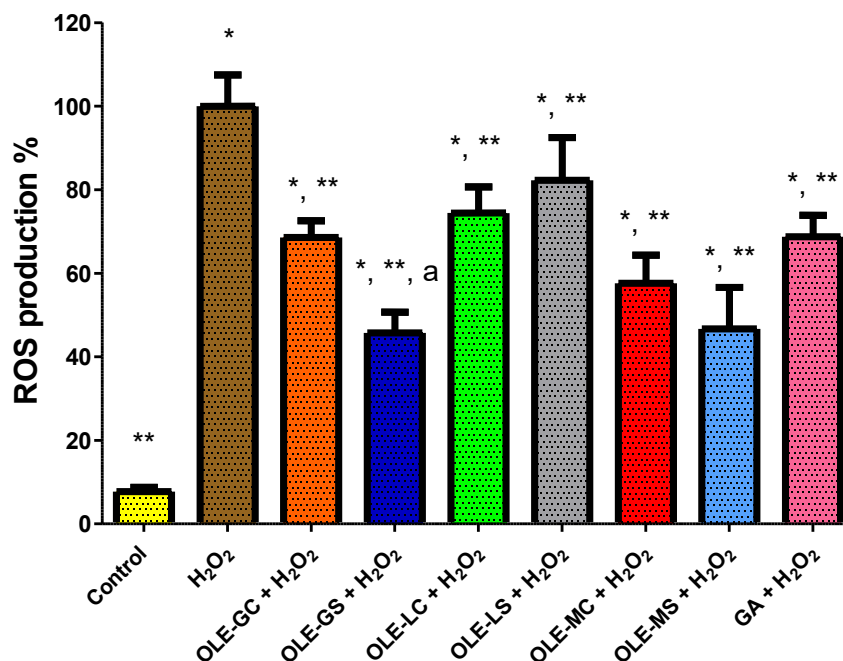


Figure 8. Reactive oxygen species (ROS) production in HUVECs treated with OLE-G, OLE-GS, OLE-L, OLE-LS, OLE-M, OLE-MS and GA (0.5 $\mu\text{g}/\text{mL}$ GAE) in culture medium, and subsequent treatment with 500 μM H₂O₂ for 1 h. Data are expressed as % ROS production compared to 100% (cell treated with H₂O₂). *, Significantly different from Control, $p < 0.05$; **, Significantly different from H₂O₂, $p < 0.05$; a, significantly different from OLE-G and GA, $p < 0.05$.

4.3.6. Permeation of antioxidants contained in OLE across excised rat intestine

The epithelium of excised rat jejunal tract was selected among known *ex vivo* intestinal models for studies of the permeability of antioxidant molecules because its tight junctions are similar in size and number to those of the human jejunum (Legen et al., 2005). Only the OLEs extracted from the Maurino and Giarrappa varieties that showed a greater antioxidant ability than the Leccino were tested for permeation through the intestinal epithelium. The OLEs were tested keeping constant either the concentration of the extract or the amount of polyphenols present in the extracts expressed in mg of GAE per mL. Figures 9a and 9b report the percentage of antioxidant molecules permeating through the intestinal epithelium over time. As can be seen, all the OLEs tested have the same permeation profile, regardless of the concentration or amount of antioxidant molecules applied. However, by comparing the data in figure 9a with those in figure 9b, it can be seen that the OLEs obtained from the Giarrappa variety have a significantly higher permeability than those obtained from the Maurino variety. These results, together with those shown in Figure 8, allow us to conclude that the OLEs from the Giarrappa variety are more permeable and, in particular, those obtained from plants subjected to water stress have a higher antioxidant activity.

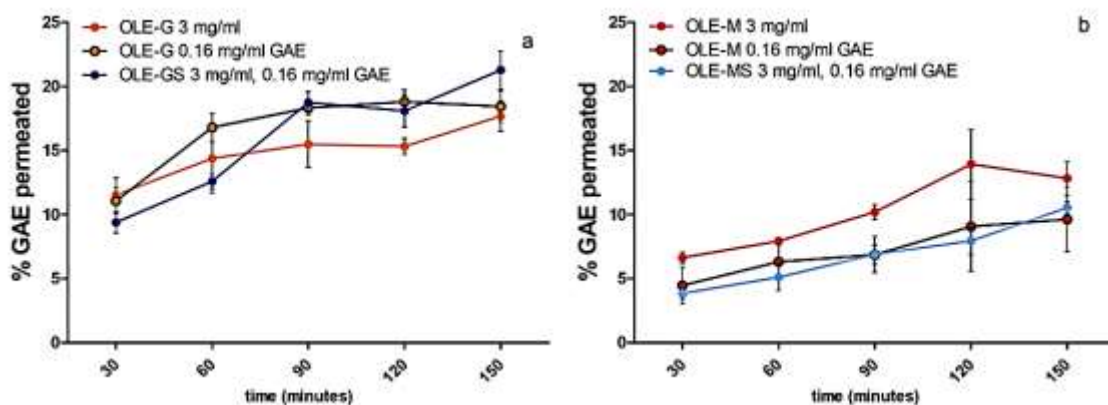


Figure 9. Data on the permeation of antioxidant molecules contained in a) OLE-G and OLE-GS and in b) OLE-M and OLE-MS in phosphate buffer, pH 7.4, 0.13 M, at the same concentration of extract (3 mg/ml) or at the equivalent gallic acid concentration (GAE) of 0.16 mg/mL across the excised jejunal rat epithelium (n = 3)

4.4. Discussion

Olea europaea L. is one of the most abundant, ancient, and economically valuable crops in the Mediterranean. Olive leaves are an unavoidable by-product of olive oil production, accounting for 25% of the dry weight of the total pruning residue (more than 6 kg/L of olive oil produced) (Espeso et al., 2021). Olive leaves are known to be rich in phenolic derivatives, mainly consisting of simple phenols, flavonoids, and secoiridoids, which may have various beneficial biological effects thanks to their antimicrobial, antioxidant, antiviral, and cardioprotective properties (Borjan et al., 2020). The accumulation of phenolic compounds is a well-known response to various abiotic stresses. As drought will be one of the major challenges in the Mediterranean region, research on cultivar-specific antioxidant properties under controlled or stressful conditions may be useful to identify which cultivars have the highest antioxidant content and potential health benefits, thus turning olive leaves from agricultural waste into a health or pharmaceutical product.

In this work, the antioxidant effects of olive leaves extracts of the olive cultivars ‘Giarraffa’, ‘Leccino’ and ‘Maurino’ are compared with those of the same leaves subjected to water stress. As also reported in other studies (Denaxa et al., 2020) (Petridis et al., 2012), drought stress of olive plants increased their antioxidant responses. In the present study, the antioxidant capacity (FRAP) and total phenols (TPC) reached their highest levels in the drought-stressed plants at the end of the experimental period, after four weeks of total water deprivation. At this time point, in OLE-GS and OLE-MS, the increase in the antioxidant capacity response is reflected by an accumulation of polyphenols. OLE-LS maintained a lower antioxidant capacity, although the polyphenol content increased. In fact, the antioxidant activity of an extract depends not only on the quantity of the polyphenols, but also on the type and the synergistic interactions that occur (Xie et al., 2015). The chemical structure heavily determines the antioxidant properties of phenolics: catechol moieties, multiple hydroxyl groups and conjugation with electron donating groups at the 4-position of the aromatic ring are factors that positively influence antioxidant activity (Xie et al., 2015). UHLC-MS characterization of the phenolic compounds present in the leaf extracts revealed differences between cultivars and also on the basis of water supplementation. Oleuropein, a (3,4-dihydroxyphenyl) ethanol (hydroxytyrosol) ester with alpha-glucosylated elenolic acid, is commonly reported as the main component of olive phenolic extracts (Valente et al., 2020), and it is well known for its pharmacological effects related to its free-radical scavenging properties (Borjan et al., 2020). In this study, oleuropein was found as the main component of leaf phenolic extracts in OLE-MS and OLE-LS. According to the

antioxidant capacity calculated for single phenolic compounds by Xie et al. (Xie et al., 2015) OLE-MS is rich of high-performance compounds, such as oleuropein, dihydroquercetin, and flavon-7-glucosides of both luteolin and apigenin, with a probable consequent decrease in the free form of these flavones. Similarly, OLE-LS showed an increase in the content of these compounds compared to OLE-L; however, the constant level of the highly antioxidant-performance dihydroquercetin and the lower amount of the phenolics' increase under stress conditions can have contributed to the lower FRAP response of OLE-LS compared to OLE-MS. Synergistic effects should be taken into account when considering the results of OLE-GS. The lower levels of all phenolics detected in OLE-GS compared to OLE-G do not justify its greater antioxidant power. As suggested by Dias et al. (Dias et al., 2021), it is possible that the stress condition increased the use in radical scavenging more than it affected phenolic synthesis, or that the molecules detected were in combination with some other compounds not revealed.

The antioxidant activity of olive leaves extract was evaluated on HUVECs cells. All OLEs showed no cytotoxicity at the concentrations analysed (1-50 µg/mL), however it can be observed in Figure 4 that the viability decreased slowly with increasing concentration especially with OLE from Giaraffa subjected or not to water deficit. Similar results were found by Fabiano et al. (Fabiano et al., 2021) and indicate that a high concentration of polyphenols present in olive extract exerts a cytotoxic effect, whereas a low concentration increases cell proliferation, as already demonstrated (Babich & Visioli, 2003). Olive leaves have scavenging activity against multiple ROS and could display cardioprotection. The ability of polyphenols presents in OLEs to inhibit ROS production was evaluated in this study. All OLEs tested, in particular OLE from Giaraffa and Maurino subjected to water deficit were able to reduce ROS production compared to untreated cells. Considering that these extracts have a higher antioxidant activity and polyphenols content than the others, these differences could be related to a synergic effect between the antioxidant compounds present (Morelo Dal Bosco, 2015). Therefore, the protective effect of OLEs could be related to a determined concentration and combination of antioxidants present in the extract. Finally in this study, we evaluated the ability of antioxidants present in OLE from Giaraffa and Maurino to cross the excised intestinal wall. As reported in figure 8b OLE from Giaraffa has a significantly higher permeability than Maurino. In fact, a permeation of total polyphenols at 20% of the applied dose (0.16 mg/mL GAE) was observed in OLE from Giaraffa whereas that from Maurino was about 10%. These results indicate that OLE from Giaraffa is more permeable through the intestine compared to OLE from Maurino probably because the antioxidants present in this extract are more stable than those present in Maurino when they encounter the rat intestinal tissue. Indeed, various factors should be considered in the study of the transport of bioactive compounds in the intestine, such as concentration and degradation processes (Cuffaro et al., 2023). In conclusion, the extracts subjected to water stress studied in this work, OLE-GS, OLE-MS and OLE-LS, have been shown to have antioxidant activity on HUVECs, thus providing protection against oxidative damage. Between all the extracts, OLE from Giaraffa and Maurino, showed better performance on HUVECs than the variety from Leccino. Although OLE-GS showed a decrease in the total amount of phenolic compounds compared to the same extract not subject to water stress, it has more antioxidant capacity and greater permeability across the rat intestine than OLE-MS. The results obtained allow us to conclude that the antioxidants activity probably depends on the permeation ability of the single molecules contained, thus, encouraging us to continue the studies on OLE subjected to water deficit.

5. Combination of Two Kinds of Medicated Microparticles Based on Hyaluronic Acid or Chitosan for a wound Healing Spray Patch

As extensively documented in literature, olive leaf extract (OLE) is an important resource due to its antioxidant and antibiotic properties, rendering it particularly adapted for wound management. In this study, we incorporated OLE into microparticles (MPs) composed of hyaluronic acid (MPHA-OLE) or chitosan (MPCs-OLE) with the objective of developing a spray patch for treating wounds in poorly accessible anatomical areas. The MPs underwent thorough characterization, focusing on particle size and their ability to safeguard OLE from degradation, absorb wound exudate, and regulate OLE release. Additionally, *in vitro* studies were carried out on fibroblasts using the scratch wound healing test to verify the impact of medicated and non-medicated MPHA and MPCs, as well as various mixtures of the two types in different proportions. The MP size consistently remained below 5 μm , making them well-suited for application as a spray in targeted zones. MPCs-OLE exhibited a controlled release profile, with approximately 60% of the encapsulated polyphenols being released after 4 hours. Both MPHA and MPCs demonstrated accelerated wound healing properties. The optimal mixture was composed of 50% MPHA-OLE and 50% MPCs-OLE, proving highly effective in accelerate wound healing process. The mixtures of MPHA-OLE and MPCs-OLE explored in this investigation displayed characteristics ideal for a spray patch, thus giving a second life to the waste products of olive growers.

5.1 Introduction

Olive leaves, often considered as agricultural by-products resulting from pruning during harvesting, are commonly disposed of by burning, contributing to the emission of greenhouse gases (Salomone & Ioppolo, 2012). For this reason the utilization of olive leaves emerges as a sustainable and ecologically alternative to their disposal. This study is specifically focused on the leaves of the *Olea europaea* *Olivastra seggianese* cultivar, a particular variety of olive grown in the Monte Amiata area of southern Tuscany, Italy. This particular tree, limited in distribution to the provinces of Grosseto and Siena, shown longevity, resilience to hard climatic conditions (prevalent in Monte Amiata), and an ability to combat parasitic adversities (Flamini et al., 2003). It is well reported that olive leaf extract (OLE) derived from this cultivar shown antimicrobial and antioxidant properties as well as the olive oil. Deep research has also highlighted its potential as an antihypertensive, antiatherogenic, anti-inflammatory, hypoglycemic, and hypocholesterolemic agent (Şahin & Bilgin, 2018). The features of this extract make it exceptionally compelling for wound applications. For this reason, the object of this study was to incorporate Olive Leaf Extract (OLE) into microparticles (MPs) composed of hyaluronic acid (HA) or chitosan (Cs), with the aim of develop a spray patch for the treatment of wounds in anatomical areas difficult to protect using traditional methods. HA, is a biomaterial with wound healing applications. In particular its efficacy is due to its properties in accelerating the wound healing process. These include its capacity to bind to specific surface receptors CD44 and RHAMM, crucial for cell migration and proliferation. Moreover, it is well known that the synthesis of HA is enhanced in a highly hydrated microenvironment, stimulating the increase, proliferation, and migration of fibroblasts, endothelial cells, and keratinocytes, essential for the formation of an HA rich granulation tissue (W. Y. Chen & Abatangelo, 1999). Also Cs was deeply investigated in wound healing. It has demonstrated the ability to promote macrophage migration, facilitating the phagocytosis of foreign bodies. Moreover, Cs activates cells such as leukocytes, fibroblasts, involved in inflammatory phase, expediting the transition from the inflammatory phase to the proliferative phase. Cs based MPs form a transparent, compact, and resistant film on wounds, while HA based MP doesn't own these features. In particular, Cs, as OLE, exhibits antibacterial properties (Singla & Chawla, 2001). Medicated microparticles of HA and Cs, loaded with OLE, could be efficiently applied as a spray for the wounds healing treatment. This could give several

benefits such as absorbing wound exudate due to the water absorbing properties of the polymers, promoting wound healing, addressing bacterial infections and gradually releasing OLE in order to prolong the antibacterial efficacy with a of lower request of frequent administration. The prospect of combining HA and Cs in spray patches could enhanced wound treatment, allowing a synergistic effect between HA and Cs formulations.

5.2. Materials and method

5.2.1. Materials

Olive leaves extract (OLE) preparation was carried out according to the previously reported procedure from *Olea europaea* var. *Olivastra seggianese* cultivar (De La Ossa et al., 2021). The leaves from which OLE was extracted were collected at CNR-IVALSA, Follonica (GR), Italy. Briefly, the freshly harvested olive leaves were freeze-dried (Freeze Dryer Modulyo, Edwards, Latina, Italy), then grounded in the presence of dry ice. The powder was dispersed in deionized water (1:5 w/v) and homogenized (IKA-ULTRA-TURRAX T25, Milan, Italy) for 5-min at 8000 rpm. Then the mixture was sonicated (Digital Ultrasonic Cleaner, Argolab 40 KHz, Milan, Italy) for 20 min at 35 °C, 40 KHz. The resulting suspension was centrifuged for 5 min at 4000 rpm and the supernatant was filtered through a 0.45 µm cellulose acetate filter. The filtrate was lyophilized (VirTis adVantage-53, Stereoglass, Perugia, Italy. Freezing -35 °C, 180 min; drying -30 °C, 360 min; -10 °C, 240 min; 25 °C, 180 min) and kept in the freezer until use. Gallic acid and Folin–Ciocalteu reagent, as well as all the inorganic salts were purchased from Sigma (Milan, Italy). Hyaluronic acid (HA) was purchased from Contipro (Dolní Dobrouc, Czech Republic), had a molecular weight of 454.8 ± 103.6 kg/mol (determined by Debye plot method, zetasizer, Malvern). Commercial chitosan, minimum 90% deacetylated from shrimp shell (Chito-clear FG90, Primex, Drammen, Norway) and average viscometric molecular weight of 590 kDa (Zambito et al., 2008) was converted into a chitosan·HCl powder (Cs). Cs was prepared by making an aqueous chitosan suspension (12 g in 2000 mL) to pH 4.7 with 1 N HCl (about 43.5 mL) and lyophilizing the resulting solution after filtration. Murine embryonic fibroblasts BALB/3T3 clone A-31 cell line was purchased from the American Type Culture Collection LGC standards (ATCC HTB-37, Milan, Italy) and propagated as indicated by the supplier. Dulbecco's modified Eagle medium (MEM), complete Dulbecco's modified Eagle medium (DMEM), non-essential amino acid, 0.01 M pH 7.4 Dulbecco's phosphate-buffered saline (DPBS), phosphate buffered-saline free of calcium and magnesium (PBSA), fetal bovine serum (FBS), and Hank's balanced solution were purchased from Sigma (Milan, Italy). Cell proliferation reagent (WST-1) was provided by Roche diagnostic (Milan, Italy). *Staphylococcus aureus* 33591 and *Pseudomonas aeruginosa* 27853 were purchased from ATCC (Milan, Italy). Tryptone Soy Broth (TSB) and Tryptone Soy Agar (TSA) were purchased from Oxoid (Basingstoke, UK).

5.2.2. Total Polyphenol Content (TPC) Determination in Olive Leaves Water Extract (OLE)

The TPC in OLE was determined following the Folin–Ciocalteu colorimetric method as previously described (Beconcini et al., 2018). Briefly, 1.58 mL of water and 100 µL of Folin–Ciocalteu reagent were added to a 50 µL aliquot of an OLE solution. After three min, 300 µL of sodium carbonate solution (1.9 M) was added and the absorbance was measured spectrophotometrically (Lambda 25 Perkin Elmer, Milan, Italy) at a wavelength of 765 nm after two hours of incubation in the dark. The TPC was therefore determined by referring to the calibration curve obtained with gallic acid and expressed as mg per g of lyophilized OLE.

5.2.3. Bactericidal Assays

The reference strains *Staphylococcus aureus* and *Pseudomonas aeruginosa* were used in the present study. For liquid cultures, bacteria were grown in TSB at 37 °C with shaking. Enumeration of colony-forming units (CFU) was performed by serially diluting bacterial suspensions and plating them on TSA. CFU were counted after an incubation of 24 h at 37 °C. The bactericidal

activity of OLE was evaluated against *S. aureus* and *P. aeruginosa* in 5% TSB. To this aim, bacterial strains were grown in TSB until exponential phase, and a number of approximately 5×10^4 CFU/mL, contained in a volume of 10 μ L, were added to a mix solution composed by 50 μ L of OLE (ranging from 2.5 to 20 mg/mL), 5 μ L TSB, and 35 μ L of water. The samples were incubated at 37 °C with shaking for 3 and 24 h. Following incubation, samples were 10-fold diluted in LB and plated on TSA to determine the number of CFU. Bactericidal activity was defined as a reduction of at least 3 Log₁₀ in the number of viable bacteria as compared to the inoculum.

5.2.4. Preparation of Microparticles (MP) Using the Spray-Drying Technique

MP based on HA (MPHA) or Cs (MPCs) medicated with OLE (MPHA-OLE, MPCh-OLE), were prepared by spray-drying. A 0.5% w/v solution of HA or Cs in water was prepared and spray-dried. The medicated MP were prepared by adding OLE (10 mg/mL in deionized water) dropwise to the polymer solution under magnetic stirring in a polymer:OLE 10:1 wt ratio. The solutions obtained were nebulized using a spray-dryer (Büchi Mini Spray Dryer B-191, Cornaredo, Italy) setting the following conditions: feed flow 600/700 mL/min, aspirator 100%, pump flow rate 15%, air temperature 175-180 °C inlet, and 80 °C outlet temperature. To ensure the homogeneity of the nebulization, the solution was kept under continuous magnetic stirring.

5.2.5. Determination of the OLE Content in Medicated MP

To verify that the OLE content in the MPHA-OLE and MPCs-OLE corresponded to the nominal content (10 wt %), 10 mg of medicated MP were dissolved in 1 mL of deionized water. The solution was then analyzed for the TPC. To rule out any interference, the same procedure was applied to non-medicated MP.

5.2.6. Dimensional and Morphological Analysis: Scanning Electron Microscopy (SEM)

The morphology (shape and surface characteristics) of the dried MP coated by metallization with 24 kt gold in a vacuum chamber at 15 mA for 20 min was observed by scanning electron microscope analysis (SEM, model JEOL JSM 300, Tokyo, Japan). ImageJ software was used to evaluate the MP average diameter. The images were divided into six grids with an area of 600 μ m². The mean diameter was calculated based on 40 measurements.

5.2.7. Thermogravimetric Analysis (TGA)

The thermal stability of the MPHA-OLE, MPCs-OLE, and free OLE was investigated by using thermal gravimetric analysis (TA Instruments Q500 TGA, New Castle, DE, USA). The instrument was calibrated using weight standards (1 g and 100 mg) and the temperature was calibrated using nickel standard. All standards were supplied by TA Instruments Inc. The samples (10–15 mg) were heated at 40 °C in a platinum crucible for the drying procedure and maintained in N₂ flux (90 mL/min) for 30 min. Then, the samples were heated from 40 °C to 600 °C with a heating rate of 10 °C/min under nitrogen (90 mL/min) and maintained at 600 °C for 3 min. Mass change was recorded as a function of temperature and time. TGA experiments were carried out in duplicate.

5.2.8. Determination of OLE Stability in MP

The stability of the polyphenols in OLE was determined in wound simulating buffer (pseudo extracellular fluid PECF, 0.11 M NaCl; 0.03 M KCl; 0.03 M NaH₂PO₄ e 0.3 M NaHCO₃, pH 8) (Singh & Pal, 2008). Ninety mg of MPHA-OLE, MPCs-OLE, or free OLE was suspended in 2 mL of PECF and immersed in a thermostated bath at 37 °C temperature under continuous stirring. The final OLE concentration was 4.5 mg/mL. At 30 min intervals, for a total of 4 h, 50 μ L were withdrawn, acidified with 1 M HCl, and analyzed for TPC quantification.

These tests were performed in quadruplicate.

5.2.9. Determination of the MP Swelling Degree

A previously reported technique was used to determine the MP swelling degree (Sadeghi et al., 2021). Briefly, 20 mg of each type of the MP under study were suspended in 2 mL of PECF pH 8 at 37 °C. After predetermined time intervals, the suspensions were filtered through paper filters. Each filter was then placed in a test tube and centrifuged at 2000 rpm for 2 min in order to remove excess water and weighed. To accurately evaluate the weight of the swollen MP, the same filters used for the tests were previously immersed in PECF, centrifuged at 2000 rpm for 2 min, and weighed and the weight of the swollen sample was calculated by difference. The swelling degree was calculated according to the equation

$$\text{Swelling degree (\%)} = [(W_s - W_{fs}) / (W_d - W_{fd})] \times 100$$

where W_d and W_{fd} are the initial weights of dry sample and dry support filter, respectively. W_s and W_{fs} are the swollen weights of sample and support filter, respectively. The swelling degree at each time point was determined in triplicate.

5.2.10. Study of the Release Profiles from Medicated MP

The OLE release from the medicated MP was determined by placing 100 mg of MPHAOLE or MPCs-OLE in 5 mL of PECF pH 8 in a thermostated beaker at 37 °C, under stirring. At predetermined time intervals, samples of 50 μ L were taken from the suspension and analyzed, after filtration (0.45 μ m cellulose acetate filters), for TPC quantification.

5.2.11. Cell Culture Techniques

Biological evaluations of polymeric MP were conducted using the BALB/3T3 clone A31 murine embryonic fibroblast cell line.

5.2.12. Cell Viability and Proliferation Test by WST-1 Assay

The cytotoxicity of MPHA, MPHA-OLE, MPCs, MPCs-OLE, and free OLE samples was evaluated by the WST-1 assay. The cells were seeded in 96-well plates, at a concentration of 7×10^3 cells per well and allowed to proliferate for 24 h at 37 °C and 5% CO₂. Stock dispersions of MP were prepared, previously made sterile by keeping them 20 min under UV, in DMEM without serum. Samples were diluted to obtain concentrations in the 0.5–50 μ g/mL range of OLE, either free or loaded into MP, considering 1/10 wt of loading. After 24 h, the culture medium was removed and replaced with the samples, and left in contact with the cells for 4 h. At the end of the incubation time, the cells were incubated at 37 °C for 4 h with WST-1 diluted 1/10. The amount of formazan produced was evaluated by measuring the absorbance at 450 nm with a microplate reader. The cytotoxicity of MP mixtures composed of MPHA and MPCs, medicated and not, was also evaluated in the ratios 25:75, 50:50, and 75:25 (abbreviations: MPHA25MPCs75, MPHA50MPCs50, MPHA75MPCs25, MPHA25MPCs75-OLE, MPHA50MPCs50, MPHA75MPCs25-OLE) at the final MP concentration of 30 μ g/mL.

5.2.13. In Vitro Scratch Wound Healing Assay

The scratch wound healing assay is a method developed to assess in vitro the ability of cell migration and proliferation (Felice et al., 2015). The cells were seeded, in 12-well plates, 1.25×10^5 cells per well in DMEM medium containing 1% calf serum. Complete confluence was achieved after 24 h at 37 °C and 5% CO₂. The resulting monolayer was scratched with a sterile pipette with p200 tip. After scratching, the wells of the plate were washed three times with PBSA to remove debris and various dead cells. Then 2 mL of each sample to be tested was added. MPHA, MPHA-OLE, MPCh, MPCh-OLE, and three mixtures composed of medicated and non-medicated MPHA and MPCh were analyzed (MPHA25MPCs75, MPHA50MPCs50, MPHA75MPCs25, MPHA25MPCs75-OLE, MPHA50MPCs50-OLE, and MPHA75MPCs25-OLE) at a concentration of 30 μ g/mL, and the free OLE at a concentration of 3 μ g/mL. In the control tests,

the cells were incubated in the presence of the culture medium alone (DPBS). Micrographic images of each well were acquired by means of a camera with a 4×-objective (Nikon Eclipse Ts2R) at time zero and after 24 h. The acquired images were analyzed using the ImageJ Software to determine the percentage of healing of the inflicted scratch.

The following formula was used to determine the percentage of healing over time

$$\text{Wound healing (\%)} = \frac{[(\text{Area T0} - \text{Area T})/\text{Area T0}] \times 100}{}$$

where Area T0 is the area at time zero, Area T is the area at 24 h.

5.3. Results

5.3.1. TPC Determination in OLE

OLE was characterized in previous studies (De la Ossa et al., 2019). The main components of this OLE are similar to those already found in OLE from other varieties of *Olea europaea*. In this work, the same olive leaves were used from which the extract was previously obtained. For this reason, we only verified that the re-prepared extract had the same polyphenol content and the same antimicrobial activity as the extract previously obtained (Hashmi et al., 2015). The content of total polyphenols (TPC) in the lyophilized OLE was in line with the previous one, resulting in 79.47 ± 6.99 mg per g of lyophilized OLE. Although reference is made to TPC, it should be kept in mind that the Folin-Ciocalteu reagent is not specific for phenolic compounds and could also react with other molecules present in the extract with reducing characteristics (Cesare et al., 2021).

5.3.2. OLE Antibacterial Activity

In order to verify that the OLE used in this study had antimicrobial activity as already reported (De la Ossa et al., 2021) was tested against *S. aureus* and *P. aeruginosa*, representative of Gram-positive and Gram-negative bacterial species respectively often involved in infection of wounds (Bessa et al., 2015). OLE, tested at 5 mg/mL, showed a bacteriostatic effect against *S. aureus* after both 3 and 24 h of incubation, figure 1, whereas at 10 and 20 mg/mL OLE exerted a strong bactericidal effect, Figure 1. No antibacterial activity was observed when OLE was tested against *P. aeruginosa* until a concentration of 20 mg/mL (data not shown). These latter results are in agreement with previous studies that reported low susceptibility of *P. aeruginosa* to a number of plants derived oil extracts and in particular to olive oil extracts (Warnke et al., 2013) and might be due to the intrinsic tolerability of this bacterial species to antimicrobials.

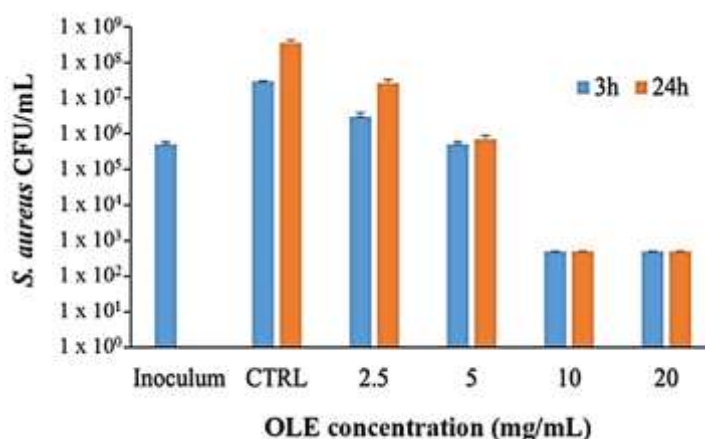


Figure 1. Antibacterial activity of OLE against *S. aureus* ATCC 33591 after 3 and 24 h of incubation in 5% TSB. Control (CTRL) represents bacteria incubated in the absence of OLE. Bactericidal activity was defined as a reduction in the numbers of viable bacteria of ≥ 3 -log colony forming units (CFU)/mL at any incubation time tested. Data are reported as mean \pm SD (n = 3).

5.3.3. MP Characterization

Both MPHA-OLE and MPCs-OLE contained the nominal amount of OLE, i.e., 10% by weight. This result was indeed expected, since the spray-drying technique ensures that the active ingredient does not degrade during drying. Figure 2 shows the SEM micrographs of MPHA, MPCs, MPHA-OLE, and MPCs-OLE. In all cases, the majority of MP have a spherical shape, although some irregularly shaped MP can be observed. The average sizes of MPHA, MPHA-OLE, MPCs, and MPCs-OLE are 4.7 ± 1.8 , 4.3 ± 1.3 , 4.5 ± 1.6 , and 4.0 ± 1.2 μm , respectively. This testifies to some dimensional dispersion, since, after all, smaller particles adsorbed on larger ones are observed in Figure 2. However, the average size is in all cases less than 5 μm and this makes the MP suitable for their topical administration (Garcia et al., 2021). It is also observed that the size of non-medicated MP does not differ significantly from medicated ones. Finally, it is noted that all kind of MP have a smooth surface even if in some cases they are collapsed. This is not surprising, rather, it suggests a hollow capsule morphology characteristic of the MP obtained by the spray-drying technique.

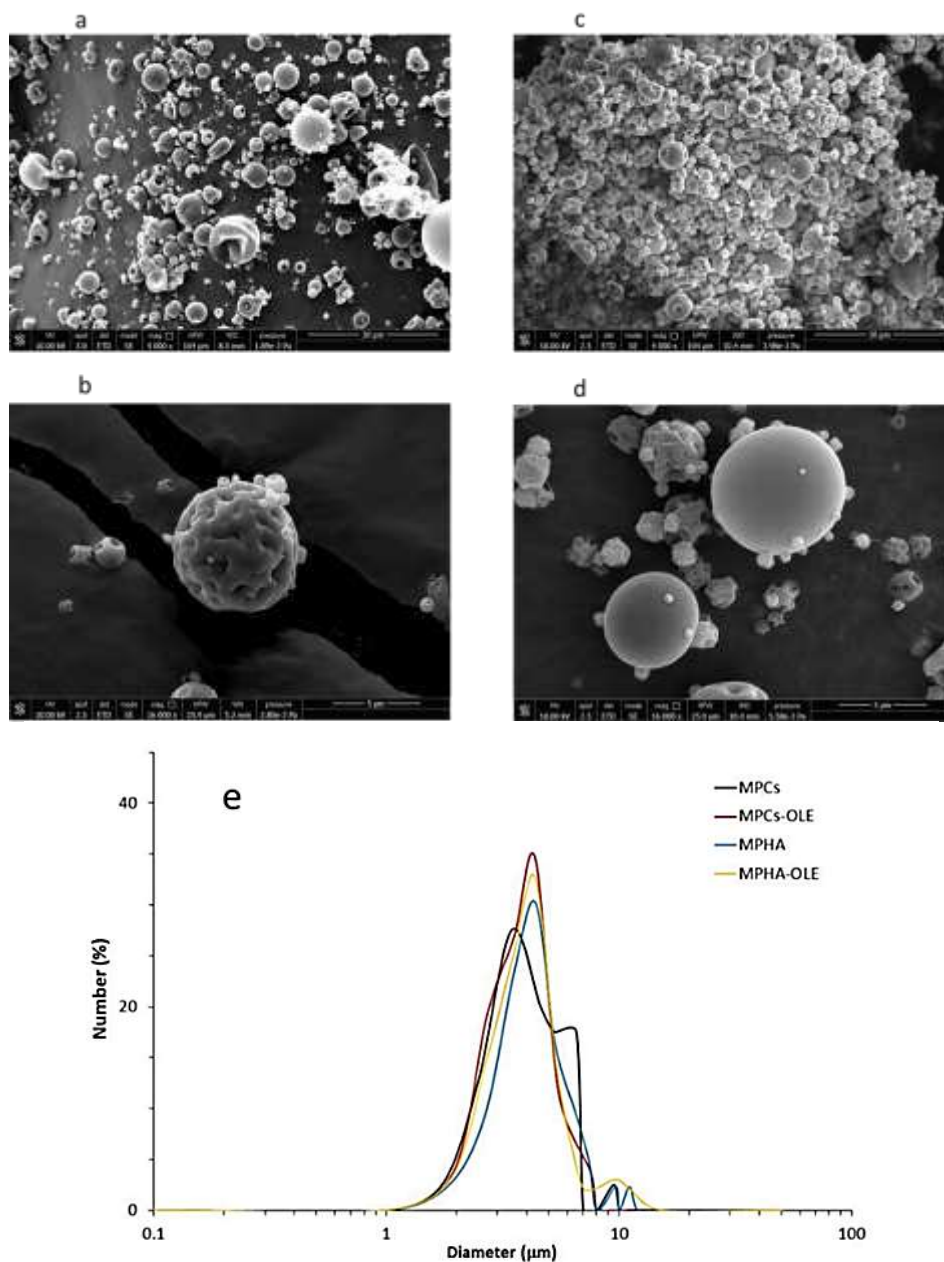


Figure 2. SEM micrographs of (a) MPHA; (b) MPHA-OLE; (c) MPCs; (d) MPCs-OLE; (e) Number (%) vs. diameter size distribution curves of MP.

5.3.4. TGA Analysis

TGA analysis is a widely used technique to evaluate the thermal stability of compounds in which the loss of mass as a function of temperature is measured. Figure 3 a,b show the thermogravimetric curves of MPHA, MPHA-OLE and MPCs, and MPCs-OLE, respectively, in comparison with free OLE. Figure 3 c,d show the derivative of the respective thermogravimetric curves. Figure 3 shows that the weight loss of the samples decreases with increasing temperature. The degradation temperature (T_d), which corresponds to the point of intersection between the starting-mass baseline and the tangent to the TGA curve at the point of maximum gradient reported in Figure 3, shows two degradation phenomena for OLE; the first around 170 °C and the second around 270 °C. The degradation curves of MPHA-OLE and MPCs-OLE are not significantly different from the curves of non-medicated MP. In the case of MPHA and MPHA-OLE (Figure 3c) a main degradation peak is observed at 230 °C with a shoulder at a higher temperature, indicating the overlapping of the breaking of the $\beta(1-3)$ glycosidic bonds and the decomposition of carbonyl groups as reported in the literature (Sahiner et al., 2019). In the case of MPCs and MPCs-OLE (Figure 3d), a degradation peak around 230 °C is observed, which could be attributed to the polysaccharide backbone depolymerization and pyrolytic decomposition of chitosan (Mezzetta et al., 2017). Despite the presence of OLE, its degradation profile is not revealed by the analysis of MPHA-OLE and MPCs-OLE particles. In particular, the first peak of OLE degradation at 170 °C totally disappears, suggesting an effective encapsulation of OLE in both MP types, with consequent protection of the extract from decomposition.

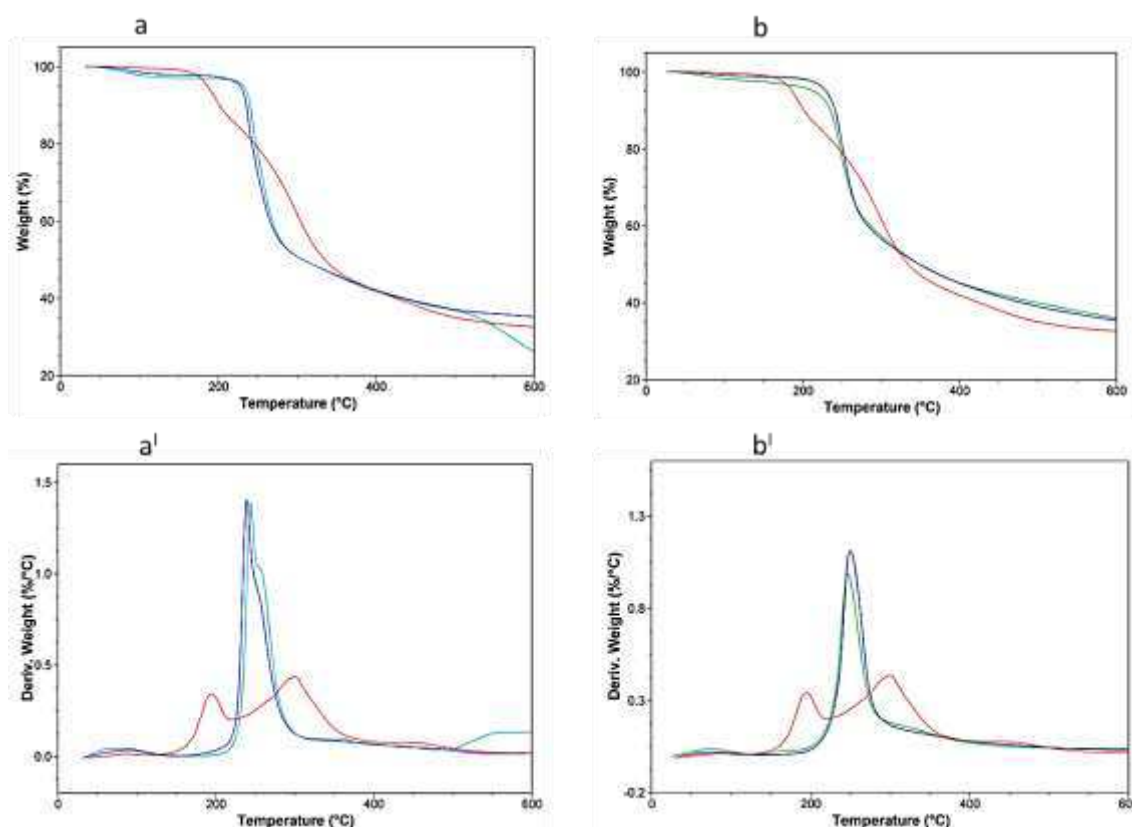


Figure 3. Thermogravimetric curves for (a) green MPHA, blue MPHA-OLE, red OLE; (b) green MPCs, blue MPCs-OLE, red OLE, and the respective derivative curves (c) and (d) ($n = 2$).

5.3.5. Determination of OLE Stability in MP

OLE stability in PECF medium was assessed by monitoring the variation of reactivity with the Folin–Ciocalteu reagent. Figure 4 shows the degradation curves of OLE in PECF medium over time, thus expressed as decreasing TPC % value. It is observed that the MPHA-OLE follows a

degradation profile completely superimposable to that of non-encapsulated OLE showing their inability to slow down the degradation of OLE in solution. This could be due to a rapid release of OLE by the MPHA. Instead, in Figure 4 it is observed that after 4 h the MPCs-OLE are able to maintain the TPC at about 80% of the initial content. This testifies that chitosan microparticles are able to protect OLE from degradation even in the simulated wound exudate medium.

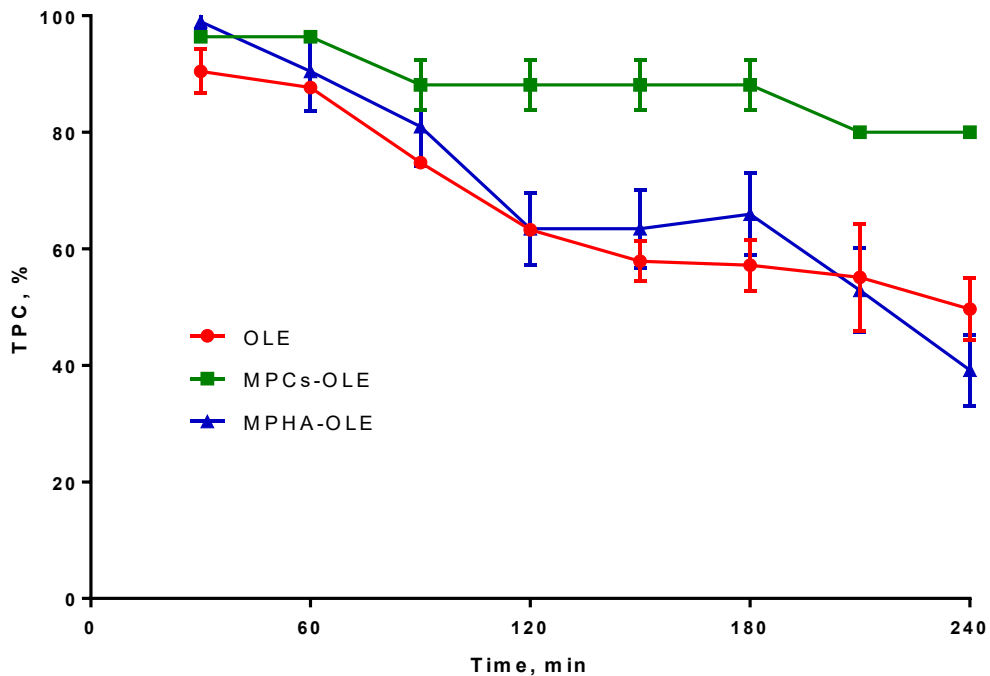


Figure 4. OLE stability in pseudo extracellular fluid (PECF) at 37 °C. Means \pm SD (n = 4).

5.3.6. Determination the MP Swelling Degree

The swelling profiles of medicated and non-medicated MPHA and MPCs are displayed in Figure 5. In Figure 5a it is observed that the MPHA swelling is very fast and reaches its equilibrium at the first time point (5 min). Furthermore, it retains the absorbed PECF for the entire experimental time (1 h). Differently, the MPHA-OLE show a swelling peak after 10 min, corresponding to a 50% increase of its initial weight. Evidently, the interaction between HA and OLE increased the osmotic force of the MP. In Figure 5b the MPCs show a maximum of absorption after 5 min. On the other hand, MPCs-OLE show a swelling peak after 30 min, with a swelling degree lower than that of non-medicated MPCs. Contrary to what observed with MPHA-OLE, the presence of OLE in the polymer matrix determines an interaction between the hydrocolloid and the polyphenols, which reduces the swelling behavior of MPCs-OLE (Talón et al., 2017). These data suggest that all MP under study are particularly suitable for the preparation of a spray patch. In fact, a high hydration and swelling power is an essential property as it makes the formulation ideal for absorbing water from the exudate (Pagano et al., 2020).

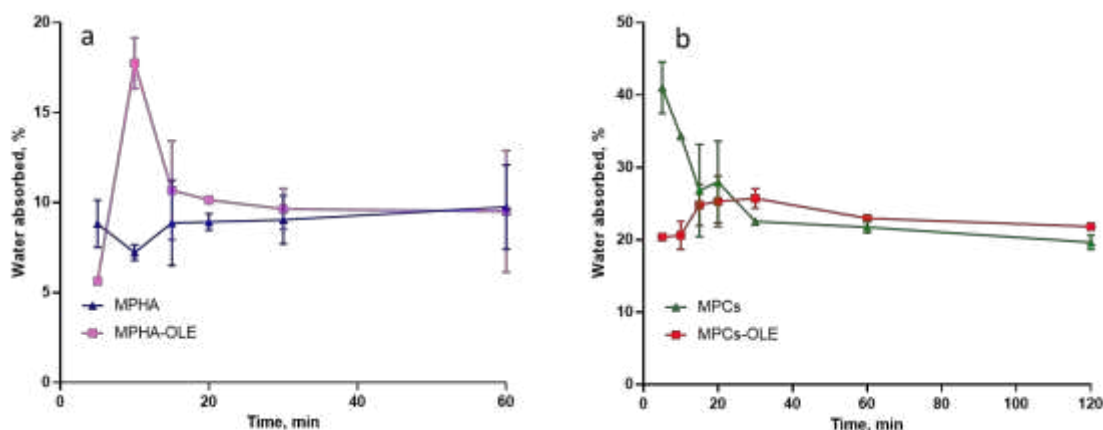


Figure 5. Swelling curves of a) MPHA and MPHA-OLE and b) MPCs and MPCs-OLE in pseudo extracellular fluid (PECF) at 37°C. Bars represent the means \pm SD of values obtained from three independent experiments.

5.3.7. Study of Release Profile from Medicated MP

To follow the release profiles of the active ingredients from the MP, the Folin–Ciocalteu analytical method was chosen, which allows identification of all the antioxidant species present in the solution. This methodology seemed more effective in this context precisely because most of the active molecules present in the extract such as oleuropein, hydroxyl-tyrosol, apigenin-7-O-glucoside, luteolin-7-O-glucoside (De la Ossa et al., 2021) respond positively to the assay. Figure 6 shows the TPC percentage released over time by MPHA-OLE or MPCs-OLE in PECF, with respect to the TPC value of loaded OLE. From the data reported in Figure 6, it can be observed that in the case of MPHA-OLE the release is complete after 15 min. Moreover, in the present experimental conditions, in which there is a large excess of PECF, it is observed that the MPHA-OLE dissolve after forming a compact gel on the bottom of the container, which erodes quickly. The inability of HA to protect OLE from degradation, shown in Figure 4, may depend on OLE being completely released from the HA-based microparticles after just 15 min from the start of the release study. In the case of the MPCs-OLE the release was followed for a total time of 4 h. In fact, as seen in Figure 4, the OLE released after 4 h in PECF begins to degrade; therefore, the release kinetics at longer times could be distorted by the simultaneous degradation of the OLE already released. Contrary to what has been observed with MPHA-OLE, MPCs-OLE does not erode in the PECF alkaline buffer. In Figure 6, the release profile for MPCs-OLE shows that after 5 min about 25% of OLE is released. This may be due to a desorption of the OLE adsorbed on the external surface of the MP. In the subsequent 4 h, the release occurs slowly and reaches the value of about 60%. These data are in agreement with those previously obtained for a similar device [16]. The shape of the release curve, together with the swelling data shown in Figure 5a and the fact that the MPCs-OLE does not dissolve in the alkaline buffer, suggest that the release is controlled by the diffusion of the OLE from the MP.

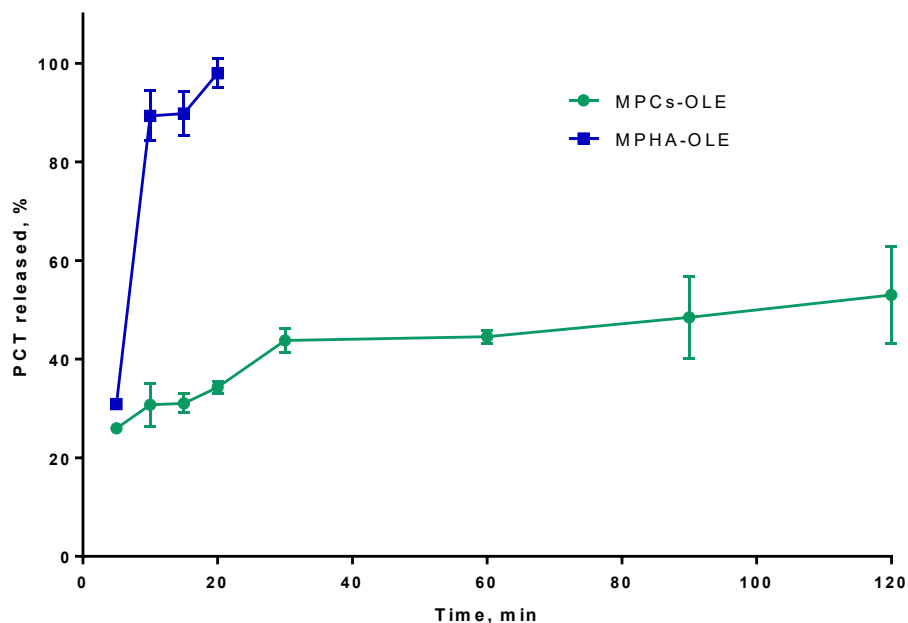


Figure 6. OLE release curves from MPHA-OLE or MPCs-OLE in pseudo extracellular fluid (PECF) at 37 °C. Means \pm SD (n = 3)

5.3.8. Cell viability and proliferation test by WST-1 assay

MPHA, MPHA-OLE, MPCs, MPCs-OLE and free OLE, underwent to *in vitro* biological investigations for the evaluation of cytotoxicity. Cells from the BALB/3T3 clone A31 murine fibroblast line were incubated with MPs for 4 hours and subsequently analyzed by the WST-1 colorimetric assay. This assay was performed to select the best concentration to be used in subsequent wound healing studies. Both MPHA and MPHA-OLE did not show cytotoxicity for all the assayed concentrations, in the range 5-500 μ g/ml. The cell viability value was always found to be over 75% of control cells viability (cells grown in the absence of MP), indicating a high biocompatibility of the same (Figure 7a). Instead, the MPCs and MPCs-OLE at the lowest tested concentrations (5-50 μ g/mL) showed cell viability values around 60-80%, while at higher concentrations (75-500 μ g/mL) they showed values of cell viability around 20-40% (Figure 7a). Free OLE also showed no cytotoxicity for the analyzed concentrations in the range 0.5-50 μ g/ml. However, it was possible to observe that with increasing concentration the percentage of cell viability decreases slowly (Figure 7b). The results of the toxicity tests led to the choice of the maximum non-toxic concentration in subsequent wound healing tests of 30 μ g/mL for MP which contain 0.3 μ g/ml of OLE. For this reason, the cytotoxicity of mixtures of HA and Cs based MP was also tested, by keeping constant the total MP concentration (30 μ g/ml) but changing the relevant MP ratio (25/75; 50/50; 75/25 of MPHA and MPCs, either medicated or not). None of the tested mixtures were found to be toxic at the chosen concentration (Figure 7c).

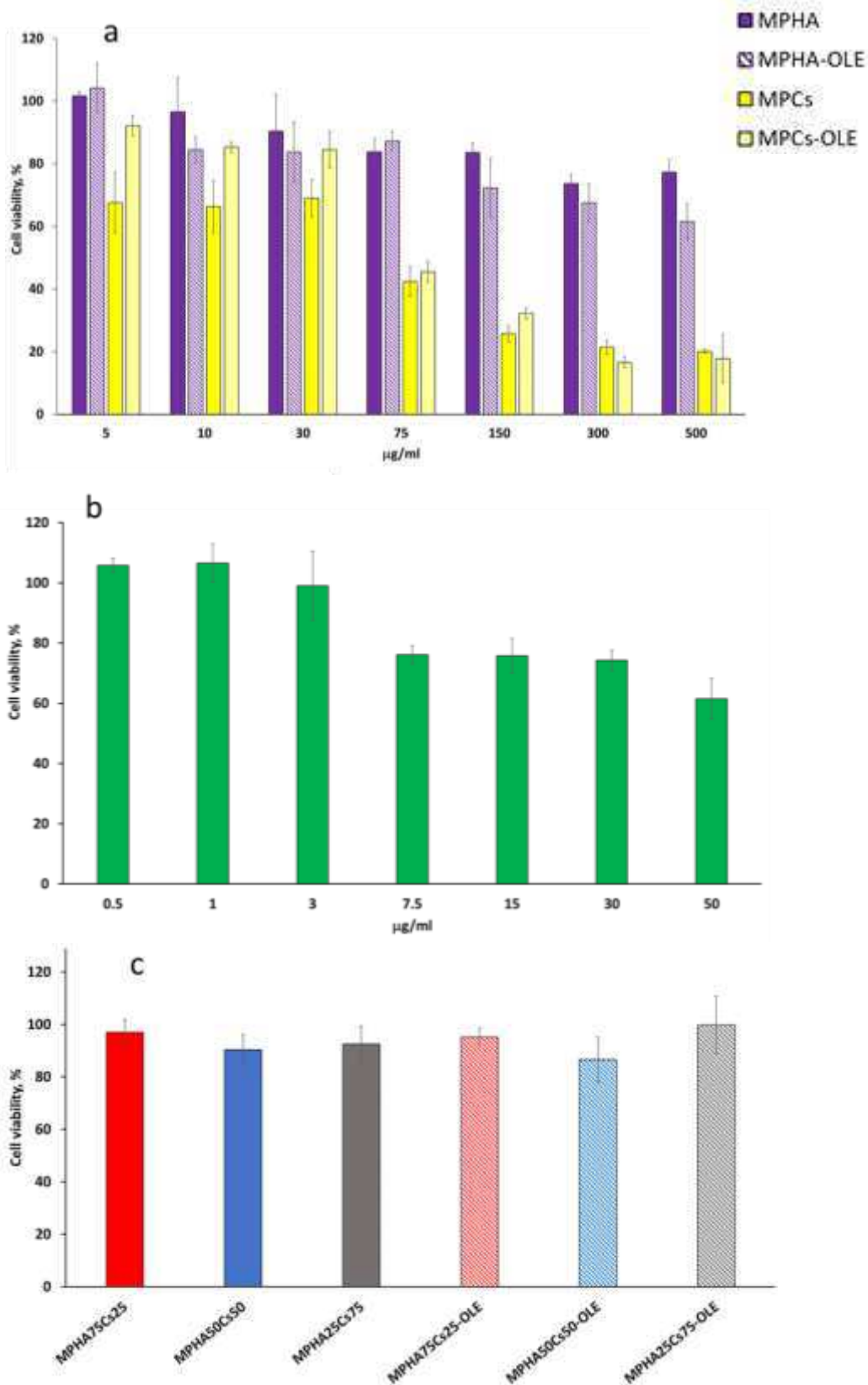


Figure 7. BALB/3T3 clone A31 murine embryonic fibroblast cell viability after 4 h of incubation with a) MPHA, MPHA-OLE, MPCs, MPCs-OLE; b) free OLE; c) mixtures of MPHA and MPCs medicated or not (30 µg/ml total MP concentration). Data are expressed as % viable cells compared to 100% of control (untreated cells). Bars represent the means \pm SD of values obtained from eight independent experiments.

5.3.9. *In vitro* scratch wound healing assay

In the wound healing studies performed by scratch test, cell migration was evaluated in a two-dimensional manner on monolayer of Balb/3T3 cells, with respect to time. The *in vitro* scratch test is the first choice method for analyzing cell migration because it does not require any specialized equipment and all the necessary materials are available in any laboratory performing cell culture studies (Liang et al., 2007). The technique involves the creation of a thin and linear "wound" by scratching a monolayer of cells and subsequent acquisition of images of the cells that migrate towards the space created (Grada et al., 2017). Low serum concentrations (1% FBS) in the cell medium were used to reduce cell proliferation and promote cell migration. Figure 8 displays a panel of micrographs, processed with ImageJ. From this first qualitative investigation it is possible to note that at time zero only the edges of the scratch are present and that after 24h it is possible to observe the migration from the margin towards the center of the simulated wound.

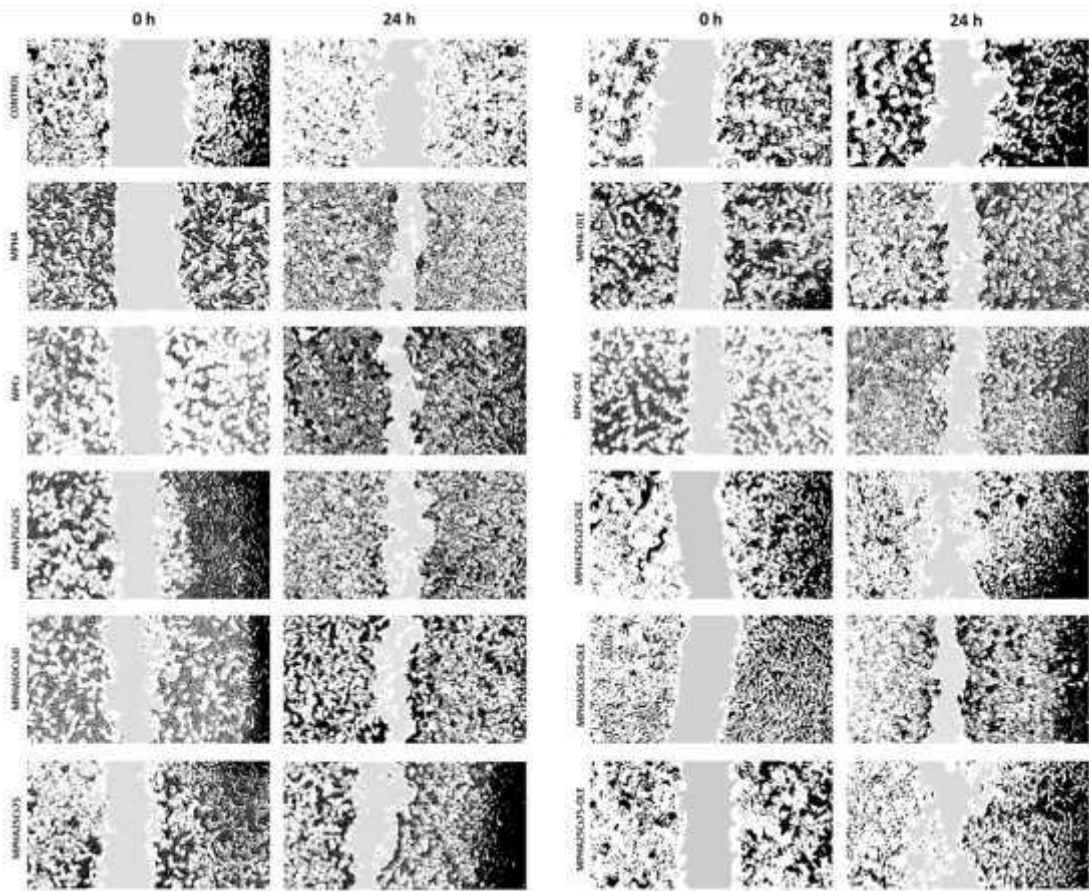


Figure 8. Representative micrographs (4× magnification) of BALB/3T3 clone A31 murine embryonic fibroblast cell monolayers, processed with ImageJ software. CTRL, plain MPHA, MPCs, and their mixtures are displayed on the left side panel; OLE and medicated MP, as well as their mixtures are on the right side of the panel.

Figure 9 shows the wound healing percentages for all the studied samples. From the data in Figure 9 it can be observed that OLE is not able to accelerate the healing of wounds but even slows it down, as a % healing was significantly lower than the control. This data appears in contrast to other literature studies in which OLE was found to be active both as an antibacterial and as an accelerator of wound healing. The tested concentrations were higher than that applied in the present work, though (De la Ossa et al., 2021). MPHA and MPCs were found to be very effective in promoting wound healing and the differences were not significant. Likewise, no significant differences were observed between medicated and non-medicated MP.

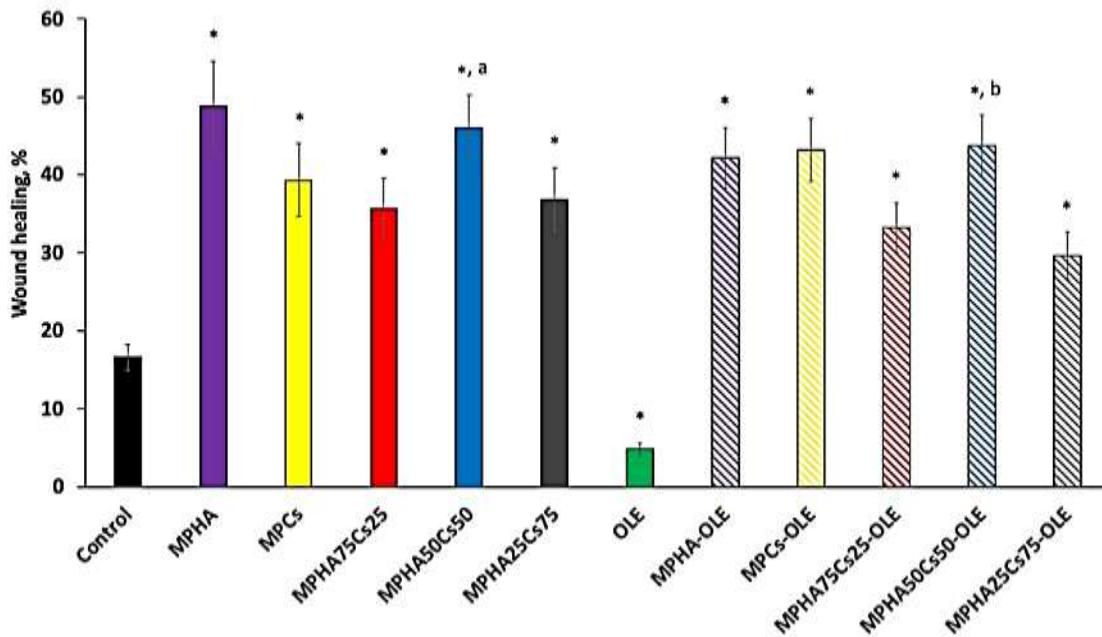


Figure 9. Wound closure rates expressed as percentage of scratch closure after 24 h compared to initial area. Control consists in untreated cells. Bars represent the means \pm SD of values obtained from six independent experiments. * $P < 0.05$ vs control; a $P < 0.5$ vs MPHA75Cs25 and MPHA25Cs75; b $P < 0.5$ vs MPHA75Cs25-OLE and MPHA25Cs75-OLE.

From a careful observation of the photomicrographs shown in Figure 8 it is possible to observe how BALB/3T3 clone A31 cells treated with MPHA promote cell proliferation. It is in fact known how HA acts in the first phase of wound healing, that is, in the proliferative phase (Kawano et al., 2021). The qualitative analysis of the images also allowed to note how the presence of MPCs rather favours cell migration. In fact, Cs, by mimicking the glycosaminoglycans portion of the extracellular matrix, allows cells to activate the mechanisms of cell migration, which represents the second phase of healing (Kawano et al., 2021; Matica et al., 2019). This interesting observation prompted us to evaluate the opportunity to create a device capable of promoting cell proliferation in the wound site thanks to the presence of HA and simultaneous cell migration thanks to the presence of Cs (W. Y. Chen & Abatangelo, 1999). Furthermore, the dual function of Cs would favour both cell migration but also an important antimicrobial action (Matica et al., 2019), the latter strengthened by the OLE loaded in the MP (Sudjana et al., 2009). In Figure 9 it is observed that the MPHA50MPCs50 mixture, medicated or not, have a significantly higher wound healing activity than all the other mixtures tested, probably because an equal quantity of both polymers is necessary to obtain the right modulation of proliferation and cell migration in the wound healing process.

5.4. Discussion

The OLE-loaded HA and Cs-based MP studied in this work were shown to have characteristics suitable for making a spray patch, thus giving a second life to the waste products of olive growers. The particles of the spray patches were less than 5 μm of size, were able to swell by absorbing the wound exudate water, were able to slowly release OLE and protect it from degradation, and were able to accelerate wound healing. A mix containing 50% MPHA-OLE and 50% MPCs-OLE, although shown by in vitro scratch studies to be unable to significantly improve the performance of unmixed HA- or Cs-based MP, nevertheless, it turned out to be very interesting. Firstly the MPCs, unlike the MPHA, were able to control the release of OLE and to protect it from degradation; secondly, it was observed from the photomicrographs that the MPCs can promote

the migration of fibroblasts, whereas the MPHA can promote their proliferation. However, in vivo studies will be necessary before a possible synergistic effect of the two MP types can be stated. In such studies, the microparticles are intended for application on the wound as a spray.

6. Olive Leaf Extract For Corneal Wound Healing

The olive leaf extract (OLE) has been studied for its properties in wound healing application (Fabiano et al., 2021). Water stress, meaning the lack of water administration, represent a resource for the production of plants with a higher metabolite content than those grown under normal conditions (Cesare et al., 2021). Olive leaves extracts of the Giarrappa varieties obtained from trees subjected to water stress (OLE-GS) (Cerri et al., 2024) were used in this study. The aim of this work was to prepare eye drops formulations medicated with OLE-GS for corneal wound healing. Different chitosan derivatives based on a quaternary ammonium chitosan food grade derivative (QA-Ch 50-190 KDa) conjugated with methyl- β -CD (MCD), coded QA-Ch-MCD (Piras et al., 2018) were applied. The ability of ophthalmic drops based on different prepared polymers medicated or not with OLE-GS to accelerate the healing of corneal wounds was evaluated on a model of corneal cell monolayers of HCE-T cell line. The samples tested for the wound healing assay were: OLE-GS, QA-Ch-MCD, QA-Ch-MCD/OLE-GS, QA-Ch/MCD, QA-Ch/MCD/OLE-GS, Ch/MCD, Ch/MCD/OLE-GS, Ch, Ch/OLE-GS, MCD and MCD/OLE-GS. All medicated formulation tested excepted Ch/OLE-GS were able to improve the scratch closure significantly better than the control. QA-Ch-MCD/OLE-GS was able to accelerate the scratch closure in a better way compared to all other formulation tested and compared to OLE-GS alone. The ability of the tested samples to protect against H₂O₂ induced oxidative damage was evaluated on HCE-T cell line. All formulations containing OLE-GS and OLE-GS alone were able to increase cell viability following H₂O₂ induced oxidative damage. A Draize test was performed using male New Zealand albino rabbits. The OLE-GS and QA-Ch-MCD/OLE-GS showed no signs of irritation, swelling or redness after 24 hours. In conclusion OLE-GS has been shown to improve corneal wound healing on the model used. Furthermore, when this is used complexed with QA-Ch-MCD there is an even more marked effect.

6.1. Introduction

Wound Healing Society described a wound as the result of “disruption of normal anatomic structure and function”. Recently, different strategies have been developed in order to obtain a faster and less painful wound healing process. The olive leaf extract (OLE) has been extensively studied for its antimicrobial and antioxidant features. Such properties are commonly exploited in wound healing application to resolve inflammation and preserve from infection (Fabiano et al., 2021). Furthermore water stress, meaning the lack of water administration, can represent a resource for the production of plants with a higher metabolite content than those grown under normal conditions (Cesare et al., 2021). For this reason olive leaves extracts of the Giarrappa varieties obtained from trees subjected to water stress (OLE-GS) were used for a following study (Cerri et al., 2024). The aim of this work was to develop eye drop formulations medicated with OLE-GS for corneal wound healing. Moreover, in a recent investigation, the capacity of cyclodextrins to solubilize poorly soluble compounds and the attributes of mucoadhesive polymers were scrutinized. To achieve this, methyl- β -cyclodextrin (MCD) was linked to a water-soluble mucoadhesive chitosan derivative using the hexamethylene diisocyanate (HMDI) spacer. The resultant conjugate exhibited notable complexing capabilities, mucoadhesive traits, and cytocompatibility. In this particular study, the water-soluble cyclodextrin-polymer complex, named as QA-Ch-MCD, was derived from a pH-independent water-soluble quaternary ammonium chitosan (QA-Ch). The QA-Ch, synthesized previously and recognized for its mucoadhesive properties, proved to be a potent enhancer for the absorption of hydrophilic, hydrophobic, and macromolecular drugs across diverse epithelia, including the intestinal, corneal (Zambito & Colo, 2010) and buccal membranes (Piras et al., 2018). In order to treat the eye diseases, patients generally prefer the convenience of eye drop therapy. However, utilizing eye drops for treatment proves to be complicated due to their poor bioavailability. This is due to the rapid clearance of drugs from the precorneal area, the primary site of drug action/absorption

in the eye. Protective mechanisms, such as blinking, basal tearing, reflex actions, and nasolacrimal drainage, contribute to the swift elimination of drugs. To address this issue and enhance the bioavailability of drugs administered through eye drops, one strategy involves minimizing the rate of elimination. This can be achieved by incorporating mucoadhesive polymers, such as QA-Ch-MCD, into the formulation (Zambito & Colo, 2010). For this reason different chitosan derivatives based on a quaternary ammonium chitosan food grade derivative (QA-Ch 50-190 kDa) conjugated with methyl- β -CD (MCD), coded QA-Ch-MCD (Piras et al., 2018) were applied. The ability of ophthalmic drops based on different prepared polymers medicated or not with OLE-GS to accelerate the healing of corneal wounds was evaluated on a model of corneal cell monolayers of HCE-T cell line, using the assay proposed for the work in the previously chapter.

6.2. Materials and method

6.2.1. Materials

Olive leaf extracts of the Giarruffa varieties subjected to water stress (OLE-GS) was collected at Life Sciences Department of the University of Siena, Siena (SI). Folin-Ciocalteu reagent, gallic acid, 1-ethyl-3-(3-dimethyl-aminopropyl) carbodiimide hydrochloride, cellulose membrane tubing MW cut-off 12.5 kDa, low-molecular-weight chitosan, dimethyl sulfoxide (DMSO), 1,6-hexamethylene diisocyanate (HMDI), and triethylamine (TEA) were purchased from Merck (Darmstadt, Germany). QA-Ch was synthesized according to (Zambito et al., 2008) and conjugated with MCD as already described (Cesari et al., 2020). The resulting QA-Ch-MCD had a molecular weight of 603 kg/mol and the following features: 8.8% acetylation degree, 33.1% degree of quaternarization with $n = 4$ (diethyldimethylene ammonium) length pendant chains, and 45.5% MCD degree of functionalization. All aqueous solutions/dispersions were prepared in mq water. Commercial chitosan, minimum 90% deacetylated from shrimp shell (Chito-clear FG90, Primex, Drammen, Norway) and average viscometric molecular weight of 590 kDa (Fabiano et al., 2021) was converted into a chitosan-HCl powder (Cs). Cs was prepared by making an aqueous chitosan suspension (12 g in 2000 mL) to pH 4.7 with 1 N HCl (about 43.5 mL) and lyophilizing the resulting solution after filtration. HCE-T human cell lines were obtained from the American Type Culture Collection (ATCC) and used at passages 19-29. Dulbecco's Modified Eagle Medium (DMEM), fetal bovine serum (FBS), L-glutamine, non-essential amino acids, and 100 U/mL penicillin and 100 mg/mL streptomycin, trypsin-EDTA, Dulbecco phosphate buffer solution, resazurin, and wheat germ agglutinin (WGA) were purchased from Gibco (Invitrogen corporation) (Da Silva et al., 2016).

6.2.2. Synthesis of Quaternarized Chitosan QA-Ch

The reaction to obtain the quaternarized chitosan, between starting chistoan and DEAE-Cl was conducted according to a previously documented procedure (Piras et al., 2018). Briefly, 3.0 g of chitosan (Ch) was dissolved in a round botton three-way flask containing 120 mL of 0.1 M HCl, and the mixture was stirred overnight. The resulting solution (pH<2.0) was adjusted to pH=4.7. Subsequently, 12.0 g of DEAE-Cl and 18 mL of 15% NaOH were sequentially added under vigorous stirring, maintaining a controlled temperature of 65 °C. Stirring and heating were sustained for 2 hours. The pH was maintained around the value of 8 by intermittent additions of 7.5% NaOH. Following this, the mixture was neutralized to pH=7 using 1 M HCl. The resulting viscous solution was underwent to dialysis through cellulose acetate membranes (14 kDa cutoff) in H₂O. The water was changed every 8-15 hours over a period of 3 days. Subsequently, the solution was filtered using cellulose acetate discs (pore size 0.45 μ m) and finally subjected to freeze-drying. This process to obtain the quaternarized derivative of chitosan, named as QA-Ch.

6.2.3. Synthesis of QA-Ch-Metil-β-Cyclodextrin conjugate (QA-Ch-MCD)

Synthesis was carried out as reported from Piras et al. 2018 (Piras et al., 2018). 400 mg of QA-Ch was accurately weighed. These were added to 8 mL of dimethyl sulfoxide (DMSO) and kept under magnetic stirring overnight in a two-necked round bottom flask under an inert nitrogen (N₂) atmosphere. The resulting solution was slowly added dropwise to 720 μL of hexamethylene diisocyanate (HMDI) combined with 10 mL of DMSO. The resulting solution was heated to 70°C, mixed with 65 μL of triethylamine (TEA) and kept under magnetic stirring for 3 hours. An inert atmosphere was maintained for the entire duration in order to complete the activation of the polymer. The resulting product was precipitated and cold washed with diethyl ether at 4°C. Subsequently, the product was redissolved in 3 mL of DMSO and 2.7 g of MCD in 8 mL of DMSO was added. 150 μL of TEA were added to the resulting mixture and kept under magnetic stirring for 3 hours at 70°C. The solution was then slowly dripped into hot water (about 90°C, 30 mL) and left to stir for 1 hour. After cooling, the reaction mixture was transferred to a dialysis tube with ethyl cellulose with a molecular weight cutoff of 12.5 kDa and dialyzed against water for 3 days. At the end of this process, the water-soluble material was separated from the dispersion by centrifugation at 20,000 rpm for 30 minutes at 4°C using a centrifuge. The supernatant was finally obtained after centrifugation.

6.2.4. Lyophilization

Lyophilization was carried out using a VirTis AdVantage wizard 2.0, SP Scientific freeze-dryer. The synthesized products underwent manual lyophilization after being placed in Petri dishes containing their respective aqueous solutions. The congealing temperature was set at -40°C, and the sublimation conditions were maintained at a pressure range of 30-40 mTorr with a temperature ranging from 15°C to 20°C. The duration of the lyophilization process varied between 15 and 17 hours for different samples.

6.2.5. Characterization of the QA-Ch-MCD conjugate

The QA-Ch-MCD conjugate was characterized through NMR measurements using a Bruker Avance II spectrometer operating at 250.13 MHz. The experiments were conducted at a constant temperature of 25°C±0.1°C. During data acquisition, the samples were dissolved in deuterated water (D₂O) at a concentration of 1%-2%.

6.2.6. Cell Culture Techniques

Biological evaluations of polymeric complexes were conducted using the HCE-T human corneal epithelial cell line.

6.2.7. Cell Viability assay

Cells were seeded in 96-well at 2×10^5 /well in 0,2 mL with standard medium, consisted of DMEM, 10% Fetal Bovine Serum, 0.1 mg/mL streptomycin, and 1000 IU/mL penicillin and incubated 24 h at 37 °C in 5% CO₂ environment. OLE-GS was tested in the concentration range of 10-500 μg/ml, while QA-Ch-MCD, QA-Ch and Ch were tested in the concentration range of 5-100 μg/ml. OLE-GS, QA-Ch-MCD and QA-Ch were dissolved in water mq, while Ch was dissolved in a solution of acetic acid 1%. For all samples the dilutions tested were carried out using medium. The cytotoxicity of the polymeric complexes was also evaluated. The development of the polymeric complexes and the polymeric mixture complexes was performed as reported in the following chapter. After 24 hours, the medium was removed and 100 μL of each sample was added. The plates were left in the incubator for 24 hours and subsequently the samples were removed, two washes were performed with 1x PBS and then 200 μL of a 20% resazurin solution in medium was added. After two hours of incubation, the plates were analyzed in fluorescence with Synergy MX excitation wavelength 530 nm and emission 590 nm. The assay was executed 3 times.

6.2.8. Preparation of polymeric complexes

The preparation of polymeric complexes was carried out by mixing OLE-GS and the polymer solutions in a 10:1 weight ratio. The mixtures were maintained in agitation for 1h at room temperature before the use. Then 500 μ L of the obtained solution were mixed with 500 μ L DMEM in volume ratio 1:1. For the OLE-GS the final concentration of 100 μ g/mL and was chosen to carry out the scratch test assay. For the polymeric mixture the amount of MCD and QA-Ch was chosen according to the characterization carried out after the synthesis.

6.2.9. OLE-GS stability study in simulated tear fluid (STF)

Polyphenols present in OLE-GS, both in their free form or complexed with QA-Ch-MCD, QA-Ch/MCD, Ch/MCD, Ch, and MCD, were investigated for stability in simulated tear fluid (STF) at pH 7.4. The STF composition included 50 mL of solution containing 336.4 mg of NaCl, 55.5 mg of KCl, 1.3 mg of glucose, 96.2 mg of NaHCO₃, 335 mg of albumin, and 1.3 mg of CaCl₂ (Asim et al., 2021). For each sample, 10 mg of Lyophilized OLE-GS were suspended in 2 mL of STF, while for the polymeric complexes, the mixture was formulated with the same weight ratios according with their formulation maintaining constant 10 mg of OLE-GS for 2 mL of solution. Subsequently, these solutions were placed in a water bath thermostated at 35 °C under continuous stirring. At 30-minute intervals, over to 4 hours, 50 μ L of STF was withdrawn and subjected to analysis for Total Phenolic Content (TPC). All experiments were meticulously conducted in duplicate to ensure the reliability and consistency of the obtained results.

6.2.10. Total polyphenols content (TPC)

The assessment of Total Phenolic Content (TPC) was conducted for the entire duration of the stability experiment. This approach enabled the determination of the percentage of polyphenols remaining unaltered in OLE-GS, both when the extract was complexed with QA-Ch-MCD or not. The evaluation was performed using the Folin-Ciocalteu spectrophotometric method, providing evaluation of the preservation of polyphenols contained in OLE-GS over time when complexed QA-Ch-MCD or not (Singleton et al., 1999). The absorbance was measured at 765 nm. The results were derived from a standard curve constructed with gallic acid (GA) (Sigma-Aldrich) and were reported as milligrams of gallic acid equivalent (GAE) per 100 grams of fresh weight (FW).

6.2.11. Differential Scanning Calorimetry (DSC)

The thermal behavior of OLE, QA-Ch-MCD, and QA-Ch/MCD was analyzed by a differential scanning calorimeter (TA DSC, Q250, USA, temperature accuracy \pm 0.05 °C, temperature precision \pm 0.008 °C, enthalpy precision \pm 0.08%). Dry high purity N₂ gas with a flow rate of 50 cm³ min⁻¹ was purged through the sample. 3-5 mg of each sample was loaded in pinhole hermetic aluminum crucibles and the phase behavior was explored under nitrogen atmosphere in the temperature range of -90 -140 °C with a heating rate of 10 °C min⁻¹. The temperature calibration was performed considering the heating rate dependence of the onset temperature of the melting peak of indium. The enthalpy was also calibrated using indium (melting enthalpy Δ mH=28.71 J g⁻¹). DSC experiments were carried out in duplicate.

6.2.12. *In vitro* Scratch Test Wound healing assay

The cells were seeded, in 12-well plates, 1.25×10^5 cells per well in DMEM medium containing 10% FBS serum. Complete confluence was achieved after 24 h at 37 °C and 5% CO₂. The resulting monolayer was scratched with a sterile pipette with p200 tip. After scratching, the wells of the plate were washed three times with PBS to remove debris and various dead cells. Then 2 mL of each sample to be tested was added. OLE-GS was tested in free form in a range of concentrations of 50 and 250 μ g/mL. Later the polymeric complexes were tested formulated as reported in their preparation. Micrographic images of each well were acquired using a camera with a 4x-objective at time zero and after 24 h. The acquired images were analyzed using the ImageJ Software to

determine the percentage of healing of the inflicted scratch. The following formula was used to determine the percentage of healing over time:

$$\text{Wound healing (\%)} = \frac{[(\text{Area T0} - \text{Area T})/\text{Area T0}] \times 100}{}$$

Where Area T0 is the area at time zero, Area T is the area at 24 h.

6.2.13. Antioxidant activity assay

The viability of the HCE-T was assessed by the resazurin assay. For this purpose, 2×10^5 cells per well were seeded in 96 well plates and placed in an incubator at 37 °C with 5% CO₂. The cells, 24 hours after seeding, were incubated for 24 hours with all formulations tested and OLE alone at concentrations chosen for the wound healing assay. At the end of the 24 hours treatment, 3 times washing with fresh PBS was carried out in order to completely remove any residual, then in order to develop an oxidative damage, cells were incubated one hour with 7.5 mM H₂O₂. The resazurin reagent was added after completely removing H₂O₂ from the wells through a suitable washing with PBS for 3 times (Migone et al., 2022).

6.2.14. In Vivo study

Two solutions were prepared for administration to rabbits. The first solution comprised 2 mg/mL of OLE-GS in its free form, while the second solution contained 2 mg/mL of OLE-GS complexed with 0.2 mg/mL of QA-Ch-MCD. Both solutions were formulated in water. Male New Zealand albino rabbits, weighing between 3.0-3.5 kg, were selected for the study and were treated in strict accordance with the guidelines outlined in Directive 2010/63 of the Council of the European Community. The procedures were approved by the Animal Protection Committee of the University of Pisa, in compliance with Legislative Decree 2014/26 dated 12 March 2019. The animal protocol received official approval from the Italian Ministry of University and Research (authorization no. 192/2019-PR). Administration involved instilling one drop (50 µl) of each study formulation into the rabbit's lower conjunctival sac. Subsequently, each rabbit's eye underwent meticulous monitoring over a 24 hours period, with observations recorded at specific time intervals from the initiation of the study (30, 60, 120, 360, and 1440 minutes). An overall irritation index (I_{irr}) was calculated by adding the total clinical evaluation scores for each observation time. A score of 2 or 3 in any category or an I_{irr} greater than 4 is considered an indicator of a clinically significant irritation. The monitoring aimed to detect any signs of conjunctival/corneal edema and/or hyperemia, providing valuable insights into the ocular effects of the administered formulations (Fabiano et al., 2022; Lallemand et al., 2005).

6.2.15. Statistics analysis

All data are presented as means \pm standard deviation (SD). The statistics analysis was performed with one-way ANOVA followed by Bonferroni post-test. $P < 0.05$ was considered indicative of a significant difference.

6.3. Results

6.3.1. Synthesis and characterization of QA-Ch and QA-Ch-MCD

By prior investigations (Zambito et al., 2006), the NMR analysis, using two-dimensional maps, demonstrated that the resulting derivatives exhibited the characteristic structure of ammonium conjugates (N⁺-Ch). Specifically, these derivatives manifested as N, O-[N, N-diethylaminomethyl (diethylidimethylene ammonium)_n] methylchitosans, featuring diminutive side chains of proximate quaternary ammonium groups. These quaternary ammonium groups were found to be partially substituted on the chitosan repeating units. In particular, both the degree of substitution (GS) and the average number of quaternary ammonium groups within each small chain (n) exhibited pronounced sensitivity to the pH of the reaction mixture. Maintaining the pH

at a precise value of 8 proved to be necessary for achieving reproducibility in the reaction. We synthesized QA-Ch-MCD because MCD, according to study reported in literature, led to a conjugate with higher solubility property. The resulting QA-Ch-MCD had a molecular weight of 603 kg/mol and by the interpretation of ^1H NMR spectrum demonstrated the following features: 8.8% acetylation degree, 33.1% degree of quaternarization with $n = 4$ (diethyldimethylene ammonium) length pendant chains, and 45.5% MCD degree of functionalization (figure 1).

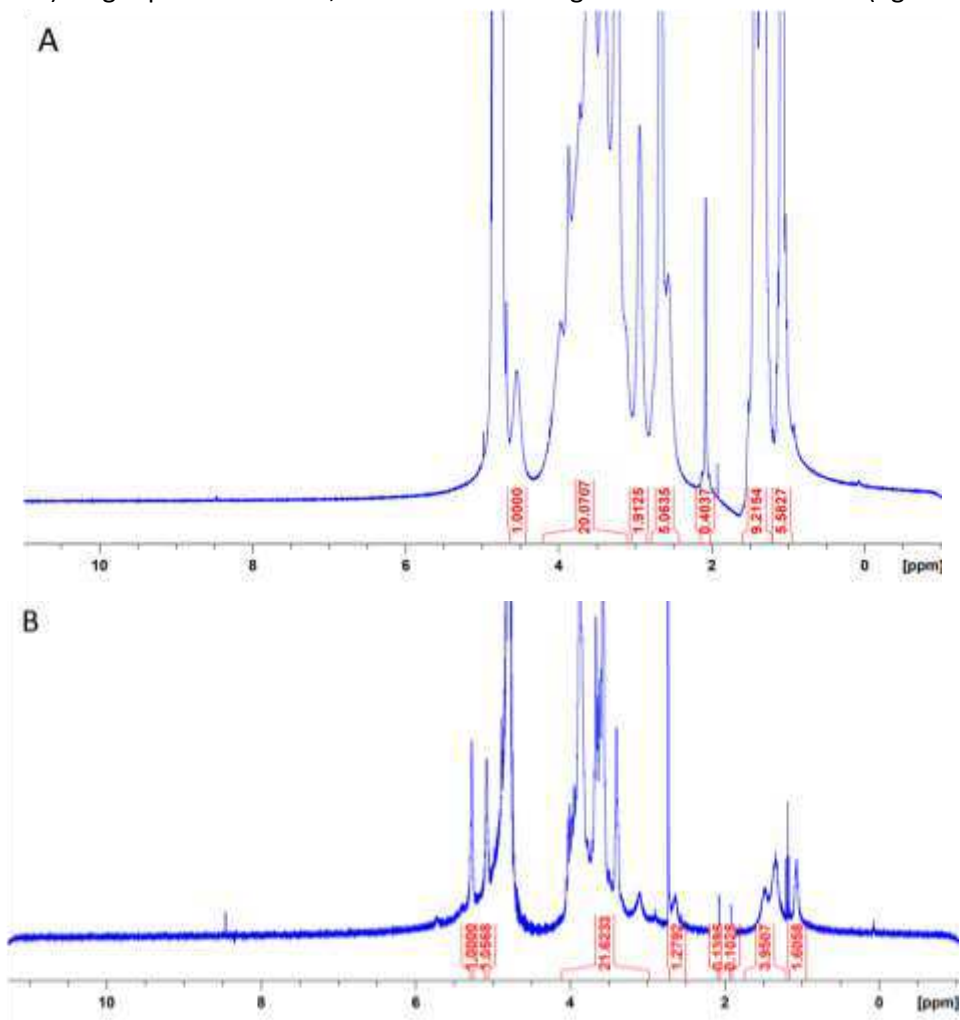


Figure. ^1H -NMR spectra of QA-Ch (A) and QA-Ch-MCD (B). Notes: QA-Ch (300 MHz, D₂O): $\delta = 4.5$ (s, anomeric), 4.2–2.2 (m, protons of the pyranosidic ring, methylene protons of pendant quaternized chains $-\text{CH}_2\text{CH}_2\text{N}+(\text{CH}_2\text{CH}_3)_2\text{CH}_2-$ and $-\text{CH}_2\text{N}(\text{CH}_2\text{CH}_3)_2$), 2.0 (s, methyl protons of N-acetylglucosamine), 1.6–1.1 (m, methyl protons of the ethyl moieties closed to ammonium pendants $\text{N}^+ \text{CH}_2\text{CH}_3$), and 1.1–0.8 ppm (m, methyl protons of the terminal part of DEAE chains $\text{N}(\text{CH}_2\text{CH}_3)_2$). QA-Ch-MCD (300 MHz, D₂O) $\delta = 5.13$ and 4.95 (s, MCD anomeric), 4.2–2.6 (m, protons of the pyranosidic ring, methylene protons of pendant quaternized chains $-\text{CH}_2\text{CH}_2\text{N}+(\text{CH}_2\text{CH}_3)_2\text{CH}_2-$ and $-\text{CH}_2\text{N}(\text{CH}_2\text{CH}_3)_2$, methylene protons closed to the N of the spacer $-\text{NHCH}_2(\text{CH}_2)_4\text{CH}_2\text{NH}_2$); 2.5 (s, methylene protons of not protonated N of the DEAE pendant $-\text{CH}_2\text{N}(\text{CH}_2\text{CH}_3)_2$), 2.0 (s, methyl protons of N-acetylglucosamine), 1.7–1.1 (m, methyl protons of the ethyl moieties close to ammonium pendants $\text{N}^+(\text{CH}_2\text{CH}_3)_2$, and methylene protons of the central part of spacer chain $-\text{NHCH}_2(\text{CH}_2)_4\text{CH}_2\text{NH}_2$), and 1.0–0.7 ppm (m, methyl protons of the terminal part of DEAE chains $-\text{N}(\text{CH}_2\text{CH}_3)_2$). Compounds in bold correspond to peaks in the spectra. Abbreviations: DEAE, 2-diethylaminoethyl chloride; MCD, methyl- β -cyclodextrin; QA-Ch, quaternary ammonium-chitosan; QA-Ch-MCD, methyl- β -cyclodextrin-quaternary ammonium chitosan; s, singlet; m, multiplet.

6.3.2. OLE-GS stability study in STF

The evaluation of the stability of polyphenols contained in OLE-GS in simulated tear fluid (STF) was performed using the Folin-Ciocalteu reagent (figure 2). The degradation curves of OLE-GS in the STF medium, reported in the figure, illustrate a decline in Total Phenolic Content (TPC) over time. Non-encapsulated OLE-GS demonstrated an inability to impede the degradation of polyphenols in the solution, potentially attributed to the rapid oxidation of antioxidant molecules present in OLE-GS. However, as shown in the figure, after 4 hours, all formulations exhibited a capacity to slow down the polyphenol degradation of OLE-GS. Specifically, QA-Ch-MCD/OLE-GS and QA-Ch/MCD/OLE-GS formulations were particularly effective, maintaining the TPC at approximately 76% and 73% of the initial content, respectively. This observation underscores the protective capability of QA-Ch-MCD in protecting OLE-GS from degradation in simulated tear fluid.

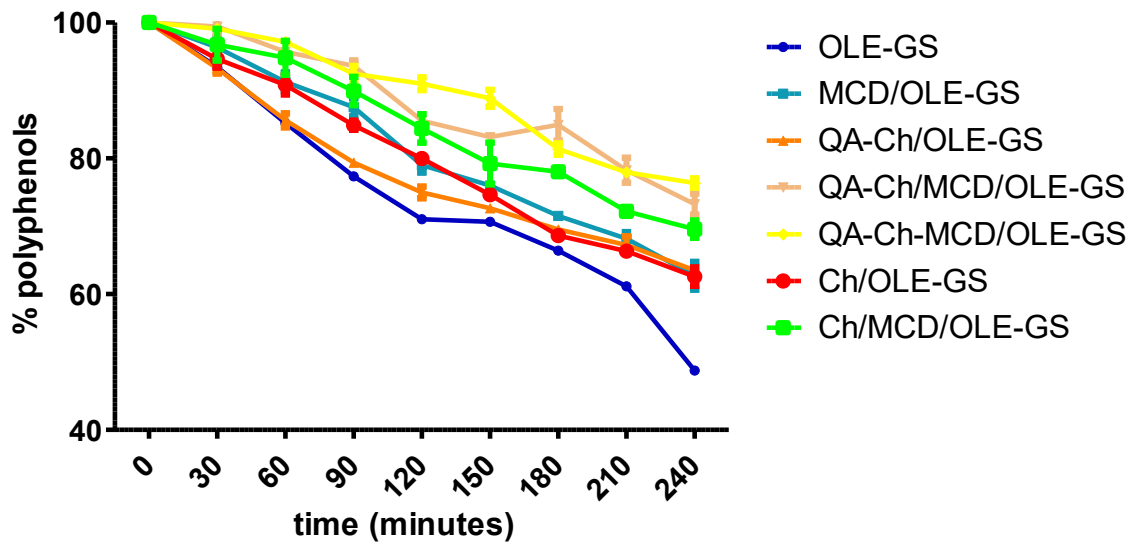


Figure 2. OLE-GS stability in simulated tear fluid (STF) at 37 °C. Means \pm SD (n = 2).

6.3.3. DSC

The thermal characteristics of the three samples were scrutinized within the temperature range of -90 to 140 °C. In the case of OLE-GS, a degradation of the extract was identified, starting at 120 °C, as evident from the scattering of the thermogram line (figure 3). A similar behaviour was observed when OLE-GS was mixed with QA-Ch-MCD. In the QA-Ch-MCD/OLE-GS freeze-dried sample, a different effect on OLE-GS by the polymer was observed. Within the temperature range associated with the degradation of OLE-GS, no detectable degradation phenomena were noted. This safeguarding effect is attributed to the plausible intercalation of OLE-GS into the polymer matrix.

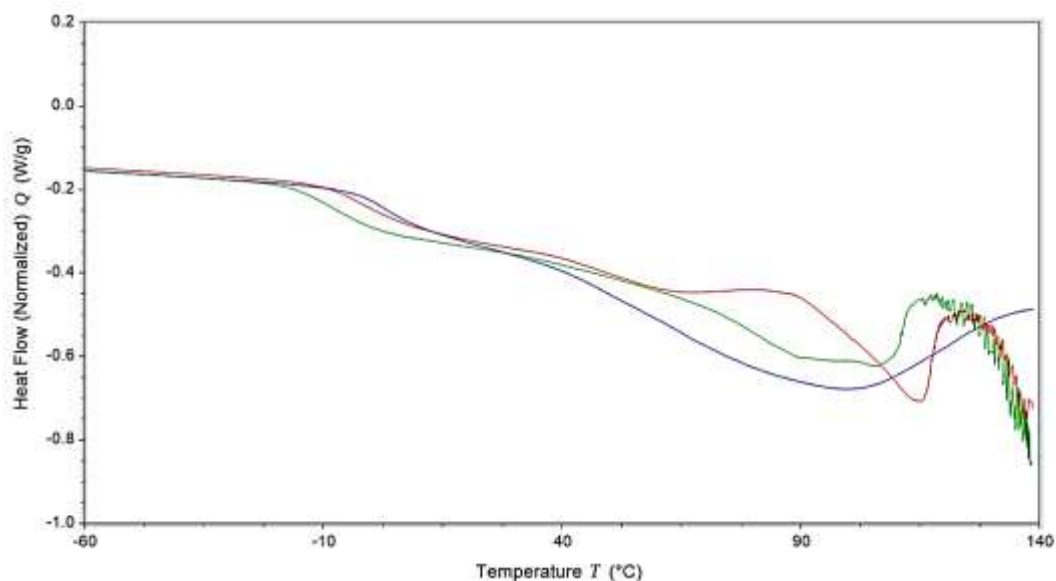


Figure 3. DSC analysis for red OLE-GS, blue QA-Ch-MCD/OLE-GS freeze-dried, green QA-Ch-MCD/OLE-GS mixture; (n = 2).

6.3.4. Biological investigation: Cell viability assay ad in vitro scratch test

OLE-GS, Ch, MCD, QA-Ch and QA-Ch-MCD underwent to *in vitro* biological investigations for the evaluation of cytotoxicity. The HCE-T cells line were incubated with polymeric material and free OLE-GS 24 hours at 37 °C in 5% CO₂ environment and subsequently analyzed by the resazurin colorimetric assay. This assay was performed in order to choose the right concentration to be used in subsequent wound healing studies. OLE-GS did not show cytotoxicity for all tested concentration in a range 10-500 µg/ml. Both Ch and MCD did not show cytotoxicity for all the assayed concentrations, in the range 5-100 µg/ml. The cell viability value was always found to be over 80% of control cells viability (cells grown in the absence of any treatment), indicating a high biocompatibility of the same (figure 4). Instead, the treatment of cells with QA-Ch showed an evident toxicity also at the lowest tested concentration of 5 µg/mL showing cell viability values around 40% (range of concentration tested 5-100 µg/mL). The treatment of cells with QA-Ch-MCD show an absence of toxicity at the concentrations of 5-10 µg/mL, while for the concentration of 50-100 µg/mL was found a cell viability value around 75% of control cells viability (cells grown in the absence of any treatment). For this results the concentration of 10 µg/mL of QA-Ch-MCD was chosen to carry out the following tests. For the other polymeric material was chosen the concentration according to the weight ratio contained in QA-Ch-MCD. For the Ch was selected the same concentration of QA-Ch, in order to verify if the modification occurred on the native Ch could improve their ability compared with the starting one.

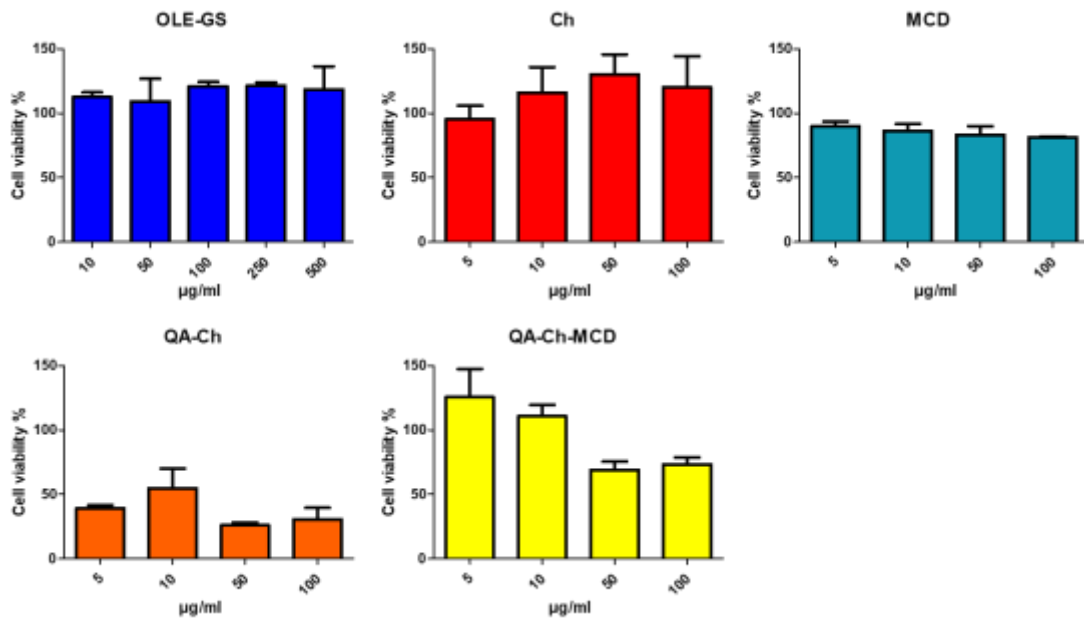


Figure 4. HCE-T viability after 24 h of incubation with: OLE-GS; Ch, MCD, QA-Ch and QA-Ch-MCD in culture medium. Data are expressed as % viable cells referred to 100% control (untreated cells). Data are reported as mean \pm SD (n = 6).

For OLE-GS some concentrations were tested for the *in vitro* scratch test assay in order to verify the optimal concentration to carry out the following experiment. For this reason the HCE-T cells were seeded, in 12-well plates, 1.25×10^5 cells per well in DMEM medium containing 10% FBS serum. Complete confluence was achieved after 24 h at 37 °C and 5% CO₂. After 24 h the % of healing of wound was significant different from the untreated cells using the concentration of 100 µg/mL (figure 5). The concentration of 100 µg/mL if OLE-GS was chosen to prepare the polymeric complexes using the concentration of polymeric material selected in the previously performed cell viability assay.

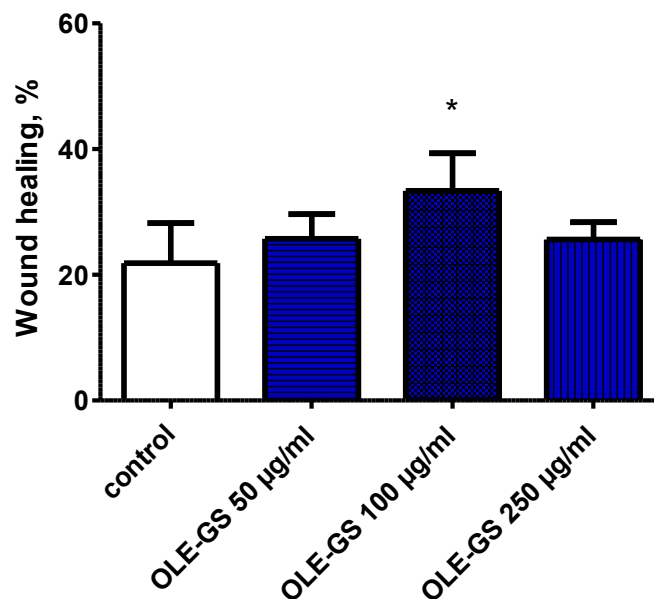


Figure 5. Scratch test assay for OLE-GS alone in range of concentration 50-250 µg/mL. Wound closure rates expressed as percentage of scratch closure after 24 h compared to initial area.

*P<0.05 vs control

Cytotoxicity investigations were conducted to assess the safety of the polymer complexes. The synthesis of polymeric complexes was carried out as detailed in the relevant paragraph. For all polymeric complexes and mixtures, no observed toxicity was noted, except in the cases of QA-Ch and QA-Ch/OLE-GS, where cell viability values were approximately 35%. Notably, this adverse effect was absent when QA-Ch was physically mixed with MCD, both in the presence and absence of OLE-GS. This interesting behavior may be attributed to the interaction between the positive charge on the quaternary ammonium of QA-Ch and the hydroxyl groups of MCD, leading to the formation of hydrogen bonds (figure 6) (Cesari et al., 2020). Based on these findings, it was decided not to include QA-Ch and QA-Ch/OLE-GS in the wound healing test due to their observed toxicity, while all other prepared formulations will be utilized for further assessments.

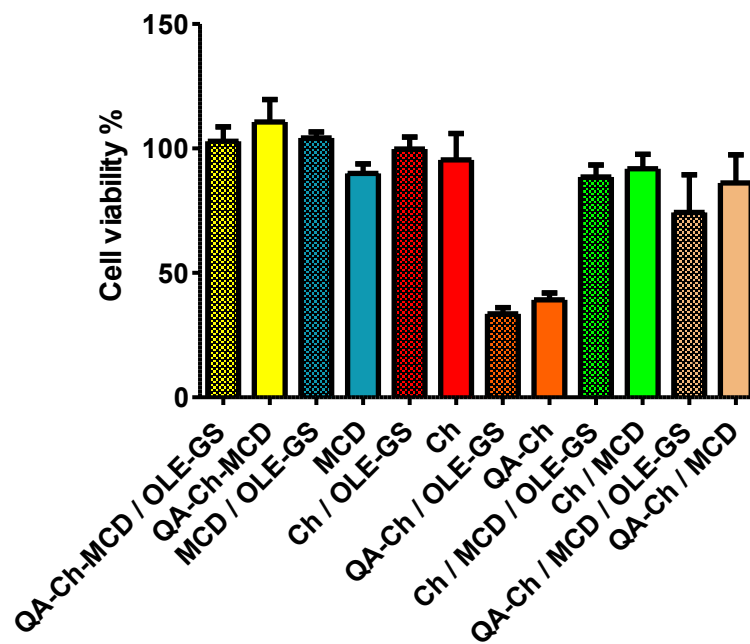


Figure 6. HCE-T viability after 24 h of incubation polymeric complexes and polymeric material in culture medium. Data are expressed as % viable cells referred to 100% control (untreated cells). Data are reported as mean \pm SD (n = 6).

The evaluation of wound healing activity was conducted both for the polymeric material alone and for polymeric complexes. The figure illustrates that the polymeric material alone lacks the capability to effectively heal wounds compared to the control (figure 7). Subsequently, the polymeric complexes were tested. All formulations, with the exception of Ch/OLE-GS, exhibited a significant improvement in wound healing compared to the control. Notably, QA-Ch-MCD/OLE-GS demonstrated superior efficacy in reducing the scratch compared to all other formulations tested, including OLE-GS alone (figure 8). A distinctive behavior is observed in Ch/OLE-GS formulations that not appear different from the control.

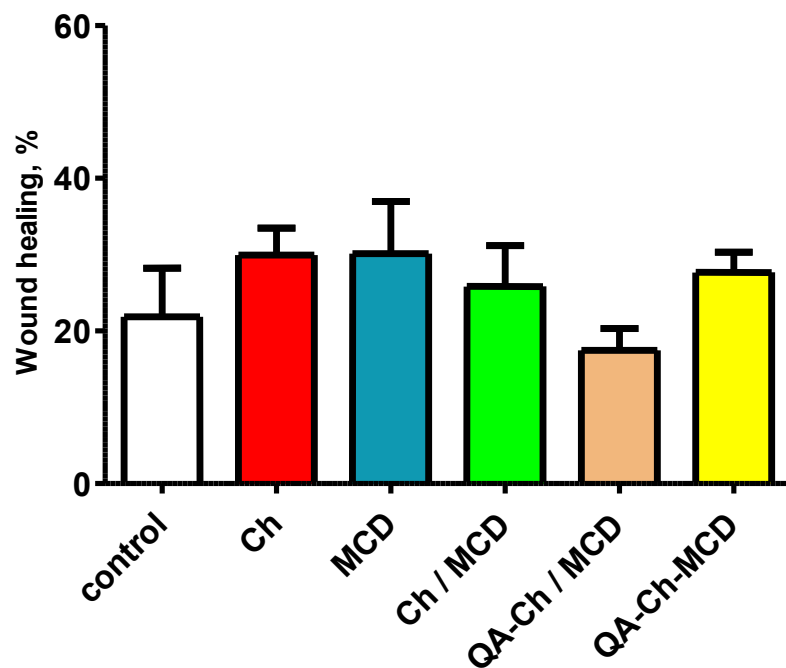


Figure 7. Scratch test assay for the polymeric material. Wound closure rates expressed as percentage of scratch closure after 24 h compared to initial area.

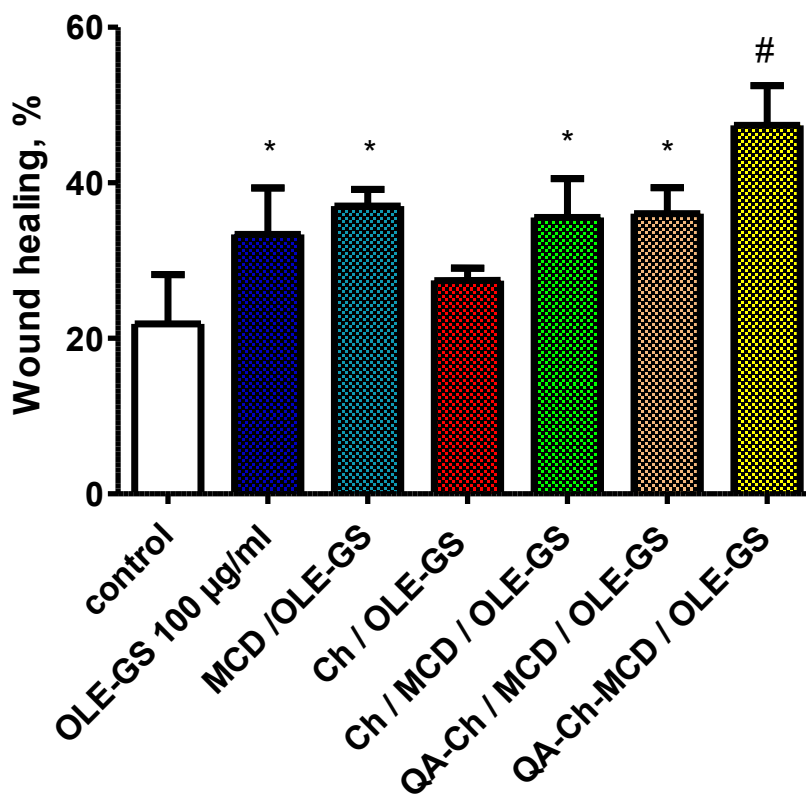


Figure 8. Scratch test assay for OLE-GS alone and the polymeric complexes. Wound closure rates expressed as percentage of scratch closure after 24 h compared to initial area. *P<0.05 vs control; #P<0.5 vs all

6.3.5. Antioxidant activity assay

The assessment of protective activity against oxidative damage resulting from H₂O₂ treatment was conducted. The results show that all formulations containing OLE-GS and OLE-GS alone are able to increase cell viability following H₂O₂ induced oxidative damage. Cell viability following oxidative damage is around 50% compared to the control (cells not subjected to oxidative damage). All vehicles alone, are capable of containing oxidative damage except MCD (figure 9).

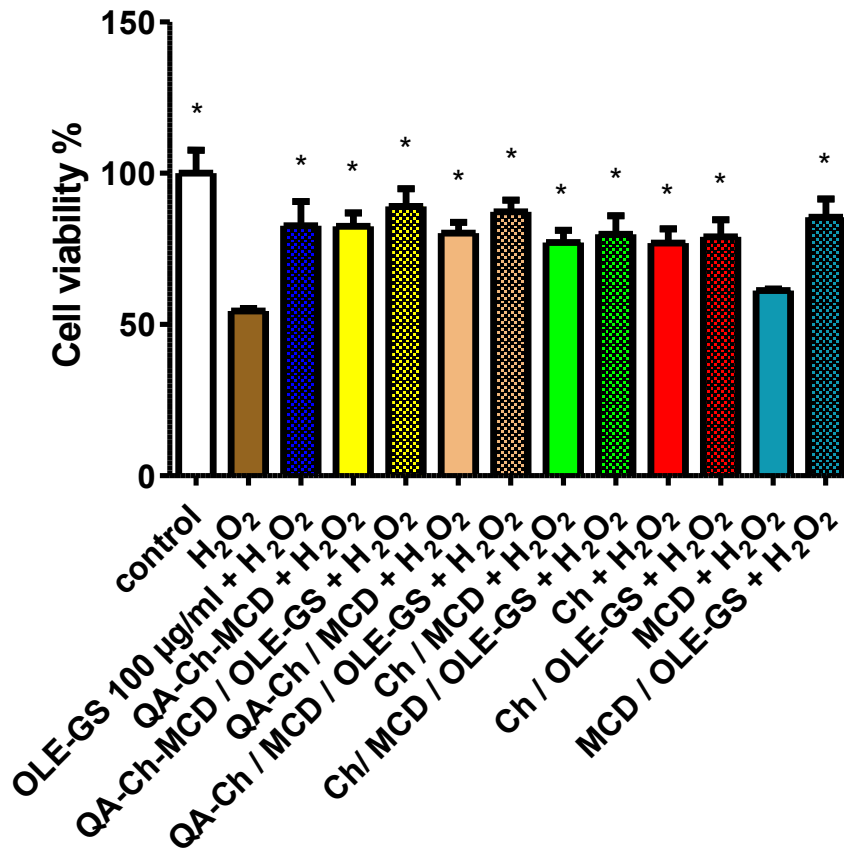


Figure 9. HCE-T viability after 24 h pre-treatment with tested formulation in culture medium, and subsequent 1 h treatment with 7.5 mM H₂O₂. Data are expressed as % viable cells compared to negative control (H₂O₂). *, significantly different from H₂O₂, p<0.05.

6.3.6. *In Vivo* study: Draize test

In the modified Draize test, the eye drops containing 0.2% OLE-GS exhibited no signs of conjunctival redness, secretion, or conjunctival edema throughout the entire experimental period, as depicted in the accompanying figure. The combined I_{irr} score for both eye drop formulations remained consistently below three. Therefore, it can be inferred that both OLE-GS and QA-Ch-MCD/OLE-GS demonstrate good ocular tolerability (figure 10).













OLE-GS	QA-Ch-MCD/OLE-GS	
		Non treated eye
		30 min
		60 min
		120 min
		360 min
		1440 min

Figure 10. Modified Draize test representation. On the first row are shown the untreated eyes of rabbit used as reference; on the left column the same rabbit right eye after instillation of one drop of eye drops containing 0.2% (m/V) OLE-GS at times: 30 min, 1 h, 2 h and 6 h, 24 h respectively; on the right column the same rabbit left eye after instillation of one drop of eye drops containing 0.2% (m/V) QA-Ch-MCD/OLE-GS at times: 30 min, 1 h, 2 h and 6 h, 24 h respectively.

6.4. Discussion

The literature has highlighted the superior ability of QA-Ch to form complexes compared to native Ch. This characteristic is further emphasized in the case of QA-Ch-MCD, showing enhanced complexation compared to conjugated MCD (Cesari et al., 2020). The conjugation of MCD with QA-Ch has not only demonstrated improved affinity and stability but has also exhibited various advantages, making it a favorable choice for formulating biocompatible eye drops capable of efficiently complexing natural or synthetic molecules. The dsc analysis provides insights into the interaction between OLE-GS and QA-Ch-MCD affirming the theme of complexation between these. Additionally, stability experiments reveal that all polymers used can mitigate the degradation of polyphenols over time. Notably, QA-Ch-MCD stands out as the most promising polymer in safeguarding antioxidant molecules from degradation in simulated

tear fluid (STF). This superior performance is attributed to the excellent complexing capacity of QA-Ch-MCD. In summary, the research underscores the advantageous properties of QA-Ch and its conjugate QA-Ch-MCD, especially in the context of complex formation and stability, making them valuable candidates for the development of biocompatible formulations, such as eye drops. The findings also highlight the potential application of QA-Ch-MCD in protecting antioxidant compounds in various pharmaceutical contexts (Zambito et al., 2022). The conjugation of the quaternarized derivative QA-Ch with MCD results in the formation of a highly soluble polymer. However, it has been observed that QA-Ch carries a toxicity concern attributed to the positive charge on the quaternary nitrogen. To address this issue, the conjugation of QA-Ch with MCD is employed, fostering the establishment of hydrogen bonds between the hydroxyl groups of MCD and the quaternary nitrogen of QA-Ch. This interaction, whether of a chemical or physical nature (conjugated or mixed), effectively mitigates the toxicity of QA-Ch, rendering it suitable for the development of polymeric complexes for drug delivery applications. The process of deriving QA-Ch from native Ch not only enhances its solubility in water but also augments its capacity for complexation. Dynamic Light Scattering (DLS) analyses conducted after the formation of polymer complexes reveal the absence of stable nanosystems in formulations, except for Ch/OLE-GS. In fact, Ch/OLE-GS successfully forms stable self-assembly nanosystems, providing a plausible explanation for its distinct behavior in wound repair experiments compared to other formulations containing OLE-GS. The distinctive behavior observed in Ch/OLE-GS formulations may be attributed to the formation of self-assembling nanoparticles in this case. The resulting stiffer structure potentially restricts the interaction between OLE-GS and the polymer. Indeed, analysis using dynamic light scattering (DLS) confirmed that only the combination of Ch and OLE-GS is capable of forming self-assembling nanoparticles with a size of 172 ± 2 nm and a polydispersity index (PDI) of 0.29 ± 0.02 . OLE-GS exhibits noteworthy wound-healing properties, either when employed independently or in conjunction with complexing agents. A preliminary study, conducted to determine the optimal concentration of OLE-GS, reveals a crucial threshold effect. Concentrations of 250 $\mu\text{g/mL}$ and 50 $\mu\text{g/mL}$ prove ineffective in promoting wound healing, underscoring the significance of the concentration of 100 $\mu\text{g/mL}$ that appears significantly different from the control. At this concentration, OLE-GS demonstrates a pronounced and statistically significant improvement in wound healing compared to the control group. This concentration-dependent behavior aligns with observations in the existing literature, where similar trends have been reported for various extracts. It is hypothesized that the antioxidant molecules within an extract possess the capacity to enhance cell proliferation within a specific concentration range. Beyond this threshold, higher concentrations may lose their efficacy for this particular purpose (Ruszymah et al., 2012). The complexation of OLE-GS with QA-Ch-MCD demonstrates a notable enhancement in the wound-healing effects within the proposed *in vitro* model, aligning with existing literature findings on the positive impact of complexation. This outcome not only underscores the efficacy of the complexation process but also suggests a promising alternative application for this specific polymer in wound healing. Additionally, significant insights emerge from the assessment of antioxidant activity in both the tested polymer complexes and the individual polymers. All samples, with the exception of MCD, exhibit the capability to decrease oxidative stress damage induced by H_2O_2 . This indicates the potential of these polymer complexes, as well as the individual polymers, in countering oxidative stress, further emphasizing their relevance in biomedical applications. OLE-GS has been reported for its antioxidant properties and its ability to provide protection against oxidative stress damage. This protective effect is attributed to the presence of antioxidant molecules, particularly polyphenols, within OLE-GS. The antioxidant effect of chitosan polymers may be attributed to various mechanisms, predominantly through its scavenging capacity. The most well-supported mechanism involves its chelating action towards metal ions. Additionally, there is evidence suggesting that chitosan can scavenge free radicals and chelate metal ions by donating hydrogen or lone pairs of electrons. The robust metal-ion chelating ability exhibited by chitosan underscores its potential as a natural product antioxidant (Ivanova & Yaneva, 2020). These

considerations hold significance not only for the primary objective of facilitating wound repair in the cornea but also for the secondary application of the eye drop's antioxidant activity in combating corneal inflammation. This dual functionality underscores the potential versatility and broader therapeutic benefits of the eye drop formulation, positioning it as a valuable tool in addressing both wound healing and inflammation management in the context of corneal health.

7. Stabilization of nano-aggregates based on thiolated hydroxypropil- β -cyclodextrin for pulmonary delivery

Positive perspectives are arising for the development of formulations containing cyclodextrins as solubility enhancers and mucoadhesive polymers (Levy et al., 2019). Such formulations are able to interact with the mucous layer improving the bioavailability and local retention of poorly soluble drugs. Thiolated cyclodextrins are mucoadhesive excipients, with the thiol moieties able to bind to the cysteine residues of the mucins and establishing disulphide bridges (Grassiri et al., 2022). Meanwhile, mucoadhesive nanoparticles consisting of thiolated cyclodextrins are thought for increasing drug delivery, improving drug stability and solubility of easily oxidizable poorly water soluble active ingredients. In particular, cross-linked thiolated cyclodextrins can be used to enhance the beneficial pharmacological properties of corticosteroids, such as dexamethasone (DMS), and natural polyphenol products for the treatment of inflammatory lung diseases (Trotta & Scalia, 2017). The olive leaf extract (OLE) is particularly rich in polyphenols widely used in therapy due to their antioxidant and anti-inflammatory properties. OLE has been extensively studied for its beneficial effects on the cardiovascular level as well as for its antioxidant, anti-inflammatory properties (Fabiano et al., 2021). Moreover, water stress, meaning the lack of water administration, can represent a resource for the production of plants with a higher metabolite content than those grown under normal conditions. In particular, a dried extract of olive leaves of the Giaraffa variety subjected to drought stress was used for this work (OLE-GS).

7.1. Introduction

Inhalation is a widely employed method of drug administration, serving as a pivotal route for various medical applications. It proves instrumental for the targeted delivery of local drugs, such as treatments for bronchial diseases, chemotherapy, and antibiotics. Simultaneously, it plays a crucial role in administering systemic drugs, including insulin therapy and gene therapy (Levy et al., 2019). This versatile approach ensures the effective and efficient distribution of medications, offering tailored solutions for a spectrum of medical needs (Perinel et al., 2017). An inhalation device plays a critical role in ensuring targeted deposition of drugs at specific sites within the lungs. In the case of drugs designed for topical action, inhalation administration presents the advantage of requiring a relatively lower drug dose. This allows for direct action on the target organ, resulting in a reduction of systemic side effects and a quicker onset of action. On the other hand, for systemic drugs, this delivery route offers the opportunity to bypass challenges associated with poor absorption through the gastrointestinal tract. Additionally, it provides the potential for achieving more favourable pharmacokinetic profiles, enhancing the overall effectiveness and efficiency of drug therapy (Boe et al., 2001). Respiratory diseases currently represent an enormous and growing health and economic burden across Europe, with over 600,000 deaths and 6 million hospitalizations per year (Gibson et al., 2013). Despite growing medical needs in respiratory medicine, there has been limited introduction of new effective drugs in the past 40 years. Respiratory medicine lags behind other fields like cardiovascular, metabolic, or neurological, with fewer innovative therapies and a higher rate of failures (Guo et al., 2021). Positive perspectives are arising for the development of aerosolized formulations containing cyclodextrins (CD) as solubility and absorption enhancers for pulmonary delivery (Qin et al., 2023; Schwarz et al., 2017). CD are cyclic oligosaccharides consisting of α -D-glucopyranoside units and linked in a cyclic form by α -(1-4)-glycosidic bonds. CD are employed in pharmaceutical formulations for delivering poorly soluble drugs or forming complexes with natural extracts. The formation of CD complexes with poorly soluble molecules in aqueous solution induces chemical-physical changes in the guest molecule. This complexation results in increased stability by protecting active principles against oxidative and thermal degradation,

hydrolysis, and masking unpleasant odours and tastes (Li et al., 2019). In ocular applications, CD contribute to forming water-soluble complexes, improving drug absorption, ensuring aqueous stability, and minimizing irritation (Kurkov & Loftsson, 2013). Recently, a derivative of hydroxypropyl- β -cyclodextrin (HP- β -CD), thiolated hydroxypropyl- β -cyclodextrin (HP- β -CD-SH), has been synthesized, exhibiting notable mucoadhesive properties, forming disulfide bonds with cysteine-rich subdomains of mucus glycoproteins, thus further promoting drug absorption compared to parent CD (Grassiri et al., 2022). To the best of our knowledge, Miyajima and his colleagues were the first to suggest that α CD and γ CD self-associate to form aggregates in aqueous solutions (Miyajima et al., 1983). CD were found to form transient clusters that dissociate during the manipulation of CD dispersion in water and, therefore, are difficult to detect, for example, by ^1H NMR. With the advent of new techniques for studying nanosystems, including dynamic light scattering, CD self-aggregates have received increasing attention from researchers. In fact, it has been demonstrated that with the formation of CD nanoaggregates, biopharmaceutical benefits are obtained; for example, better penetration of CD aggregates through mucus (Calleja et al., 2014), or better promotion of ocular bioavailability of topically administered drugs compared to non-aggregated CD (Loftsson et al., 2012). Hence the idea of exploiting the thiol groups present on thiolated CD to prepare cross-linked nanoparticles. The objective of this work is to compare the ability of cross-linked thiolated CD nanoparticles to promote the activity of two different active ingredients, namely dexamethasone (DMS) and olive leaf extracts (OLE), compared to transient CD nanoaggregates. DMS was chosen as a model drug due to its poor solubility in water and its widespread use in lung administration. While OLE was chosen because the usefulness of natural polyphenols for the treatment of inflammatory lung diseases is reported (Trotta & Scalia, 2017). Hereby, medicated cross-linked HP- β -CD-SH nanoparticles were prepared and nebulized onto lung epithelial cell monolayers to evaluate the DMS permeation or the antioxidant effect of OLE in comparison to formulations based on non-cross-linked HP- β -CD-SH or HP- β -CD.

7.2. Materials and methods

7.2.1. Materials

Hydroxypropyl- β -cyclodextrin (HP- β -CD) MW 1380 Da (SR: 0.6), dexamethasone (DMS), thiourea, Ellman's reagent (2,2'-dinitro-5,5'-dithiobenzoic acid), L-cysteine hydrochloride monohydrate, tris(hydroxymethyl)aminomethane, Sephadex G-15, RPMI-1640 medium (RPMI), Insulin-Transferrin-Selenium (ITS), Trypsin-EDTA and Triton X-100, a mixture of antibiotics consisting of an aqueous solution of penicillin (10,000 U/mL) and streptomycin (10,000 $\mu\text{g}/\text{mL}$), 10 mM phosphate buffer pH 7.3 without Ca^{2+} and Mg^{2+} (PBSA), Hanks' Balanced Salt Solution (HBSS), Dulbecco phosphate buffered saline (DPBS), DMSO, DMSO- d_6 , and a trypsin-EDTA buffer solution containing 0.25% trypsin were all purchased from Sigma-Aldrich (Darmstadt, Germany). The reagents 1,8-Bis-Maleimidotriethilen Glicole (BM(PEG)2), PM: 308,29 g/mol and 1,11-Bis-Maleimidotriethilen Glicole (BM(PEG)3), PM: 352.34 g/mol were purchased from Thermo Fisher Scientific. Cell proliferation reagent (WST-1) was provided by Roche diagnostic (Milan, Italy). Human lung adenocarcinoma NCI-H441 epithelial cell line was purchased from the American Type Culture Collection LGC standards ((ATCC HTB-174), Milan, Italy) and propagated as indicated by the supplier. Olive leaf extracts of the Giarruffa varieties subjected to water stress (OLE-GS) was supplied by Life Sciences Department of the University of Siena, Siena (SI), Italy and previously characterised (Cerri et al., 2024).

7.2.3. Synthesis and purification of thiolated hydroxypropyl- β -cyclodextrin (HP- β -CD-SH)

The synthesis and purification of HP- β -CD-SH was performed as previously described (Grassiri et al., 2022). Briefly, 400 mg of HP- β -CD were solubilized in 2 mL of 10% acetic acid, and 2.14 g of

thiourea were dissolved at 40 °C under stirring in 8 mL of 0.44 M HCl. Subsequently, the thiourea solution was added dropwise to that of HP- β -CD. The resulting mixture was irradiated in a microwave device (Microwave Biotage Initiator) with temperature regulation and maximum power set at 90 Watts. Irradiation was carried out for 5 minutes at 87°C and for 50 minutes at 80°C. After this first phase, hydrolysis was started by adding a few drops of 10 M NaOH until a pH of approximately 8-9 was reached. The resulting mixture was further microwave irradiated for 3 minutes at 80°C. Purification was carried out by drying the product using a rotary evaporator (BÜCHI, Italy) at a temperature of 30–40 °C. Subsequently, the solid obtained was subjected to five washes, each with 20 mL of acetone, each followed by centrifugation for 20 minutes (5000 rpm; room temperature). The product was freeze-dried (VirTis freeze-dryer, freezing temperature -40 °C, drying at 30-40 mTorr, up to 16 °C) and subsequently dissolved in Milli-Q water at a concentration of 100 mg/mL. Purification was completed by size exclusion chromatography, using a chromatographic column with a diameter of 1.5 cm and a length of 30 cm, packed with Sephadex G-15 resin (22 cm). Milli-Q water was used as the mobile phase.

7.2.4. Synthesis and purification of nanoparticles based on HP- β -CD-SH (HP- β -CD-SH-NP)

The cross-linker BM(PEG)2, or BM(PEG)3 was used to form stabilized HP- β -CD-SH clusters and transformed them into nanoparticles. To a solution of HP- β -CD-SH 10 mg/mL in HBSS left stirring at room temperature overnight, variable volumes of BM(PEG)2 were added, at a concentration of 6.2 mg/mL in DMSO, or BM(PEG)3, at a concentration of 7 mg/mL in DMSO, left stirring for 2 hours at 4°C in a tilting plate. To stop the reaction, for each mL of solution, 50 μ L of cysteine at a concentration of 62 mg/mL in HBSS were added. The dispersion was incubated at room temperature for 15 minutes and subsequently ultracentrifuged (Thermo Fisher Sorvall MTX150) at 100,000 rpm for 20 minutes at 4°C thus obtaining a pellet with a gelatinous consistency. For purification, the HP- β -CD-SH-NP pellet dispersed in 1 mL of Milli-Q water was extruded 3 times (Avanti Polar Lipids mini extruder) through a filter with a diameter of 0.1 μ m. After each extrusion approximately 0.8 mL of solvent was discarded and the volume was brought back to 1 mL with Milli-Q water before repeating the extrusion. For cell viability assays HP- β -CD-SH-NP was diluted to the desired concentration with RPMI medium. For the nebulization tests the sample was diluted with HBSS.

7.2.5. Characterization of HP- β -CD-SH-NP and study of the reaction by NMR

NMR analyzes were performed using a Bruker 400 UltraShieldTM spectrometer operating at 400 MHz for the ¹H core. During acquisition, the temperature (18 °C) was controlled via the Varian control unit (accuracy + 0.1 °C). HP- β -CD-SH was solubilized in DMSO-d6 or D₂O at a concentration of 10 mg/mL. To control the reaction, the cross-linker BM(PEG)3 was dissolved in DMSO-d6 and added to HP- β -CD-SH solution. The reaction was monitored for 24 hours.

7.2.6 Determination of the association constant for cyclodextrins/DMS and cyclodextrins/OLE-GS

For this analysis the Benesi-Hildebrand method was used as previously described (Grassiri et al., 2022). Dispersions at different concentrations ranging from 0 to 100 mg/mL of HP- β -CD, or HP- β -CD-SH or HP- β -CD-SH-NP in HBSS were prepared. To determine the cyclodextrin/DMS association constant, 500 μ L of a 5.8 μ M DMS solution were added to 500 μ L of these dispersions. These were left to stir overnight at room temperature. The same procedure was repeated to determine the cyclodextrin/OLE-GS association constant by adding 500 μ L of OLE-GS 0.6 mg/mL in HBSS to 500 μ L of each cyclodextrin dispersions. For the samples containing DMS the analysis of the filtered solutions was carried out using UV at a wavelength of 258 nm, for those containing OLE-GS a wavelength of 290 nm was used.

7.2.7. Study of the complexation of DMS with HP-β-CD-SH-NP

The complexation of DMS with HP-β-CD-SH-NP was carried out by two different loading modes. In one case DMS was complexed with HP-β-CD-SH followed by reaction with cross-linker, in the second DMS was added to a preformed HP-β-CD-SH-NP dispersion. In both cases HP-β-CD-SH or HP-β-CD-SH-NP were dispersed in HBSS (10 mg/mL). To each mL of each of these dispersions, 10 μL of 25 mg/mL dexamethasone in ethanol was added and left to incubate overnight at room temperature. In order to compare the two preparation methods, at the end of the preparation the average size of the dispersions was determined by light scattering (Zetasizer nano series Malvern). Three measurements were carried out for each sample and the data obtained were analyzed in terms of average diameter expressed in percentage cumulative intensity and polydispersity index (PDI).

7.2.8. Biological investigation

In vitro biological evaluations were conducted on Human lung adenocarcinoma NCI-H441 epithelial cell line. NCI-H441 cells were grown in RPMI medium with 1% pen/strep and 10% FBS at 37°C in a 5% CO₂ atmosphere, as previously described (Vizzoni et al., 2023).

7.2.9. Cell Viability Assay

Cytotoxicity studies were performed using the WST-1 assay as previously described (Vizzoni et al., 2023). Cells were seeded into 96-well plates, at a concentration of 4×10^4 cells per well, and allowed to proliferate for 24 hours at 37°C, 5% CO₂. After 24 hours, the culture medium was removed and replaced with the samples under study. The cell viability of DMS solutions in RPMI was evaluated in a concentration range between 0.02 and 2 mg/mL, those of HP-β-CD and HP-β-CD-SH between 5 and 100 mg/mL and that of OLE-GS in a range between 0.001 and 0.5 mg/mL. For the viability study of HP-β-CD-SH-NP, a concentration of 10 mg/mL was tested, while the toxicity of all cyclodextrins complexed with DMS was evaluated at concentrations of 10 and 0.25 mg/mL, respectively. After 4 hours of incubation, cells were washed with RPMI, culture medium was then added and incubated at 37°C for 2 hours with WST-1. The amount of formazan produced was evaluated at 450 nm. Before carrying out the subsequent nebulization studies, the selected formulations, all in HBSS, had been studied for their dimensions, PDI and ζ potential by light scattering (Zetasizer nano series Malvern). Three measurements were carried out for each sample.

Therefore, the tested samples had the following composition:

- 0.25mg/mL DMS (code DMS);
- 0.25mg/mL DMS containing 10 mg/mL of HP-β-CD (code HP-β-CD/DMS);
- 0.25mg/mL DMS containing 10 mg/mL of HP-β-CD-SH (code HP-β-CD-SH/DMS);
- 0.25mg/mL DMS containing 10 mg/mL of HP-β-CD-SH-NH (code HP-β-CD-SH-NH/DMS);
- 0.3 mg/mL OLE-GS (code OLE-GS);
- 0.3 mg/mL OLE-GS containing 10 mg/mL of HP-β-CD (code HP-β-CD/OLE-GS);
- 0.3 mg/mL OLE-GS containing 10 mg/mL of HP-β-CD-SH (code HP-β-CD-SH/OLE-GS);
- 0.3 mg/mL OLE-GS containing 10 mg/mL of HP-β-CD-SH-NH (code HP-β-CD-SH-NP/OLE-GS).

7.2.10. Monolayer nebulization

The nebulization of the various samples was carried out using an Aerogen Solo[®] mesh nebulizer (Galway, Ireland) on differentiated monolayers grown on the apical side of the Transwell[®] as previously described (Vizzoni et al., 2023).

7.2.11. DMS permeation through monolayer

For the permeation experiment through the monolayer, the In Vitro Air–Liquid Interface (ALI) model was used as reported by Vizzoni et al. (Vizzoni et al., 2023). Briefly, NCI-H441 cells were seeded at a concentration of 2.5×10^4 cells per well onto 12-well Transwell[®] plates with 0.4 μm pore polyester filters and incubated for 10 days at 37 °C in a CO₂ atmosphere at 5%. 1.5 mL of

fresh medium was placed in the basolateral chamber while a 0.5 mL volume containing cells was added to the apical chamber. The medium was changed every 2 days. 48 hours after seeding, the medium in the apical chamber was removed, while that in the basolateral chamber was replaced with a polarizing RPMI medium, containing 1% ITS and 200 nM DMS. In this situation the cells are in a growth condition called ALI. DMS (0.25 mg/mL) and DMS complexed with HP- β -CD, HP- β -CD-SH and HP- β -CD-SH-NP at the concentration of 10 mg/ml. All experiments were performed in triplicate. To assess cell monolayer confluence, and during permeation studies, transepithelial electrical resistance (TEER) was measured at time 0 and hourly for 3 hours. At intervals of 0.5 h to 2.5 h, 500 μ L was withdrawn from the basolateral chamber and replaced with fresh HBSS. The samples were analyzed by high performance liquid chromatography as previously described (Grassiri et al., 2022). To quantify the amount of DMS nebulized on the cells during the experiment, the method already reported by Vizzoni et al. was followed (Vizzoni et al., 2023). Briefly, the nebulization test was carried out for 30 seconds on filter placed inside Transwell® supports. Subsequently, the filter was placed in HBSS and stirred in a shaker bath for one hour. The filter was then removed and the supernatant was analyzed spectrophotometrically at 242 nm. Experiments to quantify nebulization were performed in triplicate.

7.2.12. Permeation Data Treatment

Permeation data were treated as previously described (Zambito et al., 2009) assuming that the volume of sample nebulized onto the cell monolayer was identical for all samples under study. Briefly, for each permeation through cell monolayer a value of permeation flux was calculated from the following equation:

$$\text{Flux} = dM/dt \cdot 1/A$$

that is the slope of the linear portion of the cumulative amount permeated per unit surface area (0.33 cm²) vs. time plot. For each plot, the linear regression analysis was extended to the set of data points that gave the best fit, as judged from the r² value. This, in all of the cases investigated, was > 0.9. The average cumulative amount permeated per unit area in a given time was calculated to track each permeation profile and determine T_{2.5h}, which is the cumulative transport per unit area during the entire time of the experiment. Also the lag time (L) which is the time axis intercept of the regression line, was determined for each plot.

7.2.13. Evaluation of the protective effect from oxidative stress of OLE-GS nebulized on the monolayer

Before testing the ability of nebulized OLE-GS to protect cells from oxidative stress, it was necessary to determine the quantity of OLE-GS nebulized on the apical chamber. The test was carried out by spraying OLE-GS on filters placed on the Transwell, as described for DMS, for 15, 20 or 30 seconds. The nebulization time was chosen on the basis of preliminary cytotoxicity tests, so that the amount of OLE-GS sprayed on the monolayer was not cytotoxic.

To evaluate the protective effect from oxidative damage and ROS production by the complexed or free OLE-GS, the cells were seeded and treated as described in the previous paragraph.

For this test, OLE-GS (0.3 mg/mL) solubilized in HBSS in free form or complexed with HP- β -CD, HP- β -CD-SH or HP- β -CD-SH-NP all used at the concentration of 10 mg/mL was nebulized for 15 seconds via Aerogen Solo® nebulizer onto 12 monolayers as previously described (Vizzoni et al., 2023). The evaluation of the protective effect of OLE-GS from oxidative stress was carried out as already described (Cesare et al., 2021). After spraying the samples onto the monolayers, 2 hours of incubation were carried out and then washed with fresh medium. At this point, oxidative stress was performed on the pre-treated cells by incubating them for one hour with 250 μ M H₂O₂. The protective effect due to pre-treatment with nebulized samples was evaluated after removing the supernatant, washing with fresh medium and adding the WST-1 reagent. To

evaluate ROS production, the previously removed supernatant was placed in a 96-well plate, the fluorescent probe 2,7-dichloro-di-hydro-fluorescein diacetate, acetyl ester (CM-H2DCFDA) was added at a concentration of 10 μ M/well dissolved in PBS. The plate was kept in the dark at room temperature for 30 minutes and the fluorescence was subsequently determined at an excitation wavelength of 488 nm and emission of 510 nm.

7.2.14. Statistical analysis

All data are presented as mean \pm standard deviation (SD). Four replicates were performed for each experiment concerning the permeation of DMS through the cell monolayer and six for the cell viability experiments. The significance of the difference between two Flux, or L, or T2.5h values was assessed by the Student's t-test. Four replicates were performed for each experiment concerning the evaluation of the protective effect from nebulized OLE-GS oxidative stress and six for the cell viability experiments. The protective effects of the extracts against oxidative stress damage and ROS production were statistically analyzed with one-way ANOVA followed by Bonferroni post-test. $P < 0.05$ was considered indicative of a significant difference.

7.3. Results

7.3.1. Synthesis and characterization of HP- β -CD-SH-NP

HP- β -CD-SH was obtained starting from HP- β -CD via microwave reaction as reported by Grassiri et al. (Grassiri et al., 2022). By ^1H NMR analysis the degree of thiolation of HP- β -CD-SH was found to be 25%, not significantly different from that obtained previously (Grassiri et al., 2022). HP- β -CD-SH dispersions were tested for size at concentrations ranging from 5 to 20 mg/mL HP- β -CD-SH in DPBS, to verify the spontaneous formation of nanometric-sized aggregates, as well as already previously observed with other commercial cyclodextrins (Loftsson et al., 2019). Figure 1 shows the dimensions and PDI of the dispersions tested where it is observed that at concentrations between 5 and 10 mg/mL the formation of aggregates having nanometric dimensions with a low PDI is visible, while at higher concentrations a notable increase in the size and PDI. Among the concentrations of HP- β -CD-SH leading to the formation of nanoaggregates, the highest concentration was chosen, i.e. 10 mg/mL, as it makes it possible to bring a greater quantity of drug into solution. HP- β -CD-SH at the chosen concentration gives rise to the formation of unstable nanoaggregates, i.e. which form and break down continuously, as already reported for HP- β -CD (Rodrigues Sá Couto et al., 2019).

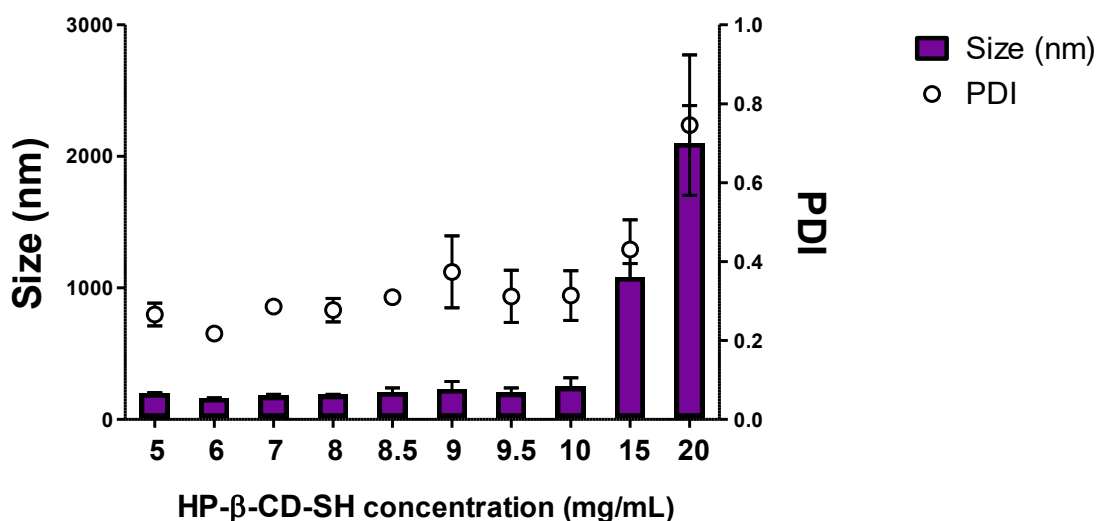


Figure 1. Size and PDI of HP- β -CD-SH dispersions in DPBS at increasing concentrations. Means \pm SD (n = 3).

In order to obtain stable nanoparticles (HP- β -CD-SH-NP), two different cross-linkers capable of forming thioether bonds with the thiol groups present on HP- β -CD-SH were chosen. In particular, the tested cross-linkers BM(PEG)2 and BM(PEG)3 are homobifunctional with a spacer arm made up of hydrophilic polyethylene glycol groups which give the molecule greater solubility in water. The maleimide moiety, present in the two cross-linkers, BM(PEG)2 and BM(PEG)3, is temporarily stable in aqueous solutions free of reactive sulfhydryl targets, but hydrolysis to non-reactive maleic acid may occur during storage, especially at pH>8. For this reason, it is advisable to use them promptly (Partis et al., 1983). The interaction between the sulfhydryl group of HP- β -CD-SH and the maleimide group of the cross-linker results in the formation of a stable thioether bond. This bond exhibits resistance to cleavage by reducing agents or physiological conditions of the buffer. Notably, the maleimide reaction is highly specific to sulfhydryls within the pH range of 6.5-7.5 (Smyth et al., 1964). Although maleimide can also react with primary amines at pH levels greater than 8, the rate of this reaction is a thousand times slower compared to its reaction with sulfhydryls at pH 7, rendering it practically negligible. In the tuning of the cross-linking conditions, different quantities of the two different cross-linkers were used following dimensional analysis to choose the best conditions for the formation of nanoaggregates. In particular, the final concentrations 0.07, 0.14, 0.27, 0.40, 0.64 mg/mL were tested for both BM(PEG)2 and BM(PEG)3. Figure 2 shows the dimensions and PDI of the aggregates that form in the conditions described. The data reported in Figure 2 show that the use of the BM(PEG)3 cross-linker allows to obtain, at all the concentrations tested, nanoparticles that are smaller or of dimensions not significantly different than those obtained with the BM(PEG)2 cross-linker. It is also observed that at the BM(PEG)3 concentration of 0.14 mg/mL, nanoparticles of smaller dimensions and with one of the lowest PDI are obtained; therefore, these conditions were chosen for the preparation of HP- β -CD-SH-NP in all subsequent experiments. The dispersion thus obtained was subsequently centrifuged and it was possible to observe the formation of a transparent precipitate with a gelatinous consistency which was considered further evidence of the formation of nanoaggregates (Akbulut et al., 2012).

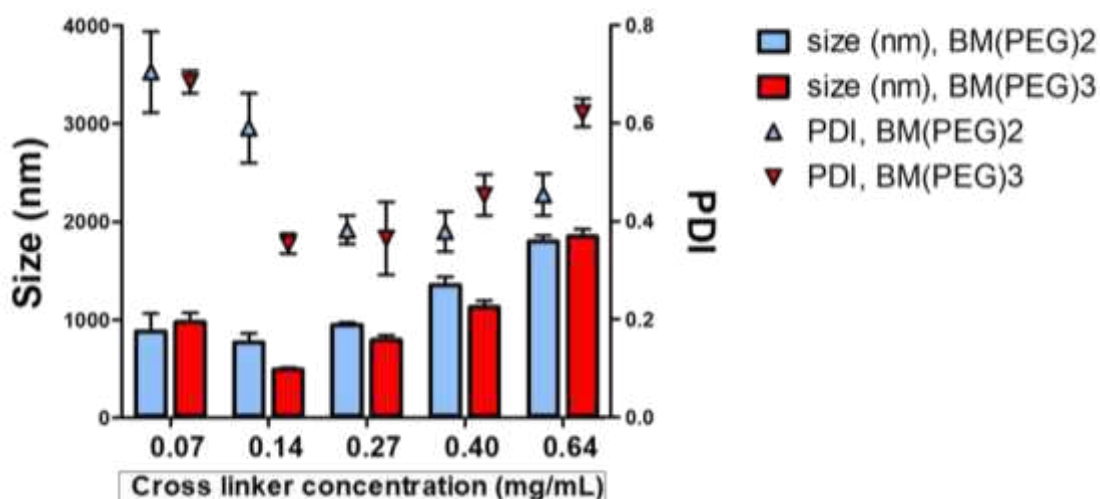


Figure 2. Influence on the reaction of two different types of cross linker, BM(PEG)2 or BM(PEG)3 at different concentrations with HP- β -CD-SH on HP- β -CD-SH-NP size (bars) and PDI (points). Means \pm SD (n = 3).

7.3.2. Determination of the association constant for cyclodextrins/DMS and cyclodextrins/OLE-GS

Cyclodextrins form inclusion complexes with lipophilic molecules, with a consequent increase in their apparent solubility. A dynamic balance is therefore established between complexed and free forms. The association constants (K_a) of the cyclodextrin/DMS and cyclodextrin/OLE-GS complexes were determined with the Benesi-Hildebrand method (Benesi & Hildebrand, 1949) in association with UV-vis spectrometry exploiting the variation in the absorption of solutions having the same content of DMS or OLE-GS and variable concentrations of cyclodextrins. K_a was calculated using the Benesi-Hildebrand equation (Cesari et al., 2020):

$$1/(A - A_0) = 1/(A' - A_0) \times 1/[CD] + 1/(A' - A_0)$$

Where [CD] represents the concentration of cyclodextrin, A and A_0 are the absorbances, in the presence and absence of CD, respectively, and A' is the absorbance when all DMS molecules are complexed with CD. For each cyclodextrin tested, a straight line was obtained based on the equation above. The K_a was calculated by dividing the intercept by the slope of the relevant straight line. Table 1 shows the K_a obtained.

Drug	HP- β -CD K_a (M^{-1})	HP- β -CD-SH K_a (M^{-1})	HP- β -CD-SH-NP K_a (M^{-1})
DMS	480.1 \pm 1.1	1573.9 \pm 4.2	639.0 \pm 0.5
OLE-GS	233.1 \pm 1.2	1418.0 \pm 13.9	900.0 \pm 6.0

Table 1. Association constants (K_a) between HP- β -CD, HP- β -CD-SH and HP- β -CD-SH NP and DMS or OLE-GS in aqueous solutions. Means \pm SD, n = 3.

As can be seen, HP- β -CD shows a lower ability than HP- β -CD-SH and HP- β -CD-NP to form complexes with DMS and OLE-GS. HP- β -CD-SH appears to have the best ability to complex both DMS and OLE-GS even compared to HP- β -CD-SH-NP. It has been reported in the literature that native cyclodextrins have a lower solubility in water than their hydroxypropylated derivatives. This phenomenon is thought to influence the ability of cyclodextrins to complex with drugs. Therefore, HP- β -CD is considered one of the best complexants in the cyclodextrin family (Loftsson et al., 2023) precisely because the random replacement of the hydroxyls with hydroxypropyl groups transforms the native crystalline cyclodextrins into amorphous mixtures of different isomers. Probably the further replacement of the hydroxyls with -SH groups leads to the formation of an even more soluble product and therefore more capable of complexing. While the cross-linking of HP- β -CD-SH with the formation of HP- β -CD-SH-NP makes it structurally more rigid and less capable of interacting with the active ingredients under study.

7.3.3. Study of DMS complexation with HP- β -CD-SH-NP

The ability of HP- β -CD-SH-NP to complex DMS was evaluated depending on whether the DMS came into contact with HP- β -CD-SH and subsequently cross-linked with the formation of HP- β -CD-SH-NP or with preformed nanoparticles. In the first case, HP- β -CD-SH-NP with dimensions of 492.2 \pm 25.50 nm (PDI 0.461) were obtained, in the second the dimensions were 495.9 \pm 46.66 nm (PDI 0.405), i.e. not significantly different from each other. From the above data it is possible to state that the drug loading method does not influence the size of the nanoparticles. For this reason, complexation following cross-linking was chosen, as this method can also be used with other active ingredients that could interfere with the cross-linking reaction.

7.3.4. Cytotoxicity studies

Figure 3 shows the cytotoxicity values of HP- β -CD and HP- β -CD-SH on NCI-H441 cells tested in a concentration range between 5 and 100 mg/mL. The concentration chosen for technological reasons of 10 mg/mL is ideal for subsequent nebulization studies on monolayers as at this concentration the two cyclodextrins do not show toxicity. These data are in agreement with those already obtained on BALB/3T3 (Grassiri et al., 2022) where HP- β -CD-SH was found to be more toxic than HP- β -CD, but safe to use. Figure 3 shows the cytotoxicity study on cells treated with increasing concentrations of DMS (Fig.4a) or OLE-GS (Fig.4b). The data in Figure 4a show that in the tested concentration range from 0.02 to 2 mg/mL DMS is not cytotoxic. For this reason, in subsequent studies, it was chosen to test DMS at the final concentration of 0.25 mg/mL, i.e. the one that on the basis of K_a remained dissolved with all types of cyclodextrins under study. From Fig.3b we can see how the OLE-GS tested at a concentration between 0.001 and 0.5 mg/mL shows cell viability values close to 80% up to a concentration of 0.3 mg/mL which further drops below 70% viability at 0.5 mg/mL concentration. For this reason, to conduct the nebulization studies on the monolayers, the highest non-toxic concentration of 0.3 mg/mL was chosen for OLE-GS.

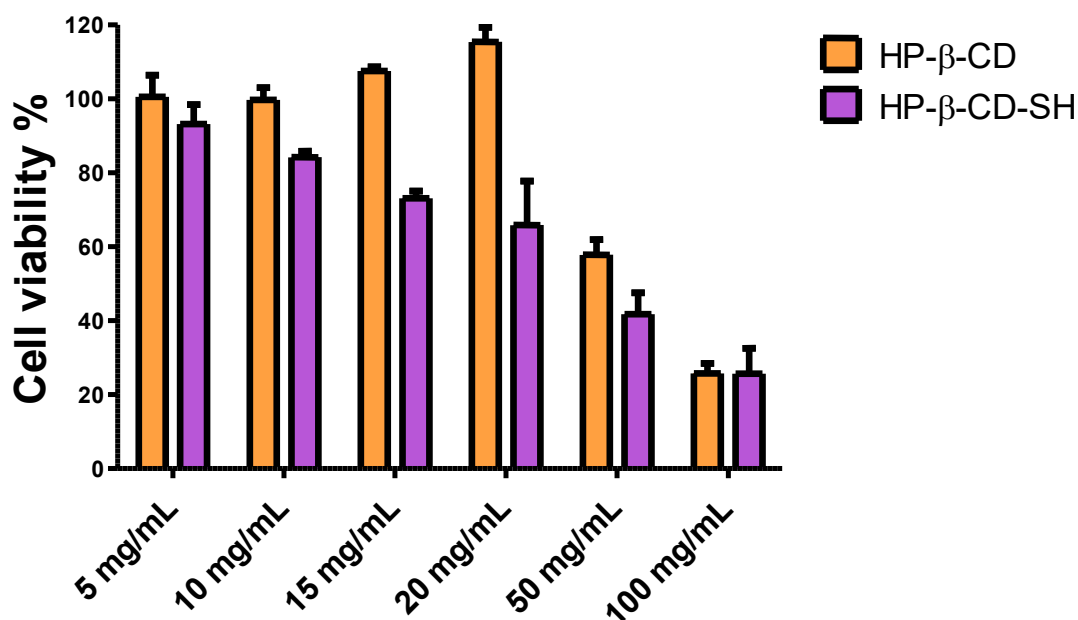


Figure 3. NCI-H441 viability after 4 h treatment with HP- β -CD or HP- β -CD-SH in culture medium. Data are expressed as % viable cells compared to control (untreated cells). Means \pm SD, n = 6.

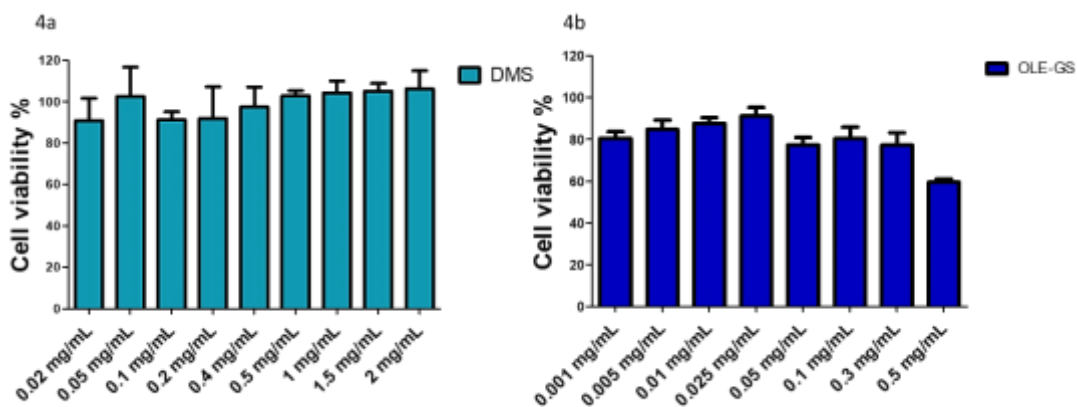


Figure 4. NCI-H441 viability after 4 h treatment with: (a) DMS and (b) OLE-GS in culture medium. Data are expressed as % viable cells compared to control (untreated cells). Means \pm SD, n = 6.

Figures 5a and 5b show the cytotoxicity data of the chosen formulations to test on the monolayers, where the non-cytotoxicity of any formulation under study is confirmed.

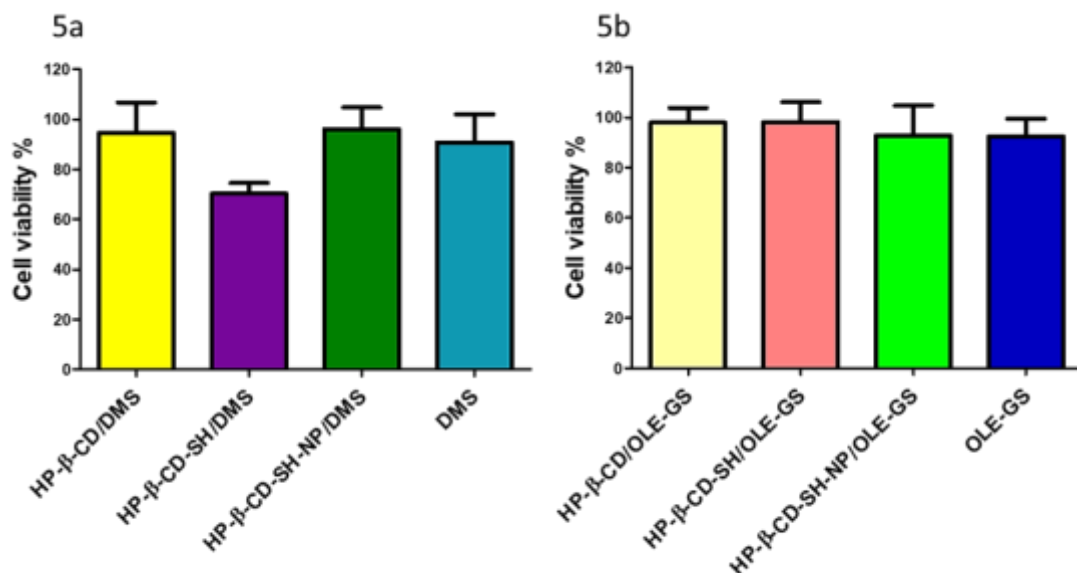


Figure 5. NCI-H441 viability after 4 h treatment with: (a) DMS (0.25 mg/mL), HP-β-CD/DMS, HP-β-CD-SH/DMS, HP-β-CD-SH-NP/DMS and (b) OLE-GS (0.3 mg/mL), HP-β-CD/OLE-GS, HP-β-CD-SH/OLE-GS, HP-β-CD-SH-NP/OLE-GS in culture medium. Cyclodextrins concentration was always 10 mg/mL. Data are expressed as % viable cells compared to control (untreated cells). Means \pm SD, n = 6.

7.3.5. Dimensional analysis and zeta potential of medicated formulations

Table 2 shows dimensions, PDI and ζ potential of HP-β-CD, HP-β-CD-SH and HP-β-CD-SH-NP dispersions complexed or not with DMS or OLE-GS. The data in Table 2 show that, in the conditions studied, nanometric-sized agglomerates are formed, in the rank order HP-β-CD < HP-β-CD-SH < HP-β-CD-SH-NP. The same trend is maintained for the complexes of the same cyclodextrins with DMS and OLE-GS obtaining higher dimensions compared to the non-medicated ones and showing a smaller increase in size for the formulations loaded with OLE-GS compared to those loaded with DMS. The PDI of the medicated dispersions were all lower than

0.5, obtaining a lower PDI in all cases for the HP- β -CD-SH based dispersions. It is not surprising for these systems that the PDI is not as low as desirable, it is in fact reported that they are composed of single cyclodextrin molecules in equilibrium with small clusters, in equilibrium with larger clusters (Messner et al., 2010). The ζ potential is significantly negative in all cases and increasingly less negative in the case of medicated and non-medicated HP- β -CD-SH-NP. Moreover, the negative charge indicates that the hydroxyl groups of the CD, as well as the thiol ones, are facing the external surface, i.e. towards the aqueous environment, making the nanosystems hydrophilic. Since some thiol groups are involved in the formation of cross-links in HP- β -CD-SH-NP, this explains the reason for the lower surface negativity of the latter. The active ingredients DMS and OLE-GS loaded in the nanosystems do not seem to influence the surface charge, indicating for both an interaction with the lipophilic internal cavity of the cyclodextrins.

Formulation	Size (nm)	Pdi	ζ -Potential (mV)
HP- β -CD	152.4 \pm 5.4	0.408 \pm 0.040	-8.05 \pm 0.61
HP- β -CD-SH	196.8 \pm 3.4	0.275 \pm 0.030	-6.89 \pm 0.49
HP- β -CD-SH-NP	431.5 \pm 7.1	0.443 \pm 0.061	-5.33 \pm 0.37
HP- β -CD/DMS	200.7 \pm 9.4	0.460 \pm 0.075	-10,00 \pm 0.78
HP- β -CD-SH/DMS	301.4 \pm 1.6	0.424 \pm 0.064	-6.53 \pm 1.14
HP- β -CD-SH-NP/DMS	492.2 \pm 5.5	0.461 \pm 0.092	-4.51 \pm 1.54
HP- β -CD/OLE-GS	165.1 \pm 5.1	0.424 \pm 0.013	-7.64 \pm 0.41
HP- β -CD-SH/OLE-GS	189.3 \pm 3.2	0.369 \pm 0.029	-9.22 \pm 1.25
HP- β -CD-SH-NP/OLE-GS	397.3 \pm 6.1	0.473 \pm 0.022	-5.66 \pm 0.56

Table 2. Diameter distribution, Pdi and ζ -potential values of HP- β -CD, HP- β -CD-SH, HP- β -CD-SH-NP and HP- β -CD/DMS, HP- β -CD-SH/DMS, HP- β -CD-SH-NP/DMS and HP- β -CD/OLE-GS, HP- β -CD-SH/OLE-GS, HP- β -CD-SH-NP/OLE-GS in HBSS. Cyclodextrins concentration was always 10 mg/mL, DMS 0.25 mg/mL and OLE-GS 0.3 mg/mL. Mean \pm SD, n = 3.

7.3.6. DMS permeation through monolayer

The quantity of DMS deposited on the Transwell® filter after 30 seconds of nebulization was preliminarily determined, resulting in 5 \pm 1 μ g for all the formulations tested. Figure 6 shows the DMS permeation data through the monolayer for all the formulations under study and for the control consisting of free DMS in suspension, which allowed the calculation of the parameters reported in Table 3. As can be seen from Figure 6 and from the Flux data reported in Table 3, when the DMS is complexed with HP- β -CD-SH there is an increase in the cumulative mass of DMS permeated over time both compared to the control and to the HP- β -CD/DMS and HP- β -CD-SH-NP/DMS formulations. The formation of disulfide bridges between -SH groups of the cyclodextrin and those of the mucin glycoproteins allow a prolongation of the residence time of the drug at the administration site with a consequent increase in bioavailability (Bernkop-Schnürch et al., 2006). In *in vitro* studies, in the absence of mucus, interactions can occur between the -SH groups of the cyclodextrin with the proteins of the cytoplasmic membranes. The DMS complexed with HP- β -CD-SH-NP showed at shorter times a higher DMS permeation than HP- β -CD but lower than HP- β -CD-SH; however, at longer times a significant variation is not observed between HP- β -CD-SH/DMS and HP- β -CD-SH-NP/DMS as demonstrated by the fact that the T2.5 values reported in Table 3 are not significantly different from each other but significantly greater than the control and HP- β -CD/DMS. The data relating to lag times (L) (Table 3) also show a significantly higher value for HP- β -CD-SH-NP/DMS compared to HP- β -CD-SH/DMS and HP- β -CD-SH/DMS indicating the need for a longer time to pass before the quasi-steady state is established, i.e. for the cellular monolayer to be saturated with the drug. This difference can be attributed to a greater rigidity of the nanoparticles compared to non-cross-linked cyclodextrins,

while it seems that at longer times the biological mechanism by which the nanoparticles are internalized has a greater influence on the DMS permeation process. The data relating to HP- β -CD-SH/DMS are in agreement with those obtained *in vivo* on the rabbit eye in a previous paper (Grassiri et al., 2022), where it was hypothesized that the better permeation of DMS complexed with HP- β -CD compared to the complex with HP- β -CD-SH could depend not only on the mucoadhesion of the cyclodextrin but also on its ability to promote absorption, as had been previously demonstrated with thiolated methyl- β -cyclodextrin (Asim et al., 2021). All these data indicate that, regarding DMS permeation, thiolation alone represents an advantage over the cross-linking reaction to form HP- β -CD-SH-NP.

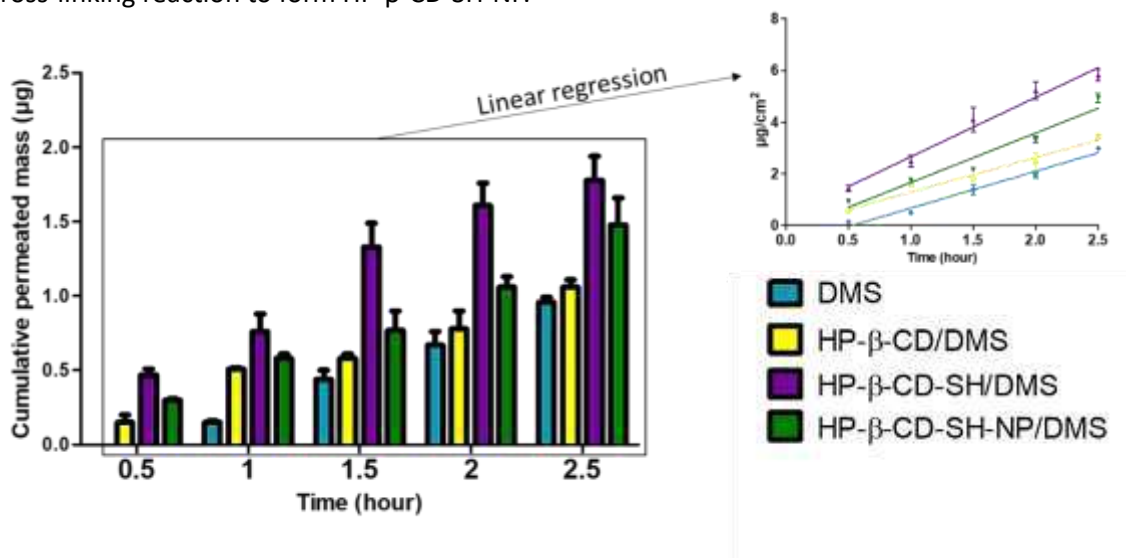


Figure 6. Data on cumulative mass of DMS permeated across NCI-H441 cell monolayer grown on Transwell®. Menas \pm SD of at least 4 runs.

Formulation	Flux ($\mu\text{g cm}^{-2} \text{h}^{-1}$)	L ^a (h)	T2.5h ^b ($\mu\text{g cm}^{-2}$)
DMS	1.43 \pm 0.04	0.53 \pm 0.03	2.91 \pm 0.09
HP- β -CD/DMS	1.33 \pm 0.09	0.04 \pm 0.01	3.21 \pm 0.15
HP- β -CD-SH/DMS	2.30 \pm 0.11 ¹	-0.04 \pm 0.02	5.39 \pm 0.48 ³
HP- β -CD-SH-NP/DMS	1.92 \pm 0.02	0.13 \pm 0.01 ²	4.48 \pm 0.55 ³

^a Lag time.

^b Cumulative transport over the whole time of experiment (2.5 h).

Table 3. Data on DMS permeation across NCI-H441 cell monolayer grown on Transwell®. Means \pm SD of at least 4 runs. ¹ $p < 0.05$ from all the other formulations; ² $p < 0.05$ from all the other formulations; ³ $p < 0.05$ from DMS and HP- β -CD/DMS.

7.3.7. Evaluation of the protective effect from oxidative stress of OLE-GS nebulized on the monolayer

The amount of OLE-GS deposited on the Transwell® filter after various nebulization times was determined. The test was carried out at 15, 20, 30 seconds of nebulization obtaining a nebulized quantity of 11.4 \pm 2.8, 50.0 \pm 7.5 and 142.4 \pm 11.7 μg , respectively. The 15 seconds of nebulization were chosen to perform the subsequent tests, because they guaranteed a non-cytotoxic dose of OLE-GS nebulized on the monolayer. Figure 7a shows data for ROS production in NCI-H441 cells subjected to oxidative stress and pretreated or not with complexed or free form OLE-GS. ROS production after cell treatment with H₂O₂ is significantly higher than ROS production in cells incubated with control (normal medium). All samples tested manage to significantly reduce the

production of ROS. In particular, when OLE-GS is complexed with cyclodextrins it limits the production of ROS significantly more effectively than when it is in free form, even if no significant differences were found between the various formulations under study. In figure 7b we can see how oxidative stress can cause an increase in cell mortality following treatment with H₂O₂. The pre-treatment of the monolayer with the formulations under study allows for a significant reduction in cell mortality. In particular, HP-β-CD-SH-NP/OLE-GS allows cell mortality to be significantly lower than all the other formulations tested. This suggests that the complexation of OLE-GS into HP-β-CD-SH NP can more effectively protect antioxidant molecules from degradation. Moreover, the ability of methyl-β-cyclodextrin to protect the antioxidant molecules contained in bergamot essential oil from degradation had previously been found (Zambito et al., 2022), as well as that of protecting the peptide dalargin (Cesari et al., 2020) had previously been found, although the hydrophobic cavity of the CD could not host the entire molecule but only a hydrophobic portion of it. This can also be hypothesized for OLE-GS which in its composition contains many high molecular weight polyphenols (Cerri et al., 2024).

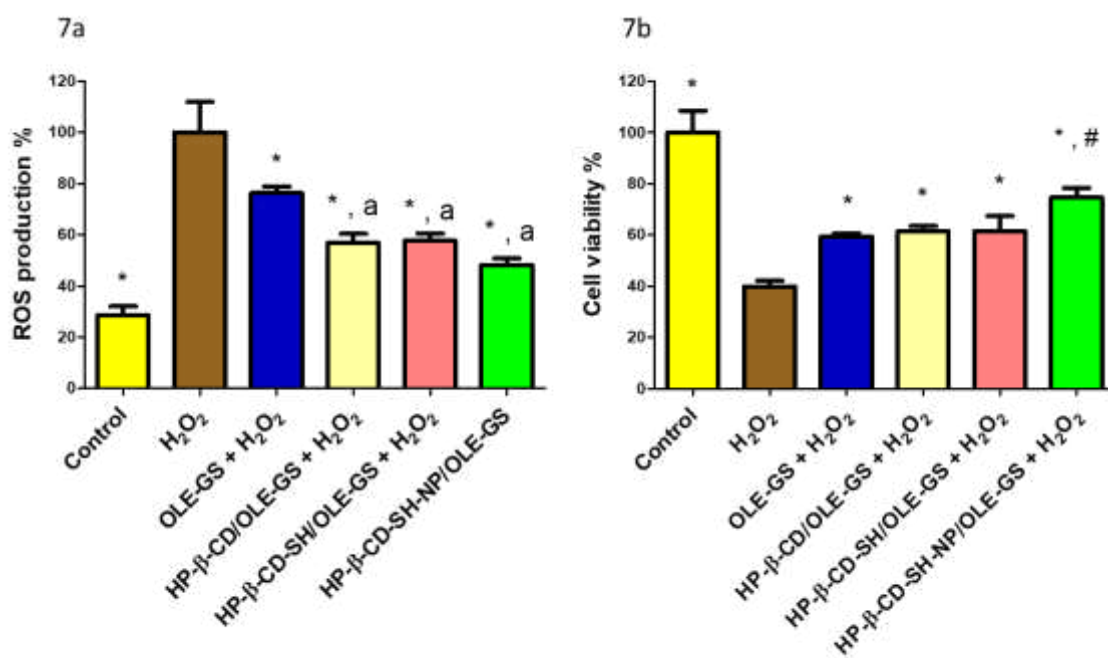


Figure 7. (a) Reactive oxygen species (ROS) production in NCI-H441 pre-treated for 2 h with nebulized OLE-GS complexed or not with all type of cyclodextrins in HBSS, and subsequent treatment with 250 μM H₂O₂ for 1 h. Data are expressed as % ROS production compared to 100% (cell treated with H₂O₂). (b) NCI-H441 viability after 2 h pre-treatment with nebulized OLE-GS complexed or not with all type of cyclodextrins in HBSS, and subsequent 1 h treatment with 250 μM H₂O₂. Data are expressed as % viable cells compared to negative control (H₂O₂). * p<0.05 from H₂O₂; ^a p<0.05 from OLE-GS + H₂O₂; [#] p<0.05 from all other.

7.4 Discussion

Historically, chemical syntheses have relied on conductive heating facilitated by external heat sources. This conventional approach is time-consuming and often inefficient, necessitating materials with high thermal conductivity for effective heat transfer to the reagents. Microwave heating represents a distinct departure from traditional methods. In this alternative process, microwaves directly engage with molecules within the reaction mixture, inducing an immediate and localized temperature elevation in substances susceptible to dipolar rotation and ion conduction—two fundamental mechanisms facilitating heat conduction from the microwave

source to the substances involved (Asim et al., 2021). In contrast to thiolation methodologies documented in the literature (Racaniello et al., 2021), the proposed synthesis offers notable advantages, being swifter, devoid of halogenated activators and organic solvents. Moreover, owing to its microwave-assisted nature, it proves more conducive to scale-up applications. The yield after purification compares favorably with that achieved by Laquintana et al. (Laquintana et al., 2019), who used a traditional approach to prepare thiolated HP- β -CD. It is crucial to consider the slightly lower thiolation degree achieved in this method, balanced against the advantage of preserving the solubility characteristics inherent in native HP- β -CD. Additionally, the maleimide fraction within both cross-linkers, BM(PEG)2 and BM(PEG)3, maintains temporary stability in aqueous solutions when reactive sulfhydryl targets are absent. However, caution is advised, as hydrolysis leading to non-reactive maleic acid may occur during storage, especially at pH levels surpassing 8. Thus, a prudent approach involves promptly dissolving and employing the reagents, discarding any unused portions (Partis et al., 1983). The interaction between the sulfhydryl group of HP- β -CD-SH and the maleimide group of the cross-linker results in the formation of a stable thioether bond. This bond exhibits resistance to cleavage by reducing agents or physiological conditions of the buffer. Notably, the maleimide reaction is highly specific to sulfhydryls within the pH range of 6.5-7.5 (Smyth et al., 1964). Although maleimide can also react with primary amines at pH levels greater than 8, the rate of this reaction is a thousand times slower compared to its reaction with sulfhydryls at pH 7, rendering it practically negligible. The optimal concentration for cross-linking HP- β -CDSH was determined to be 0.14 mg/mL for BM(PEG)3, resulting in the formation of stable nanoaggregates with a size of 493.3 ± 18.61 nm and a PDI of 0.355 ± 0.020 . These dimensions and the Polydispersity Index (PDI) align perfectly with the intended objectives of the formulation. Toxicity experiments indicate no discernible increase in toxicity post-cross-linking of HP- β -CD-SH at the concentration employed, affirming its suitability for the intended cellular treatment. However, when employing a model drug like DMS in permeation experiments, it becomes evident that cross-linking does not confer any advantage compared to thiolation alone. Thiolation alone appears to be more effective in facilitating the permeation of DMS through the monolayer, potentially attributed to the increased rigidity of the cross-linked structure, limiting drug availability for permeation. This observation suggests that HP- β -CD-SH NP may find more targeted applications compared to the use of native HP- β -CD-SH. Moreover, in evaluating the protective effect following pre-treatment via nebulization of OLE-GS, cross-linked CD-SH demonstrated a significant effect compared to all other formulations in reducing cell death induced by oxidative stress from H₂O₂. These findings imply the potential for developing promising formulations based on cross-linked HP- β -CD-SH for delivering natural extracts rich in polyphenols. Such formulations could offer a protective antioxidant effect at the application site, particularly in the case of the inhalation route.

8. Conclusion

The variety of fruits and vegetables found in the Mediterranean region represents an important heritage to be reevaluated, as they constitute a source of more resistant cultivars in extreme climatic conditions. In this study, extracts from the peel of tomatoes of an ancient native Tuscan variety and leaves from different varieties of olive trees, both obtained from plants grown under drought stress conditions, were analyzed. These extracts showed enhanced antioxidant properties compared to those obtained from plants grown under normal conditions, demonstrating new potential for biomedical applications. Furthermore, waste products from tomato and olive processing could find a new application given their strong antioxidant properties. All this could generate an advantage both from an economic point of view and in the reduction of waste production, and therefore reduce disposal costs for industries and farmers. Tomato peel extracts as well as olive leaf extracts have demonstrated antioxidant action on endothelial cells at low concentrations. A good percentage of these extracts have been shown to permeate intact through isolated rat intestine. This suggests that their integration into the diet may be valid and therefore contribute to the prevention of cardiovascular diseases. Extracts from plants grown under drought stress conditions are a good source of bioactive molecules, exhibit a protective effect on cells from oxidative stress even at low concentrations, and this constitutes an important value for the production of nutraceuticals. Furthermore, the bioactive molecules present in these extracts are widely used for the treatment and prevention of multiple pathologies. In particular, olive leaf extract can be used for the healing of wounds in the skin and cornea, as demonstrated by the works previously discussed. The molecules contained within this extract are naturally endowed with a very strong antibacterial activity, are active in the healing of wounds, and have a very marked antioxidant action. Water stress increase the production of these antioxidant molecules, making their activity even more pronounced. Furthermore, the encapsulation of these extracts manages to enhance their activity, as well as prevent their degradation, making them more active, stable, and useful for the treatment and prevention of pathologies. In conclusion, the cultivation of native plants of the Mediterranean area through water stress, in the meaning of the lack of water administration, represents a resource for the production of nutraceuticals with high antioxidant abilities. The develop of these through the use of innovative pharmaceutical forms enhances their potential use even further.

9. Acknowledgements

This work was supported by the Doctorate Degree program PEGASO of the Tuscany region.

My personal acknowledges are given to:

PhD in Life Sciences UNISI

Prof. Ylenia Zambito's research group (Department of Pharmacy, University of Pisa).

Prof. Rossella Di Stefano's research group (Cardiovascular Research Laboratory, University of Pisa).

Prof. Giampiero Cai's research group (University of Siena, Italy).

Dr. Laura Pucci (Institute of Agricultural Biology and Biotechnology, CNR – Italy).

Prof. Bruno Sarmiento's research group (i3S - Instituto de Investigação e Inovação em Saúde, University of Porto, Porto, Portugal).

10. References

- Akbulut, O., Mace, C. R., Martinez, R. V., Kumar, A. A., Nie, Z., Patton, M. R., & Whitesides, G. M. (2012). Separation of nanoparticles in aqueous multiphase systems through centrifugation. *Nano Letters*, *12*(8), 4060–4064. <https://doi.org/10.1021/nl301452x>
- Allegretta, C., Difonzo, G., Caponio, F., Tamma, G., & Laselva, O. (2023). Olive Leaf Extract (OLE) as a Novel Antioxidant That Ameliorates the Inflammatory Response in Cystic Fibrosis. *Cells*, *12*(13), 1764. <https://doi.org/10.3390/cells12131764>
- Alquraishi, R., Al-Samydai, A., Al Azzam, K. M., Alqaraleh, M., Al-Halaseh, L., Sanabrah, A., Abu Hajleh, M. N., Al Khatib, A., Alsaher, W., Negim, E.-S., & Khleifat, K. (2023). Preparation, characterization and wound-healing effect of PEGylated nanoliposomes loaded with oleuropein. *Biomedical Chromatography: BMC*, *37*(11), e5716. <https://doi.org/10.1002/bmc.5716>
- Anderson, L. J., Liu, H., & Garcia, J. M. (2017). Sex Differences in Muscle Wasting. *Advances in Experimental Medicine and Biology*, *1043*, 153–197. https://doi.org/10.1007/978-3-319-70178-3_9
- Ars.toscana.it.* (s.d.).
- Asim, M. H., Ijaz, M., Mahmood, A., Knoll, P., Jalil, A., Arshad, S., & Bernkop-Schnürch, A. (2021). Thiolated cyclodextrins: Mucoadhesive and permeation enhancing excipients for ocular drug delivery. *International Journal of Pharmaceutics*, *599*, 120451. <https://doi.org/10.1016/j.ijpharm.2021.120451>
- Avraamides, M., & Fatta, D. (2008). Resource consumption and emissions from olive oil production: A life cycle inventory case study in Cyprus. *Journal of Cleaner Production*, *16*(7), 809–821. <https://doi.org/10.1016/j.jclepro.2007.04.002>
- Babich, H., & Visioli, F. (2003). In vitro cytotoxicity to human cells in culture of some phenolics from olive oil. *Farmaco (Societa Chimica Italiana: 1989)*, *58*(5), 403–407. [https://doi.org/10.1016/S0014-827X\(03\)00048-X](https://doi.org/10.1016/S0014-827X(03)00048-X)

- Barba, A. I. O., Hurtado, M. C., Mata, M. C. S., Ruiz, V. F., & Tejada, M. L. S. D. (2006). Application of a UV–vis detection–HPLC method for a rapid determination of lycopene and β -carotene in vegetables. *Food Chemistry*, *95*(2), 328–336.
<https://doi.org/10.1016/j.foodchem.2005.02.028>
- Barbagallo, R. N., Di Silvestro, I., & Patanè, C. (2013). Yield, physicochemical traits, antioxidant pattern, polyphenol oxidase activity and total visual quality of field-grown processing tomato cv. Brigade as affected by water stress in Mediterranean climate. *Journal of the Science of Food and Agriculture*, *93*(6), 1449–1457. <https://doi.org/10.1002/jsfa.5913>
- Beconcini, D., Fabiano, A., Zambito, Y., Berni, R., Santoni, T., Piras, A. M., & Di Stefano, R. (2018). Chitosan-Based Nanoparticles Containing Cherry Extract from *Prunus avium* L. to Improve the Resistance of Endothelial Cells to Oxidative Stress. *Nutrients*, *10*(11), 1598.
<https://doi.org/10.3390/nu10111598>
- Bell, K. E., von Allmen, M. T., Devries, M. C., & Phillips, S. M. (2016). Muscle Disuse as a Pivotal Problem in Sarcopenia-related Muscle Loss and Dysfunction. *The Journal of Frailty & Aging*, *5*(1), 33–41. <https://doi.org/10.14283/jfa.2016.78>
- Benavente-García, O., Castillo, J., Lorente, J., Ortuño, A., & Del Rio, J. A. (2000). Antioxidant activity of phenolics extracted from *Olea europaea* L. leaves. *Food Chemistry*, *68*(4), 457–462. [https://doi.org/10.1016/S0308-8146\(99\)00221-6](https://doi.org/10.1016/S0308-8146(99)00221-6)
- Benesi, H. A., & Hildebrand, J. H. (1949). A Spectrophotometric Investigation of the Interaction of Iodine with Aromatic Hydrocarbons. *Journal of the American Chemical Society*, *71*(8), 2703–2707. <https://doi.org/10.1021/ja01176a030>
- Benzie, I. F., & Strain, J. J. (1996). The ferric reducing ability of plasma (FRAP) as a measure of «antioxidant power»: The FRAP assay. *Analytical Biochemistry*, *239*(1), 70–76.
<https://doi.org/10.1006/abio.1996.0292>

- Berni, R., Romi, M., Parrotta, L., Cai, G., & Cantini, C. (2018). Ancient Tomato (*Solanum lycopersicum* L.) Varieties of Tuscany Have High Contents of Bioactive Compounds. *Horticulturae*, 4(4), 51. <https://doi.org/10.3390/horticulturae4040051>
- Bernkop-Schnürch, A., Weithaler, A., Albrecht, K., & Greimel, A. (2006). Thiomers: Preparation and in vitro evaluation of a mucoadhesive nanoparticulate drug delivery system. *International Journal of Pharmaceutics*, 317(1), 76–81. <https://doi.org/10.1016/j.ijpharm.2006.02.044>
- Bessa, L. J., Fazii, P., Di Giulio, M., & Cellini, L. (2015). Bacterial isolates from infected wounds and their antibiotic susceptibility pattern: Some remarks about wound infection. *International Wound Journal*, 12(1), 47–52. <https://doi.org/10.1111/iwj.12049>
- Bodine, S. C., Latres, E., Baumhueter, S., Lai, V. K., Nunez, L., Clarke, B. A., Poueymirou, W. T., Panaro, F. J., Na, E., Dharmarajan, K., Pan, Z. Q., Valenzuela, D. M., DeChiara, T. M., Stitt, T. N., Yancopoulos, G. D., & Glass, D. J. (2001). Identification of ubiquitin ligases required for skeletal muscle atrophy. *Science (New York, N.Y.)*, 294(5547), 1704–1708. <https://doi.org/10.1126/science.1065874>
- Boe, J., Dennis, J. H., O'Driscoll, B. R., Bauer, T. T., Carone, M., Dautzenberg, B., Diot, P., Heslop, K., Lannefors, L., & European Respiratory Society Task Force on the use of nebulizers. (2001). European Respiratory Society Guidelines on the use of nebulizers. *The European Respiratory Journal*, 18(1), 228–242. <https://doi.org/10.1183/09031936.01.00220001>
- Borjan, D., Leitgeb, M., Knez, Ž., & Hrnčič, M. K. (2020). Microbiological and Antioxidant Activity of Phenolic Compounds in Olive Leaf Extract. *Molecules (Basel, Switzerland)*, 25(24), 5946. <https://doi.org/10.3390/molecules25245946>
- Calleja, P., Espuelas, S., Corrales, L., Pio, R., & Irache, J. M. (2014). Pharmacokinetics and antitumor efficacy of paclitaxel-cyclodextrin complexes loaded in mucus-penetrating

- nanoparticles for oral administration. *Nanomedicine (London, England)*, 9(14), 2109–2121. <https://doi.org/10.2217/nnm.13.199>
- Cámara, M., Fernández-Ruiz, V., Sánchez-Mata, M.-C., Cámara, R. M., Domínguez, L., & Sesso, H. D. (2022). Scientific Evidence of the Beneficial Effects of Tomato Products on Cardiovascular Disease and Platelet Aggregation. *Frontiers in Nutrition*, 9, 849841. <https://doi.org/10.3389/fnut.2022.849841>
- Cao, Y., Gong, Y., Liu, L., Zhou, Y., Fang, X., Zhang, C., Li, Y., & Li, J. (2017). The use of human umbilical vein endothelial cells (HUVECs) as an *in vitro* model to assess the toxicity of nanoparticles to endothelium: A review. *Journal of Applied Toxicology*, 37(12), 1359–1369. <https://doi.org/10.1002/jat.3470>
- Cerri, L., Parri, S., Dias, M. C., Fabiano, A., Romi, M., Cai, G., Cantini, C., & Zambito, Y. (2024). Olive Leaf Extracts from Three Italian Olive Cultivars Exposed to Drought Stress Differentially Protect Cells against Oxidative Stress. *Antioxidants (Basel, Switzerland)*, 13(1), 77. <https://doi.org/10.3390/antiox13010077>
- Cesare, M. M., Felice, F., Conti, V., Cerri, L., Zambito, Y., Romi, M., Cai, G., Cantini, C., & Di Stefano, R. (2021). Impact of Peels Extracts from an Italian Ancient Tomato Variety Grown under Drought Stress Conditions on Vascular Related Dysfunction. *Molecules (Basel, Switzerland)*, 26(14), 4289. <https://doi.org/10.3390/molecules26144289>
- Cesari, A., Recchimurzo, A., Fabiano, A., Balzano, F., Rossi, N., Migone, C., Uccello-Barretta, G., Zambito, Y., & Piras, A. M. (2020). Improvement of Peptide Affinity and Stability by Complexing to Cyclodextrin-Grafted Ammonium Chitosan. *Polymers*, 12(2), 474. <https://doi.org/10.3390/polym12020474>
- Chen, J., Lu, W.-L., Gu, W., Lu, S.-S., Chen, Z.-P., Cai, B.-C., & Yang, X.-X. (2014). Drug-in-cyclodextrin-in-liposomes: A promising delivery system for hydrophobic drugs. *Expert Opinion on Drug Delivery*, 11(4), 565–577. <https://doi.org/10.1517/17425247.2014.884557>

- Chen, W. Y., & Abatangelo, G. (1999). Functions of hyaluronan in wound repair. *Wound Repair and Regeneration: Official Publication of the Wound Healing Society [and] the European Tissue Repair Society*, 7(2), 79–89. <https://doi.org/10.1046/j.1524-475x.1999.00079.x>
- Cuffaro, D., Pinto, D., Silva, A. M., Bertolini, A., Bertini, S., Saba, A., Macchia, M., Rodrigues, F., & Digiaco, M. (2023). Insights into the Antioxidant/Antiradical Effects and In Vitro Intestinal Permeation of Oleocanthal and Its Metabolites Tyrosol and Oleocanthalic Acid. *Molecules*, 28(13), 5150. <https://doi.org/10.3390/molecules28135150>
- Da Silva, S. B., Ferreira, D., Pintado, M., & Sarmiento, B. (2016). Chitosan-based nanoparticles for rosmarinic acid ocular delivery—In vitro tests. *International Journal of Biological Macromolecules*, 84, 112–120. <https://doi.org/10.1016/j.ijbiomac.2015.11.070>
- D'Agostino, N., Taranto, F., Camposeo, S., Mangini, G., Fanelli, V., Gadaleta, S., Miazzi, M. M., Pavan, S., Di Rienzo, V., Sabetta, W., Lombardo, L., Zelasco, S., Perri, E., Lotti, C., Ciani, E., & Montemurro, C. (2018). GBS-derived SNP catalogue unveiled wide genetic variability and geographical relationships of Italian olive cultivars. *Scientific Reports*, 8(1), 15877. <https://doi.org/10.1038/s41598-018-34207-y>
- De la Ossa, J. G., El Kadri, H., Gutierrez-Merino, J., Wantock, T., Harle, T., Seggiani, M., Danti, S., Di Stefano, R., & Velliou, E. (2021). Combined Antimicrobial Effect of Bio-Waste Olive Leaf Extract and Remote Cold Atmospheric Plasma Effluent. *Molecules (Basel, Switzerland)*, 26(7), 1890. <https://doi.org/10.3390/molecules26071890>
- De la Ossa, J. G., Felice, F., Azimi, B., Salsano, J. E., Digiaco, M., Macchia, M., Danti, S., & Di Stefano, R. (2019). Waste Autochthonous Tuscan Olive Leaves (*Olea europaea* var. *Olivastra seggiane*) as Antioxidant Source for Biomedicine. *International Journal of Molecular Sciences*, 20(23), 5918. <https://doi.org/10.3390/ijms20235918>
- De La Ossa, J. G., Fusco, A., Azimi, B., Esposito Salsano, J., Digiaco, M., Coltelli, M.-B., De Clerck, K., Roy, I., Macchia, M., Lazzeri, A., Donnarumma, G., Danti, S., & Di Stefano, R.

- (2021). Immunomodulatory Activity of Electrospun Polyhydroxyalkanoate Fiber Scaffolds Incorporating Olive Leaf Extract. *Applied Sciences*, 11(9), 4006.
<https://doi.org/10.3390/app11094006>
- De Pascali, M., Vergine, M., Sabella, E., Aprile, A., Nutricati, E., Nicolì, F., Buja, I., Negro, C., Miceli, A., Rampino, P., De Bellis, L., & Luvisi, A. (2019). Molecular Effects of *Xylella fastidiosa* and Drought Combined Stress in Olive Trees. *Plants*, 8(11), 437.
<https://doi.org/10.3390/plants8110437>
- Denaxa, N.-K., Damvakaris, T., & Roussos, P. A. (2020). Antioxidant defense system in young olive plants against drought stress and mitigation of adverse effects through external application of alleviating products. *Scientia Horticulturae*, 259, 108812.
<https://doi.org/10.1016/j.scienta.2019.108812>
- Dias, M. C., Figueiredo, C., Pinto, D. C. G. A., Freitas, H., Santos, C., & Silva, A. M. S. (2019). Heat shock and UV-B episodes modulate olive leaves lipophilic and phenolic metabolite profiles. *Industrial Crops and Products*, 133, 269–275.
<https://doi.org/10.1016/j.indcrop.2019.03.036>
- Dias, M. C., Pinto, D. C. G. A., Figueiredo, C., Santos, C., & Silva, A. M. S. (2021). Phenolic and lipophilic metabolite adjustments in *Olea europaea* (olive) trees during drought stress and recovery. *Phytochemistry*, 185, 112695.
<https://doi.org/10.1016/j.phytochem.2021.112695>
- Diaz-Espejo, A., Fernández, J. E., Torres-Ruiz, J. M., Rodriguez-Dominguez, C. M., Perez-Martin, A., & Hernandez-Santana, V. (2018). The Olive Tree Under Water Stress. In *Water Scarcity and Sustainable Agriculture in Semiarid Environment* (pp. 439–479). Elsevier.
<https://doi.org/10.1016/B978-0-12-813164-0.00018-1>
- Eghrari, A. O., Riazuddin, S. A., & Gottsch, J. D. (2015). Overview of the Cornea: Structure, Function, and Development. *Progress in Molecular Biology and Translational Science*, 134, 7–23. <https://doi.org/10.1016/bs.pmbts.2015.04.001>

- El, S. N., & Karakaya, S. (2009). Olive tree (*Olea europaea*) leaves: Potential beneficial effects on human health. *Nutrition Reviews*, 67(11), 632–638. <https://doi.org/10.1111/j.1753-4887.2009.00248.x>
- Erbay, Z., & Icier, F. (2010). The Importance and Potential Uses of Olive Leaves. *Food Reviews International*, 26(4), 319–334. <https://doi.org/10.1080/87559129.2010.496021>
- Espeso, J., Isaza, A., Lee, J. Y., Sørensen, P. M., Jurado, P., Avena-Bustillos, R. D. J., Olaizola, M., & Arboleya, J. C. (2021). Olive Leaf Waste Management. *Frontiers in Sustainable Food Systems*, 5, 660582. <https://doi.org/10.3389/fsufs.2021.660582>
- Fabiano, A., De Leo, M., Cerri, L., Piras, A. M., Braca, A., & Zambito, Y. (2022). Saffron extract self-assembled nanoparticles to prolong the precorneal residence of crocin. *Journal of Drug Delivery Science and Technology*, 74, 103580. <https://doi.org/10.1016/j.jddst.2022.103580>
- Fabiano, A., Migone, C., Cerri, L., Piras, A. M., Mezzetta, A., Maisetta, G., Esin, S., Batoni, G., Di Stefano, R., & Zambito, Y. (2021). Combination of Two Kinds of Medicated Microparticles Based on Hyaluronic Acid or Chitosan for a Wound Healing Spray Patch. *Pharmaceutics*, 13(12), 2195. <https://doi.org/10.3390/pharmaceutics13122195>
- Fabiano, A., Piras, A. M., Uccello-Barretta, G., Balzano, F., Cesari, A., Testai, L., Citi, V., & Zambito, Y. (2018). Impact of mucoadhesive polymeric nanoparticulate systems on oral bioavailability of a macromolecular model drug. *European Journal of Pharmaceutics and Biopharmaceutics: Official Journal of Arbeitsgemeinschaft Fur Pharmazeutische Verfahrenstechnik e.V.*, 130, 281–289. <https://doi.org/10.1016/j.ejpb.2018.07.010>
- Fang, Z., & Bhandari, B. (2010). Encapsulation of polyphenols – a review. *Trends in Food Science & Technology*, 21(10), 510–523. <https://doi.org/10.1016/j.tifs.2010.08.003>
- Felice, F., Fabiano, A., De Leo, M., Piras, A. M., Beconcini, D., Cesare, M. M., Braca, A., Zambito, Y., & Di Stefano, R. (2020). Antioxidant Effect of Cocoa By-Product and Cherry

- Polyphenol Extracts: A Comparative Study. *Antioxidants (Basel, Switzerland)*, 9(2), 132.
<https://doi.org/10.3390/antiox9020132>
- Felice, F., Francini, A., Domenici, V., Cifelli, M., Belardinelli, E., Sebastiani, L., Cantini, C., & Di Stefano, R. (2019). Effects of Extra Virgin Olive Oil and Apples Enriched-Dark Chocolate on Endothelial Progenitor Cells in Patients with Cardiovascular Risk Factors: A Randomized Cross-Over Trial. *Antioxidants (Basel, Switzerland)*, 8(4), 88.
<https://doi.org/10.3390/antiox8040088>
- Felice, F., Zambito, Y., Belardinelli, E., Fabiano, A., Santoni, T., & Di Stefano, R. (2015). Effect of different chitosan derivatives on in vitro scratch wound assay: A comparative study. *International Journal of Biological Macromolecules*, 76, 236–241.
<https://doi.org/10.1016/j.ijbiomac.2015.02.041>
- Felice, F., Zambito, Y., Di Colo, G., D'Onofrio, C., Fausto, C., Balbarini, A., & Di Stefano, R. (2012). Red grape skin and seeds polyphenols: Evidence of their protective effects on endothelial progenitor cells and improvement of their intestinal absorption. *European Journal of Pharmaceutics and Biopharmaceutics: Official Journal of Arbeitsgemeinschaft Fur Pharmazeutische Verfahrenstechnik e.V.*, 80(1), 176–184.
<https://doi.org/10.1016/j.ejpb.2011.09.002>
- Flamini, G., Cioni, P. L., & Morelli, I. (2003). Volatiles from leaves, fruits, and virgin oil from *Olea europaea* Cv. Olivastra Seggianese from Italy. *Journal of Agricultural and Food Chemistry*, 51(5), 1382–1386. <https://doi.org/10.1021/jf020854y>
- Fore, J. (2006). A review of skin and the effects of aging on skin structure and function. *Ostomy/Wound Management*, 52(9), 24–35; quiz 36–37.
- Frati, A., Landi, D., Marinelli, C., Gianni, G., Fontana, L., Migliorini, M., Pierucci, F., Garcia-Gil, M., & Meacci, E. (2014). Nutraceutical properties of chestnut flours: Beneficial effects on skeletal muscle atrophy. *Food & Function*, 5(11), 2870–2882.
<https://doi.org/10.1039/c4fo00353e>

- Friedman, M. (2013). Anticarcinogenic, cardioprotective, and other health benefits of tomato compounds lycopene, α -tomatine, and tomatidine in pure form and in fresh and processed tomatoes. *Journal of Agricultural and Food Chemistry*, *61*(40), 9534–9550. <https://doi.org/10.1021/jf402654e>
- Frusciante, L., Carli, P., Ercolano, M. R., Pernice, R., Di Matteo, A., Fogliano, V., & Pellegrini, N. (2007). Antioxidant nutritional quality of tomato. *Molecular Nutrition & Food Research*, *51*(5), 609–617. <https://doi.org/10.1002/mnfr.200600158>
- Garcia, L. G. S., da Rocha, M. G., Lima, L. R., Cunha, A. P., de Oliveira, J. S., de Andrade, A. R. C., Ricardo, N. M. P. S., Pereira-Neto, W. A., Sidrim, J. J. C., Rocha, M. F. G., Vieira, R. S., & Brilhante, R. S. N. (2021). Essential oils encapsulated in chitosan microparticles against *Candida albicans* biofilms. *International Journal of Biological Macromolecules*, *166*, 621–632. <https://doi.org/10.1016/j.ijbiomac.2020.10.220>
- García-Valverde, V., Navarro-González, I., García-Alonso, J., & Periago, M. J. (2013). Antioxidant Bioactive Compounds in Selected Industrial Processing and Fresh Consumption Tomato Cultivars. *Food and Bioprocess Technology*, *6*(2), 391–402. <https://doi.org/10.1007/s11947-011-0687-3>
- Gibson, G. J., Loddenkemper, R., Lundbäck, B., & Sibille, Y. (2013). Respiratory health and disease in Europe: The new European Lung White Book. *The European Respiratory Journal*, *42*(3), 559–563. <https://doi.org/10.1183/09031936.00105513>
- Grada, A., Otero-Vinas, M., Prieto-Castrillo, F., Obagi, Z., & Falanga, V. (2017). Research Techniques Made Simple: Analysis of Collective Cell Migration Using the Wound Healing Assay. *The Journal of Investigative Dermatology*, *137*(2), e11–e16. <https://doi.org/10.1016/j.jid.2016.11.020>
- Grassiri, B., Knoll, P., Fabiano, A., Piras, A. M., Zambito, Y., & Bernkop-Schnürch, A. (2022). Thiolated Hydroxypropyl- β -cyclodextrin: A Potential Multifunctional Excipient for

- Ocular Drug Delivery. *International Journal of Molecular Sciences*, 23(5), 2612.
<https://doi.org/10.3390/ijms23052612>
- Guinda, Á., Castellano, J. M., Santos-Lozano, J. M., Delgado-Hervás, T., Gutiérrez-Adánez, P., & Rada, M. (2015). Determination of major bioactive compounds from olive leaf. *LWT - Food Science and Technology*, 64(1), 431–438.
<https://doi.org/10.1016/j.lwt.2015.05.001>
- Guo, Y., Bera, H., Shi, C., Zhang, L., Cun, D., & Yang, M. (2021). Pharmaceutical strategies to extend pulmonary exposure of inhaled medicines. *Acta Pharmaceutica Sinica. B*, 11(8), 2565–2584. <https://doi.org/10.1016/j.apsb.2021.05.015>
- Gupta, R. C., Lall, R., Srivastava, A., & Sinha, A. (2019). Hyaluronic Acid: Molecular Mechanisms and Therapeutic Trajectory. *Frontiers in Veterinary Science*, 6, 192.
<https://doi.org/10.3389/fvets.2019.00192>
- Han, M. K., McLaughlin, V. V., Criner, G. J., & Martinez, F. J. (2007). Pulmonary diseases and the heart. *Circulation*, 116(25), 2992–3005.
<https://doi.org/10.1161/CIRCULATIONAHA.106.685206>
- Harrer, D., Sanchez Armengol, E., Friedl, J. D., Jalil, A., Jelkmann, M., Leichner, C., & Laffleur, F. (2021). Is hyaluronic acid the perfect excipient for the pharmaceutical need? *International Journal of Pharmaceutics*, 601, 120589.
<https://doi.org/10.1016/j.ijpharm.2021.120589>
- Hashmi, M. A., Khan, A., Hanif, M., Farooq, U., & Perveen, S. (2015). Traditional Uses, Phytochemistry, and Pharmacology of *Olea europaea* (Olive). *Evidence-Based Complementary and Alternative Medicine: eCAM*, 2015, 541591.
<https://doi.org/10.1155/2015/541591>
- He, Y., Zheng, Y., Liu, C., Zhang, H., & Shen, J. (2024). Citric acid cross-linked β -cyclodextrins: A review of preparation and environmental/biomedical application. *Carbohydrate Polymers*, 323, 121438. <https://doi.org/10.1016/j.carbpol.2023.121438>

- Hernández, M., Rodríguez, E., & Díaz, C. (2007). Free hydroxycinnamic acids, lycopene, and color parameters in tomato cultivars. *Journal of Agricultural and Food Chemistry*, 55(21), 8604–8615. <https://doi.org/10.1021/jf071069u>
- https://cellbank.brc.riken.jp/cell_bank/CellInfo/?cellNo=RCB2280. (s.d.).
- <https://www.atcc.org/products/ccl-163#detailed-product-images>. (s.d.).
- <https://www.atcc.org/products/crl-1730#detailed-product-images>. (s.d.).
- <https://www.atcc.org/products/htb-174>. (s.d.).
- Huang, J., & Zhu, X. (2016). The molecular mechanisms of calpains action on skeletal muscle atrophy. *Physiological Research*, 65(4), 547–560. <https://doi.org/10.33549/physiolres.933087>
- Ighodaro, O. M., & Akinloye, O. A. (2018). First line defence antioxidants-superoxide dismutase (SOD), catalase (CAT) and glutathione peroxidase (GPX): Their fundamental role in the entire antioxidant defence grid. *Alexandria Journal of Medicine*, 54(4), 287–293. <https://doi.org/10.1016/j.ajme.2017.09.001>
- Irakli, M., Chatzopoulou, P., & Ekateriniadou, L. (2018). Optimization of ultrasound-assisted extraction of phenolic compounds: Oleuropein, phenolic acids, phenolic alcohols and flavonoids from olive leaves and evaluation of its antioxidant activities. *Industrial Crops and Products*, 124, 382–388. <https://doi.org/10.1016/j.indcrop.2018.07.070>
- Ismea, 2017. Report—I numeri della filiera del pomodoro da industria. Roma, June 2017.* (s.d.).
- Ivanova, D. G., & Yaneva, Z. L. (2020). Antioxidant Properties and Redox-Modulating Activity of Chitosan and Its Derivatives: Biomaterials with Application in Cancer Therapy. *BioResearch Open Access*, 9(1), 64–72. <https://doi.org/10.1089/biores.2019.0028>
- Jaffe, E. A., Nachman, R. L., Becker, C. G., & Minick, C. R. (1973). Culture of human endothelial cells derived from umbilical veins. Identification by morphologic and immunologic criteria. *The Journal of Clinical Investigation*, 52(11), 2745–2756. <https://doi.org/10.1172/JCI107470>

- Jesús Periago, M., García-Alonso, J., Jacob, K., Belén Olivares, A., José Bernal, M., Dolores Iniesta, M., Martínez, C., & Ros, G. (2009). Bioactive compounds, folates and antioxidant properties of tomatoes (*Lycopersicum esculentum*) during vine ripening. *International Journal of Food Sciences and Nutrition*, *60*(8), 694–708.
<https://doi.org/10.3109/09637480701833457>
- Joshi, R., Wani, S. H., Singh, B., Bohra, A., Dar, Z. A., Lone, A. A., Pareek, A., & Singla-Pareek, S. L. (2016). Transcription Factors and Plants Response to Drought Stress: Current Understanding and Future Directions. *Frontiers in Plant Science*, *7*, 1029.
<https://doi.org/10.3389/fpls.2016.01029>
- Kaliora, A. C., Dedoussis, G. V. Z., & Schmidt, H. (2006). Dietary antioxidants in preventing atherogenesis. *Atherosclerosis*, *187*(1), 1–17.
<https://doi.org/10.1016/j.atherosclerosis.2005.11.001>
- Kalra, E. K. (2003). Nutraceutical—Definition and introduction. *AAPS pharmSci*, *5*(3), E25.
<https://doi.org/10.1208/ps050325>
- Kavitha, P., Shivashankara, K. S., Rao, V. K., Sadashiva, A. T., Ravishankar, K. V., & Sathish, G. J. (2014). Genotypic variability for antioxidant and quality parameters among tomato cultivars, hybrids, cherry tomatoes and wild species. *Journal of the Science of Food and Agriculture*, *94*(5), 993–999. <https://doi.org/10.1002/jsfa.6359>
- Kawano, Y., Patrulea, V., Sublet, E., Borchard, G., Iyoda, T., Kageyama, R., Morita, A., Seino, S., Yoshida, H., Jordan, O., & Hanawa, T. (2021). Wound Healing Promotion by Hyaluronic Acid: Effect of Molecular Weight on Gene Expression and In Vivo Wound Closure. *Pharmaceuticals (Basel, Switzerland)*, *14*(4), 301. <https://doi.org/10.3390/ph14040301>
- Kawashima, Y. (2001). Nanoparticulate systems for improved drug delivery. *Advanced Drug Delivery Reviews*, *47*(1), 1–2. [https://doi.org/10.1016/S0169-409X\(00\)00117-4](https://doi.org/10.1016/S0169-409X(00)00117-4)

- Kerch, G. (2015). The potential of chitosan and its derivatives in prevention and treatment of age-related diseases. *Marine Drugs*, 13(4), 2158–2182.
<https://doi.org/10.3390/md13042158>
- Klein, G. L. (2015). THE EFFECT OF GLUCOCORTICOIDS ON BONE AND MUSCLE. *Osteoporosis and Sarcopenia*, 1(1), 39–45. <https://doi.org/10.1016/j.afos.2015.07.008>
- Klunklin, W., & Savage, G. (2017). Effect on Quality Characteristics of Tomatoes Grown Under Well-Watered and Drought Stress Conditions. *Foods (Basel, Switzerland)*, 6(8), 56.
<https://doi.org/10.3390/foods6080056>
- Kumar, N., Bhandari, P., Singh, B., Gupta, A. P., & Kaul, V. K. (2008). Reversed phase-HPLC for rapid determination of polyphenols in flowers of rose species. *Journal of Separation Science*, 31(2), 262–267. <https://doi.org/10.1002/jssc.200700372>
- Kuppusamy, P., Yusoff, M. M., Maniam, G. P., Ichwan, S. J. A., Soundharrajan, I., & Govindan, N. (2014). Nutraceuticals as potential therapeutic agents for colon cancer: A review. *Acta Pharmaceutica Sinica. B*, 4(3), 173–181. <https://doi.org/10.1016/j.apsb.2014.04.002>
- Kurkov, S. V., & Loftsson, T. (2013). Cyclodextrins. *International Journal of Pharmaceutics*, 453(1), 167–180. <https://doi.org/10.1016/j.ijpharm.2012.06.055>
- Lachowicz, M., Stańczyk, A., & Kołodziejczyk, M. (2020). Characteristic of Cyclodextrins: Their Role and Use in the Pharmaceutical Technology. *Current Drug Targets*, 21(14), 1495–1510. <https://doi.org/10.2174/1389450121666200615150039>
- Lagreca, E., Onesto, V., Di Natale, C., La Manna, S., Netti, P. A., & Vecchione, R. (2020). Recent advances in the formulation of PLGA microparticles for controlled drug delivery. *Progress in Biomaterials*, 9(4), 153–174. <https://doi.org/10.1007/s40204-020-00139-y>
- Lallemand, F., Furrer, P., Felt-Baeyens, O., Gex-Fabry, M., Dumont, J.-M., Besseghir, K., & Gurny, R. (2005). A novel water-soluble cyclosporine A prodrug: Ocular tolerance and in vivo kinetics. *International Journal of Pharmaceutics*, 295(1–2), 7–14.
<https://doi.org/10.1016/j.ijpharm.2004.12.015>

- Landi, S., Nurcato, R., De Lillo, A., Lentini, M., Grillo, S., & Esposito, S. (2016). Glucose-6-phosphate dehydrogenase plays a central role in the response of tomato (*Solanum lycopersicum*) plants to short and long-term drought. *Plant Physiology and Biochemistry: PPB*, *105*, 79–89. <https://doi.org/10.1016/j.plaphy.2016.04.013>
- Laplante, M., & Sabatini, D. M. (2012). mTOR signaling in growth control and disease. *Cell*, *149*(2), 274–293. <https://doi.org/10.1016/j.cell.2012.03.017>
- Laquintana, V., Asim, M. H., Lopedota, A., Cutrignelli, A., Lopalco, A., Franco, M., Bernkop-Schnürch, A., & Denora, N. (2019). Thiolated hydroxypropyl- β -cyclodextrin as mucoadhesive excipient for oral delivery of budesonide in liquid paediatric formulation. *International Journal of Pharmaceutics*, *572*, 118820. <https://doi.org/10.1016/j.ijpharm.2019.118820>
- Lecker, S. H., Jagoe, R. T., Gilbert, A., Gomes, M., Baracos, V., Bailey, J., Price, S. R., Mitch, W. E., & Goldberg, A. L. (2004). Multiple types of skeletal muscle atrophy involve a common program of changes in gene expression. *FASEB Journal: Official Publication of the Federation of American Societies for Experimental Biology*, *18*(1), 39–51. <https://doi.org/10.1096/fj.03-0610com>
- Legen, I., Salobir, M., & Kerc, J. (2005). Comparison of different intestinal epithelia as models for absorption enhancement studies. *International Journal of Pharmaceutics*, *291*(1–2), 183–188. <https://doi.org/10.1016/j.ijpharm.2004.07.055>
- Levy, M. L., Carroll, W., Izquierdo Alonso, J. L., Keller, C., Lavorini, F., & Lehtimäki, L. (2019). Understanding Dry Powder Inhalers: Key Technical and Patient Preference Attributes. *Advances in Therapy*, *36*(10), 2547–2557. <https://doi.org/10.1007/s12325-019-01066-6>
- Li, J., Pan, D., Yi, J., Hao, L., Kang, Q., Liu, X., Lu, L., & Lu, J. (2019). Protective effect of β -cyclodextrin on stability of nisin and corresponding interactions involved. *Carbohydrate Polymers*, *223*, 115115. <https://doi.org/10.1016/j.carbpol.2019.115115>

- Liang, C.-C., Park, A. Y., & Guan, J.-L. (2007). In vitro scratch assay: A convenient and inexpensive method for analysis of cell migration in vitro. *Nature Protocols*, *2*(2), 329–333.
<https://doi.org/10.1038/nprot.2007.30>
- Loftsson, T., & Brewster, M. E. (1996). Pharmaceutical Applications of Cyclodextrins. 1. Drug Solubilization and Stabilization. *Journal of Pharmaceutical Sciences*, *85*(10), 1017–1025.
<https://doi.org/10.1021/js950534b>
- Loftsson, T., Jansook, P., & Stefánsson, E. (2012). Topical drug delivery to the eye: Dorzolamide. *Acta Ophthalmologica*, *90*(7), 603–608. <https://doi.org/10.1111/j.1755-3768.2011.02299.x>
- Loftsson, T., Saokham, P., & Sá Couto, A. R. (2019). Self-association of cyclodextrins and cyclodextrin complexes in aqueous solutions. *International Journal of Pharmaceutics*, *560*, 228–234. <https://doi.org/10.1016/j.ijpharm.2019.02.004>
- Loftsson, T., Sigurdsson, H. H., & Jansook, P. (2023). Anomalous Properties of Cyclodextrins and Their Complexes in Aqueous Solutions. *Materials (Basel, Switzerland)*, *16*(6), 2223.
<https://doi.org/10.3390/ma16062223>
- M Ways, T. M., Lau, W. M., & Khutoryanskiy, V. V. (2018). Chitosan and Its Derivatives for Application in Mucoadhesive Drug Delivery Systems. *Polymers*, *10*(3), 267.
<https://doi.org/10.3390/polym10030267>
- MacLeod, M., Papi, A., Contoli, M., Beghé, B., Celli, B. R., Wedzicha, J. A., & Fabbri, L. M. (2021). Chronic obstructive pulmonary disease exacerbation fundamentals: Diagnosis, treatment, prevention and disease impact. *Respirology (Carlton, Vic.)*, *26*(6), 532–551.
<https://doi.org/10.1111/resp.14041>
- Matica, M. A., Aachmann, F. L., Tøndervik, A., Sletta, H., & Ostafe, V. (2019). Chitosan as a Wound Dressing Starting Material: Antimicrobial Properties and Mode of Action. *International Journal of Molecular Sciences*, *20*(23), 5889.
<https://doi.org/10.3390/ijms20235889>

- Medina-Leyte, D. J., Domínguez-Pérez, M., Mercado, I., Villarreal-Molina, M. T., & Jacobo-Albavera, L. (2020). Use of Human Umbilical Vein Endothelial Cells (HUVEC) as a Model to Study Cardiovascular Disease: A Review. *Applied Sciences*, *10*(3), 938. <https://doi.org/10.3390/app10030938>
- Messner, M., Kurkov, S. V., Jansook, P., & Loftsson, T. (2010). Self-assembled cyclodextrin aggregates and nanoparticles. *International Journal of Pharmaceutics*, *387*(1–2), 199–208. <https://doi.org/10.1016/j.ijpharm.2009.11.035>
- Mezzetta, A., Guazzelli, L., & Chiappe, C. (2017). Access to cross-linked chitosans by exploiting CO₂ and the double solvent-catalytic effect of ionic liquids. *Green Chemistry*, *19*(5), 1235–1239. <https://doi.org/10.1039/C6GC02935C>
- Migone, C., Scacciati, N., Grassiri, B., De Leo, M., Braca, A., Puppi, D., Zambito, Y., & Piras, A. M. (2022). Jellyfish Polysaccharides for Wound Healing Applications. *International Journal of Molecular Sciences*, *23*(19), 11491. <https://doi.org/10.3390/ijms231911491>
- Mirzoev, T., Tyganov, S., Vilchinskaya, N., Lomonosova, Y., & Shenkman, B. (2016). Key Markers of mTORC1-Dependent and mTORC1-Independent Signaling Pathways Regulating Protein Synthesis in Rat Soleus Muscle During Early Stages of Hindlimb Unloading. *Cellular Physiology and Biochemistry: International Journal of Experimental Cellular Physiology, Biochemistry, and Pharmacology*, *39*(3), 1011–1020. <https://doi.org/10.1159/000447808>
- Mitjans, M., Ugartondo, V., Martínez, V., Touriño, S., Torres, J. L., & Vinardell, M. P. (2011). Role of galloylation and polymerization in cytoprotective effects of polyphenolic fractions against hydrogen peroxide insult. *Journal of Agricultural and Food Chemistry*, *59*(5), 2113–2119. <https://doi.org/10.1021/jf1025532>
- Miyajima, K., Sawada, M., & Nakagaki, M. (1983). Viscosity *B*-Coefficients, Apparent Molar Volumes, and Activity Coefficients for α - and γ -Cyclodextrins in Aqueous Solutions.

Bulletin of the Chemical Society of Japan, 56(12), 3556–3560.

<https://doi.org/10.1246/bcsj.56.3556>

- Morales, R. G., Resende, L. V., Maluf, W. R., Peres, L. E., & Bordini, I. C. (2015). Selection of tomato plant families using characters related to water deficit resistance. *Horticultura Brasileira*, 33(1), 27–33. <https://doi.org/10.1590/S0102-053620150000100005>
- Morelo Dal Bosco, S. (2015). BENEFICIOS POLIFENOLICOS HOJA DE OLIVO (OLEA EUROPAEA L) PARA LA SALUD. *NUTRICION HOSPITALARIA*, 3, 1427–1433. <https://doi.org/10.3305/nh.2015.31.3.8400>
- Munin, A., & Edwards-Lévy, F. (2011). Encapsulation of natural polyphenolic compounds; a review. *Pharmaceutics*, 3(4), 793–829. <https://doi.org/10.3390/pharmaceutics3040793>
- Ortega-García, F., & Peragón, J. (2009). The response of phenylalanine ammonia-lyase, polyphenol oxidase and phenols to cold stress in the olive tree (*Olea europaea* L. cv. Picual). *Journal of the Science of Food and Agriculture*, 89(9), 1565–1573. <https://doi.org/10.1002/jsfa.3625>
- Osakabe, Y., Osakabe, K., Shinozaki, K., & Tran, L.-S. P. (2014). Response of plants to water stress. *Frontiers in Plant Science*, 5, 86. <https://doi.org/10.3389/fpls.2014.00086>
- Padalino, L., Conte, A., Lecce, L., Likyova, D., Sicari, V., Pellicanò, T. M., Poiana, M., & Del Nobile, M. A. (2017). Functional pasta with tomato by-product as a source of antioxidant compounds and dietary fibre. *Czech Journal of Food Sciences*, 35(1), 48–56. <https://doi.org/10.17221/171/2016-CJFS>
- Pagano, C., Perioli, L., Baiocchi, C., Bartoccini, A., Beccari, T., Blasi, F., Calarco, P., Ceccarini, M. R., Cossignani, L., di Michele, A., Ortenzi, R., Scuota, S., & Ricci, M. (2020). Preparation and characterization of polymeric microparticles loaded with Moringa oleifera leaf extract for exuding wound treatment. *International Journal of Pharmaceutics*, 587, 119700. <https://doi.org/10.1016/j.ijpharm.2020.119700>

- Parri, S., Romi, M., Hoshika, Y., Giovannelli, A., Dias, M. C., Piritore, F. C., Cai, G., & Cantini, C. (2023). Morpho-Physiological Responses of Three Italian Olive Tree (*Olea europaea* L.) Cultivars to Drought Stress. *Horticulturae*, *9*(7), 830. <https://doi.org/10.3390/horticulturae9070830>
- Partis, M. D., Griffiths, D. G., Roberts, G. C., & Beechey, R. B. (1983). Cross-linking of protein by ω -maleimido alkanoyl-N-hydroxysuccinimido esters. *Journal of Protein Chemistry*, *2*(3), 263–277. <https://doi.org/10.1007/BF01025358>
- Pellicanò, T. M., Sicari, V., Loizzo, M. R., Leporini, M., Falco, T., & Poiana, M. (2020). Optimizing the supercritical fluid extraction process of bioactive compounds from processed tomato skin by-products. *Food Science and Technology*, *40*(3), 692–697. <https://doi.org/10.1590/fst.16619>
- Pereira, A. P., Ferreira, I. C. F. R., Marcelino, F., Valentão, P., Andrade, P. B., Seabra, R., Estevinho, L., Bento, A., & Pereira, J. A. (2007). Phenolic compounds and antimicrobial activity of olive (*Olea europaea* L. Cv. Cobrançosa) leaves. *Molecules (Basel, Switzerland)*, *12*(5), 1153–1162. <https://doi.org/10.3390/12051153>
- Pereira, J. A., Pereira, A. P. G., Ferreira, I. C. F. R., Valentão, P., Andrade, P. B., Seabra, R., Estevinho, L., & Bento, A. (2006). Table olives from Portugal: Phenolic compounds, antioxidant potential, and antimicrobial activity. *Journal of Agricultural and Food Chemistry*, *54*(22), 8425–8431. <https://doi.org/10.1021/jf061769j>
- Perinel, S., Pourchez, J., Leclerc, L., Avet, J., Durand, M., Prévôt, N., Cottier, M., & Vergnon, J. M. (2017). Development of an ex vivo human-porcine respiratory model for preclinical studies. *Scientific Reports*, *7*(1), 43121. <https://doi.org/10.1038/srep43121>
- Perveen, R., Suleria, H. A. R., Anjum, F. M., Butt, M. S., Pasha, I., & Ahmad, S. (2015). Tomato (*Solanum lycopersicum*) Carotenoids and Lycopenes Chemistry; Metabolism, Absorption, Nutrition, and Allied Health Claims—A Comprehensive Review. *Critical*

Reviews in Food Science and Nutrition, 55(7), 919–929.

<https://doi.org/10.1080/10408398.2012.657809>

Petridis, A., Therios, I., Samouris, G., Koundouras, S., & Giannakoula, A. (2012). Effect of water deficit on leaf phenolic composition, gas exchange, oxidative damage and antioxidant activity of four Greek olive (*Olea europaea* L.) cultivars. *Plant Physiology and Biochemistry: PPB*, 60, 1–11. <https://doi.org/10.1016/j.plaphy.2012.07.014>

Biochemistry: PPB, 60, 1–11. <https://doi.org/10.1016/j.plaphy.2012.07.014>

Pietta, P.-G. (2000). Flavonoids as Antioxidants. *Journal of Natural Products*, 63(7), 1035–1042.

<https://doi.org/10.1021/np9904509>

Piras, A. M., Fabiano, A., Chiellini, F., & Zambito, Y. (2018). Methyl- β -cyclodextrin

quaternary ammonium chitosan conjugate: Nanoparticles vs macromolecular soluble complex. *International Journal of Nanomedicine*, Volume 13, 2531–2541.

<https://doi.org/10.2147/IJN.S160987>

Polera, N., Badolato, M., Perri, F., Carullo, G., & Aiello, F. (2019). Quercetin and its Natural

Sources in Wound Healing Management. *Current Medicinal Chemistry*, 26(31), 5825–

5848. <https://doi.org/10.2174/0929867325666180713150626>

Qin, L., Cui, Z., Wu, Y., Wang, H., Zhang, X., Guan, J., & Mao, S. (2023). Challenges and

Strategies to Enhance the Systemic Absorption of Inhaled Peptides and Proteins.

Pharmaceutical Research, 40(5), 1037–1055. [https://doi.org/10.1007/s11095-022-](https://doi.org/10.1007/s11095-022-03435-3)

03435-3

Racaniello, G. F., Laquintana, V., Summonte, S., Lopedota, A., Cutrignelli, A., Lopalco, A., Franco,

M., Bernkop-Schnürch, A., & Denora, N. (2021). Spray-dried mucoadhesive

microparticles based on S-protected thiolated hydroxypropyl- β -cyclodextrin for

budesonide nasal delivery. *International Journal of Pharmaceutics*, 603, 120728.

<https://doi.org/10.1016/j.ijpharm.2021.120728>

Ranieri, M., Di Mise, A., Difonzo, G., Centrone, M., Venneri, M., Pellegrino, T., Russo, A.,

Mastrodonato, M., Caponio, F., Valenti, G., & Tamma, G. (2019). Green olive leaf extract

- (OLE) provides cytoprotection in renal cells exposed to low doses of cadmium. *PLOS ONE*, *14*(3), e0214159. <https://doi.org/10.1371/journal.pone.0214159>
- Rodrigues Sá Couto, A., Ryzhakov, A., Larsen, K. L., & Loftsson, T. (2019). Interaction of Native Cyclodextrins and Their Hydroxypropylated Derivatives with Carbamazepine in Aqueous Solution. Evaluation of Inclusion Complexes and Aggregates Formation. *ACS Omega*, *4*(1), 1460–1469. <https://doi.org/10.1021/acsomega.8b02045>
- Ruszymah, B. H. I., Chowdhury, S. R., Manan, N. A. B. A., Fong, O. S., Adenan, M. I., & Saim, A. B. (2012). Aqueous extract of *Centella asiatica* promotes corneal epithelium wound healing in vitro. *Journal of Ethnopharmacology*, *140*(2), 333–338. <https://doi.org/10.1016/j.jep.2012.01.023>
- Sadeghi, D., Solouk, A., Samadikuchaksaraei, A., & Seifalian, A. M. (2021). Preparation of internally-crosslinked alginate microspheres: Optimization of process parameters and study of pH-responsive behaviors. *Carbohydrate Polymers*, *255*, 117336. <https://doi.org/10.1016/j.carbpol.2020.117336>
- Safran, T., Swift, A., Cotofana, S., & Nikolis, A. (2021). Evaluating safety in hyaluronic acid lip injections. *Expert Opinion on Drug Safety*, *20*(12), 1473–1486. <https://doi.org/10.1080/14740338.2021.1962283>
- Şahin, S., & Bilgin, M. (2018). Olive tree (*Olea europaea* L.) leaf as a waste by-product of table olive and olive oil industry: A review. *Journal of the Science of Food and Agriculture*, *98*(4), 1271–1279. <https://doi.org/10.1002/jsfa.8619>
- Sahiner, N., Suner, S. S., & Ayyala, R. S. (2019). Mesoporous, degradable hyaluronic acid microparticles for sustainable drug delivery application. *Colloids and Surfaces. B, Biointerfaces*, *177*, 284–293. <https://doi.org/10.1016/j.colsurfb.2019.02.015>
- Salomone, R., & Ioppolo, G. (2012). Environmental impacts of olive oil production: A Life Cycle Assessment case study in the province of Messina (Sicily). *Journal of Cleaner Production*, *28*, 88–100. <https://doi.org/10.1016/j.jclepro.2011.10.004>

- Šamec, D., Karalija, E., Šola, I., Vujčić Bok, V., & Salopek-Sondi, B. (2021). The Role of Polyphenols in Abiotic Stress Response: The Influence of Molecular Structure. *Plants (Basel, Switzerland)*, *10*(1), 118. <https://doi.org/10.3390/plants10010118>
- Sato, H., Genet, C., Strehle, A., Thomas, C., Lobstein, A., Wagner, A., Mioskowski, C., Auwerx, J., & Saladin, R. (2007). Anti-hyperglycemic activity of a TGR5 agonist isolated from *Olea europaea*. *Biochemical and Biophysical Research Communications*, *362*(4), 793–798. <https://doi.org/10.1016/j.bbrc.2007.06.130>
- Scherer, R., Rybka, A. C. P., Ballus, C. A., Meinhart, A. D., Filho, J. T., & Godoy, H. T. (2012). Validation of a HPLC method for simultaneous determination of main organic acids in fruits and juices. *Food Chemistry*, *135*(1), 150–154. <https://doi.org/10.1016/j.foodchem.2012.03.111>
- Schwarz, D. H., Engelke, A., & Wenz, G. (2017). Solubilizing steroidal drugs by β -cyclodextrin derivatives. *International Journal of Pharmaceutics*, *531*(2), 559–567. <https://doi.org/10.1016/j.ijpharm.2017.07.046>
- Scoditti, E., Massaro, M., Garbarino, S., & Toraldo, D. M. (2019). Role of Diet in Chronic Obstructive Pulmonary Disease Prevention and Treatment. *Nutrients*, *11*(6), 1357. <https://doi.org/10.3390/nu11061357>
- Selim, S., Albqmi, M., Al-Sanea, M. M., Alnusaire, T. S., Almuhayawi, M. S., AbdElgawad, H., Al Jaouni, S. K., Elkelish, A., Hussein, S., Warrad, M., & El-Saadony, M. T. (2022). Valorizing the usage of olive leaves, bioactive compounds, biological activities, and food applications: A comprehensive review. *Frontiers in Nutrition*, *9*, 1008349. <https://doi.org/10.3389/fnut.2022.1008349>
- Singh, B., & Pal, L. (2008). Development of sterculia gum based wound dressings for use in drug delivery. *European Polymer Journal*, *44*(10), 3222–3230. <https://doi.org/10.1016/j.eurpolymj.2008.07.013>

- Singla, A. K., & Chawla, M. (2001). Chitosan: Some pharmaceutical and biological aspects--an update. *The Journal of Pharmacy and Pharmacology*, 53(8), 1047–1067.
<https://doi.org/10.1211/0022357011776441>
- Singleton, V. L., Orthofer, R., & Lamuela-Raventós, R. M. (1999). [14] Analysis of total phenols and other oxidation substrates and antioxidants by means of folin-ciocalteu reagent. In *Methods in Enzymology* (Vol. 299, pp. 152–178). Elsevier.
[https://doi.org/10.1016/S0076-6879\(99\)99017-1](https://doi.org/10.1016/S0076-6879(99)99017-1)
- Singleton, V. L., & Rossi, J. A. (1965). Colorimetry of Total Phenolics with Phosphomolybdic-Phosphotungstic Acid Reagents. *American Journal of Enology and Viticulture*, 16(3), 144–158. <https://doi.org/10.5344/ajev.1965.16.3.144>
- Sivakumar, R., & Srividhya, S. (2016). Impact of drought on flowering, yield and quality parameters in diverse genotypes of tomato (*Solanum lycopersicum* L.). *Advances in Horticultural Science*, 3-11 Pages. <https://doi.org/10.13128/AHS-18696>
- Slimestad, R., & Verheul, M. (2009). Review of flavonoids and other phenolics from fruits of different tomato (*Lycopersicon esculentum* Mill.) cultivars. *Journal of the Science of Food and Agriculture*, 89(8), 1255–1270. <https://doi.org/10.1002/jsfa.3605>
- Smyth, D., Blumenfeld, O., & Konigsberg, W. (1964). Reactions of *N*-ethylmaleimide with peptides and amino acids. *Biochemical Journal*, 91(3), 589–595.
<https://doi.org/10.1042/bj0910589>
- Somova, L. I., Shode, F. O., Ramnanan, P., & Nadar, A. (2003). Antihypertensive, antiatherosclerotic and antioxidant activity of triterpenoids isolated from *Olea europaea*, subspecies *africana* leaves. *Journal of Ethnopharmacology*, 84(2–3), 299–305. [https://doi.org/10.1016/s0378-8741\(02\)00332-x](https://doi.org/10.1016/s0378-8741(02)00332-x)
- Steven, S., Frenis, K., Oelze, M., Kalinovic, S., Kuntic, M., Bayo Jimenez, M. T., Vujacic-Mirski, K., Helmstädter, J., Krölller-Schön, S., Münzel, T., & Daiber, A. (2019). Vascular Inflammation

- and Oxidative Stress: Major Triggers for Cardiovascular Disease. *Oxidative Medicine and Cellular Longevity*, 2019, 7092151. <https://doi.org/10.1155/2019/7092151>
- Sudjana, A. N., D’Orazio, C., Ryan, V., Rasool, N., Ng, J., Islam, N., Riley, T. V., & Hammer, K. A. (2009). Antimicrobial activity of commercial *Olea europaea* (olive) leaf extract. *International Journal of Antimicrobial Agents*, 33(5), 461–463. <https://doi.org/10.1016/j.ijantimicag.2008.10.026>
- Szabo, K., Cătoi, A.-F., & Vodnar, D. C. (2018). Bioactive Compounds Extracted from Tomato Processing by-Products as a Source of Valuable Nutrients. *Plant Foods for Human Nutrition (Dordrecht, Netherlands)*, 73(4), 268–277. <https://doi.org/10.1007/s11130-018-0691-0>
- Szejtli, J. (1998). Introduction and General Overview of Cyclodextrin Chemistry. *Chemical Reviews*, 98(5), 1743–1754. <https://doi.org/10.1021/cr970022c>
- Talhaoui, N., Taamalli, A., Gómez-Caravaca, A. M., Fernández-Gutiérrez, A., & Segura-Carretero, A. (2015). Phenolic compounds in olive leaves: Analytical determination, biotic and abiotic influence, and health benefits. *Food Research International*, 77, 92–108. <https://doi.org/10.1016/j.foodres.2015.09.011>
- Talón, E., Trifkovic, K. T., Vargas, M., Chiralt, A., & González-Martínez, C. (2017). Release of polyphenols from starch-chitosan based films containing thyme extract. *Carbohydrate Polymers*, 175, 122–130. <https://doi.org/10.1016/j.carbpol.2017.07.067>
- Tarchoune, I., Sgherri, C., Eddouzi, J., Zinnai, A., Quartacci, M., & Zarrouk, M. (2019). Olive Leaf Addition Increases Olive Oil Nutraceutical Properties. *Molecules*, 24(3), 545. <https://doi.org/10.3390/molecules24030545>
- Trotta, V., & Scalia, S. (2017). Pulmonary delivery systems for polyphenols. *Drug Development and Industrial Pharmacy*, 43(7), 1043–1052. <https://doi.org/10.1080/03639045.2017.1293680>

- Utami, N. D., Nordin, A., Katas, H., Bt Hj Idrus, R., & Fauzi, M. B. (2020). Molecular Action of Hydroxytyrosol in Wound Healing: An In Vitro Evidence-Based Review. *Biomolecules*, *10*(10), 1397. <https://doi.org/10.3390/biom10101397>
- Valente, S., Machado, B., Pinto, D. C. G. A., Santos, C., Silva, A. M. S., & Dias, M. C. (2020). Modulation of phenolic and lipophilic compounds of olive fruits in response to combined drought and heat. *Food Chemistry*, *329*, 127191. <https://doi.org/10.1016/j.foodchem.2020.127191>
- Van Eck, J., Kirk, D. D., & Walmsley, A. M. (2006). Tomato (*Lycopersicon esculentum*). *Methods in Molecular Biology (Clifton, N.J.)*, *343*, 459–473. <https://doi.org/10.1385/1-59745-130-4:459>
- Vizzoni, L., Migone, C., Grassiri, B., Zambito, Y., Ferro, B., Roncucci, P., Mori, F., Salvatore, A., Ascione, E., Crea, R., Esin, S., Batoni, G., & Piras, A. M. (2023). Biopharmaceutical Assessment of Mesh Aerosolised Plasminogen, a Step towards ARDS Treatment. *Pharmaceutics*, *15*(6), 1618. <https://doi.org/10.3390/pharmaceutics15061618>
- Wang, H., Nair, M. G., Strasburg, G. M., Chang, Y. C., Booren, A. M., Gray, J. I., & DeWitt, D. L. (1999). Antioxidant and antiinflammatory activities of anthocyanins and their aglycon, cyanidin, from tart cherries. *Journal of Natural Products*, *62*(2), 294–296. <https://doi.org/10.1021/np980501m>
- Wang, P.-H., Huang, B.-S., Horng, H.-C., Yeh, C.-C., & Chen, Y.-J. (2018). Wound healing. *Journal of the Chinese Medical Association: JCMA*, *81*(2), 94–101. <https://doi.org/10.1016/j.jcma.2017.11.002>
- Wang, S., Su, R., Nie, S., Sun, M., Zhang, J., Wu, D., & Moustaid-Moussa, N. (2014). Application of nanotechnology in improving bioavailability and bioactivity of diet-derived phytochemicals. *The Journal of Nutritional Biochemistry*, *25*(4), 363–376. <https://doi.org/10.1016/j.jnutbio.2013.10.002>

- Wang, W.-B., Kim, Y.-H., Lee, H.-S., Kim, K.-Y., Deng, X.-P., & Kwak, S.-S. (2009). Analysis of antioxidant enzyme activity during germination of alfalfa under salt and drought stresses. *Plant Physiology and Biochemistry: PPB*, 47(7), 570–577.
<https://doi.org/10.1016/j.plaphy.2009.02.009>
- Warnke, P. H., Lott, A. J. S., Sherry, E., Wiltfang, J., & Podschun, R. (2013). The ongoing battle against multi-resistant strains: In-vitro inhibition of hospital-acquired MRSA, VRE, Pseudomonas, ESBL E. coli and Klebsiella species in the presence of plant-derived antiseptic oils. *Journal of Cranio-Maxillo-Facial Surgery: Official Publication of the European Association for Cranio-Maxillo-Facial Surgery*, 41(4), 321–326.
<https://doi.org/10.1016/j.jcms.2012.10.012>
- Www.who.int.* (s.d.).
- Xie, P., Huang, L., Zhang, C., & Zhang, Y. (2015). Phenolic compositions, and antioxidant performance of olive leaf and fruit (*Olea europaea* L.) extracts and their structure–activity relationships. *Journal of Functional Foods*, 16, 460–471.
<https://doi.org/10.1016/j.jff.2015.05.005>
- Yoon, M.-S. (2017). mTOR as a Key Regulator in Maintaining Skeletal Muscle Mass. *Frontiers in Physiology*, 8, 788. <https://doi.org/10.3389/fphys.2017.00788>
- Zamani, M., Thyagarajan, S., & Olver, J. M. (2008). Functional use of hyaluronic acid gel in lower eyelid retraction. *Archives of Ophthalmology (Chicago, Ill.: 1960)*, 126(8), 1157–1159.
<https://doi.org/10.1001/archopht.126.8.1157>
- Zambito, Y., & Colo, G. D. (2010). Thiolated quaternary ammonium–chitosan conjugates for enhanced precorneal retention, transcorneal permeation and intraocular absorption of dexamethasone. *European Journal of Pharmaceutics and Biopharmaceutics*, 75(2), 194–199. <https://doi.org/10.1016/j.ejpb.2010.02.006>
- Zambito, Y., Fogli, S., Zaino, C., Stefanelli, F., Breschi, M. C., & Di Colo, G. (2009). Synthesis, characterization and evaluation of thiolated quaternary ammonium-chitosan

- conjugates for enhanced intestinal drug permeation. *European Journal of Pharmaceutical Sciences*, 38(2), 112–120. <https://doi.org/10.1016/j.ejps.2009.06.006>
- Zambito, Y., Piras, A. M., & Fabiano, A. (2022). Bergamot Essential Oil: A Method for Introducing It in Solid Dosage Forms. *Foods*, 11(23), 3860. <https://doi.org/10.3390/foods11233860>
- Zambito, Y., Uccello-Barretta, G., Zaino, C., Balzano, F., & Di Colo, G. (2006). Novel transmucosal absorption enhancers obtained by aminoalkylation of chitosan. *European Journal of Pharmaceutical Sciences: Official Journal of the European Federation for Pharmaceutical Sciences*, 29(5), 460–469. <https://doi.org/10.1016/j.ejps.2006.09.001>
- Zambito, Y., Zaino, C., Uccello-Barretta, G., Balzano, F., & Di Colo, G. (2008). Improved synthesis of quaternary ammonium-chitosan conjugates (N⁺-Ch) for enhanced intestinal drug permeation. *European Journal of Pharmaceutical Sciences: Official Journal of the European Federation for Pharmaceutical Sciences*, 33(4–5), 343–350. <https://doi.org/10.1016/j.ejps.2008.01.004>